# SKULL ASYMMETRY, EAR STRUCTURE AND FUNCTION, AND AUDITORY LOCALIZATION IN TENGMALM'S OWL, *AEGOLIUS FUNEREUS* (LINNÉ)

By R. Å. NORBERG
*Department of Zoology, University of Göteborg,*
*Fack, S-400 33 Göteborg 33, Sweden*

(*Communicated by B. B. Boycott, F.R.S. – Received 25 March 1977*)

[Plates 1–10]

## CONTENTS

The ear apertures in the skin of Tengmalm's owl, *Aegolius funereus* (Linné) (Strigiformes), are slit-like and *ca.* 24 mm long. This equals the height of the skull. The ear opening in the skin is bounded by a continuous fold of skin that is developed into a preaural and a postaural flap. The preaural flap carries the facial disk feathers that are structurally specialized to be sound transparent. They form a multi-layered, but sparse and delicate web over the ear opening. The postaural flap carries very densely packed feathers that form an anteriorly concave facial ruff. The ear folds (flaps) and the ear slit in the skin of one ear exhibit bilateral symmetry relative to

those of the other ear, but because of asymmetry of underlying skull bones the postaural folds come to be oriented in somewhat different ways in the left and right ear.

The skull bones, their constellation, and their role in the bilateral skull asymmetry are described in skulls at various stages of development (12–25 days post-hatching).

Inside the ear aperture in the skin lies the smaller ear aperture in the skull. This is *ca.* 11 mm high. The ear and skull asymmetry reaches its maximum at the ear apertures of the skull. Hence the right ear aperture of the skull lies *ca.* 6.5 mm higher than the left one. Viewed from in front, a line connecting the centres of the ear apertures deviates 12° from the horizontal. The asymmetry then decreases towards the posterior parts of the external auditory meatuses, and the flattened meatus parts extended over the eardrum exhibit complete bilateral symmetry. As projected on the vertical median plane of the head, an axis through the centre of the eardrum and the centre of the ear aperture of one ear gives an angle of vertical divergence of *ca.* 40° with the corresponding, projected, axis of the other ear. The tympanic ring, the eardrum, the middle ear, the stapedial complex, and the bony cochlea and semicircular canals exhibit complete bilateral symmetry. However, one pair of the three pairs of air spaces communicating with the middle ear, namely the superior air space, is of different shape on the two sides. The skull bones participating in the asymmetry are: the orbitosphenoid, squamosal, parietal, frontal, and the squamoso-occipital wing. Of the jaw muscles the M. depressor mandibulae and the aponeurosis 1 portion of M. adductor mandibulae externus exhibit pronounced bilateral asymmetry. Both muscles are related to the highly asymmetrical squamoso-occipital wings.

The combined volume of the middle ear cavity and the air spaces communicating with it is *ca.* 730 $mm^3$ in one ear. This is almost as much as the volume of the external auditory meatus, which is about 830 $mm^3$. The large volume of air inside the eardrum should result in (1) a lowering of the resonant frequency of the middle ear, and (2) a lowering of impedance in the stiffness controlled frequency region below the resonance frequency, with a corresponding increase in transmission of these frequencies to the cochlea. An ecological consequence to the owl of lowered middle ear impedance, and hence threshold of hearing at low frequencies, is an improvement of the owl's ability in far range *detection* of sounds containing low frequencies, such as rustling sounds made by prey moving about in vegetation. While high frequencies are potentially more useful for sound *localization* than low ones, low frequencies are less attenuated by air and less diffracted and reflected by vegetation, and therefore travel farther and are more useful for *detection* of sound at some distance.

The area ratio between the eardrum and the footplate of stapes is 35.3, which is a high value for a bird. The stapedial complex consists of two functional units that perform two different, but interrelated, movement patterns. One unit is formed by the extracolumella and the Ligamentum ascendens. This unit is rigid and rotates about its axis of rotation at the rim of the tympanic ring. It is the functional equivalent to the mammalian ear ossicles malleus and incus. The other unit is the bony stapes. It performs a pistonlike motion and corresponds to the mammalian stapes. Because of the oblique orientation of the stapedial complex relative to the plane of the tympanic ring, the force lever arm becomes longer than the resistance arm. The maximum transformer ratio attainable by the stapedial complex amounts to 1.6. The combined transformer action, due to the area ratio and the transformer action of the stapedial complex, thus becomes 56 (the possible curved-membrane effect not included). The middle ear transformer ratio thus seems to be close to the optimal one (*ca.* 65), i.e. that resulting in maximum pressure transfer to the inner ear.

The external ears are bilaterally asymmetrical in the *vertical* plane. This strongly suggests that the asymmetry is linked to *vertical directional hearing*. The mere fact that there is a *bilateral asymmetry* of the external ears strongly suggests that vertical directional hearing is based on *binaural comparison* of signals from the two ears. Indeed, the entire asymmetry would seem meaningless as to auditory localization, if the information processing at the neural level were not based on binaural com-

parison. It is suggested that the remarkably large height of the symmetrical ear slits in the skin serves the purpose of extending the effect of ear asymmetry to lower frequency domains. Data from acoustical measurements show that the vertical sensitivity pattern is different between the left and right ear for frequencies above 6000 Hz. This demonstrates that the ear asymmetry in *Aegolius* is capable of producing excellent physical cues to vertical localization of sound. A hypothesis on localization of complex noise is given; it suggests that the owl performs a binaural comparison of spectral pattern. Low frequencies (below 6000 Hz) provide intensity cues to azimuth, high frequencies intensity cues to elevation angle. In theory, the median plane ambiguity, inherent to symmetrical ears, is removed by the bilateral asymmetry. This is because the asymmetry, at some frequencies, causes interaural intensity differences at most elevation angles in the median plane. The use of interaural differences in spectral pattern in auditory localization, would remove also the problem of distinguishing 'what' from 'where', i.e. the uncertainty as to whether a specific spectral pattern should be attributed to the sound source or to a direction-dependent spectral transformation imposed by head and ear. The ear asymmetry provides the cue in the vertical plane. The hypothesis on auditory localization is summarized in a simple mathematical expression.

## 1. Introduction

Bilateral asymmetry of the external ears occurs in species belonging to nine genera of owls. The genera are: *Tyto* Billberg, *Phodilus* Geoffroy Saint Hilaire, *Bubo* Duméril, *Ciccaba* Wagler, *Strix* Linné, *Rhinoptynx* Kaup, *Asio* Brisson, *Pseudoscops* Kaup, and *Aegolius* Kaup. A literature review including all significant morphological papers on ear asymmetry among owls, published in the period between 1859 and 1975 (inclusive), is published elsewhere (Norberg 1977).

It should be stressed, however, that the outer ears are perfectly symmetrical in the majority of owl species, in fact (as far as known) in all species of the remaining 20 owl genera.

The outer ear structure is very diverse among owls, particularly among species with highly developed ears. Thus the asymmetry is achieved in substantially different ways in some genera. Comparison of external ear structure, and consideration also of other morphological characters providing cues to the evolutionary history of owls, lead to the conclusion that bilateral ear asymmetry has evolved independently in at least five lines among owls (Norberg 1977).

The genus *Aegolius* alone represents one line of independent evolution of ear asymmetry. As distinguished from most other species with bilateral ear asymmetry, it is the skull that gives asymmetry to the external ears of *A. funereus*. In this species the skull is more asymmetrical than in any species belonging to other owl genera. However, the overall ear asymmetry is about as pronounced also in *Phodilus*, *Asio*, and some *Strix* species.

Except for *A. funereus* and *A. acadicus* (Gmelin) it is only in *Strix uralensis* Pallas and *S. nebulosa* J. R. Forster that the asymmetry is known for certain to involve parts of the skull. In the other owl species with asymmetrical ears the asymmetry lies in the soft anatomy.

### 1.1. *Review of literature on the ear of* Aegolius funereus

This review is extracted from Norberg (1977).

In three papers Collett described and illustrated the asymmetrical skull of *A. funereus* (Collett 1871, sub nomine *Strix tengmalmi*; Collett 1872 and 1881, sub nomine *Nyctala tengmalmi* (Gmel.)). The 1881 paper contains information also on the ear opening in the skin. Pycraft

(1898) described the pterylography, the outer ear, and the skull, and later (Pycraft 1903) again the skull of *A. funereus* (sub nomine *Nyctala tengmalmi*). Pycraft's illustration of the left ear (1889: pl. 27:5) is misleading. Probably the left ear of the specimen illustrated was damaged. In Baird, Brewer & Ridgway (1874) there are a few sketches of the head of *A. funereus* (sub nomine *Nyctale richardsoni*). The sketch on p. 100, said to be of *N. richardsoni* is not, while that said to be of *Surnia ulula*, illustrating skull asymmetry, is of *Aegolius*. The brief notes by Stellbogen (1930, p. 690) and the two figures (fig. 3:6, 7) claimed to be of *Nyctala tengmalmi* Gm do not fit in with *A. funereus*, the underlying material certainly being misidentified. Judging by the figures I should think they are of *Athene* Boie (or possibly *Glaucidium* Boie).

Dijk (1973, p. 161) wrote, 'members of the genus *Aegolius*...have...strongly asymmetrical external and even inner ears...' With 'inner ears', however, he actually meant the external auditory meatus (Dijk, personal communication), that owes its asymmetry to asymmetries of the skull.

There are no previous descriptions of the middle ear, stapedial complex, cochlea, and semi-circular canals in *A. funereus*. These ear parts have been described in a few other owl species (references in Norberg 1977).

### 1.2. *Problems and aim*

The present study was undertaken to answer the following questions regarding structure, and to provide information that can help answer questions regarding function.

1. What is the detailed structure of the external ear in *A. funereus*, and more particularly, how pronounced is the ear asymmetry, how is it achieved, and what structures are involved?
2. Does the asymmetry extend to the middle and internal ear?
3. What is the detailed structure of the middle ear and how does it relate to the function of sound transmission?
4. What is the rôle of ear asymmetry in auditory localization?

The older papers on the ear of *A. funereus* contain few or no quantitative data. The present description is intended to give information with sufficient accuracy (i) to allow functional interpretations to be based on it, and (ii) to allow detailed future morphological comparisons with other species.

Throughout this paper, special emphasis is put on form, dimensions, and spatial relations which may be of importance for functional interpretations of hearing. Structures, such as nerves and blood vessels, which are not associated with hearing or the asymmetry have been excluded.

Various components of the middle ear's transformer action are estimated, based on the structural descriptions.

The function of ear asymmetry in auditory localization is discussed on the basis of the structure of the external ear and data from acoustic measurements.

After rejection of the subdivision of family Strigidae into the subfamilies Buboninae and Striginae (Norberg 1977), the relations between genera contained in Strigidae need to be reinterpreted. The affinity of *Aegolius* therefore is uncertain.

Although the evolutionary history of *Aegolius* is not considered in this paper, the structural description performed is meant to form a basis for future comparisons with other species. To ascertain the role played by various skull bones in the ear asymmetry, skulls of developing owls had to be examined. Upon comparison with other species, the constellation of skull

bones may provide clues to the affinity of *Aegolius*. Because of this, and because the skull bone constellation is not readily accessible (sutures obliterated in adult birds), the skull description was made complete by incorporation of all skull bones.

## 2. Material

The description is based on the following material:

Thirty-five skulls, of which nine were borrowed from Naturhistoriska Museet, Göteborg, 12 from Naturhistoriska Riksmuseet, Stockholm, 11 from Zoologisk Museum, Universitetet i Oslo, Oslo, and three from Zoologisk Museum, Universitetet i Bergen, Bergen. When particular specimens are referred to in this paper, the above sources are denoted G, S, O and B, respectively, whereas N denotes specimens in my possession.

Ten dead but fresh and intact (cold-stored) owls, most of which were obtained from the Natural History Museums in Göteborg and Stockholm.

Three dead but fresh and intact young owls, aged 12–25 days (unfledged), representing different stages of skull development. They were selected from 13 young found dead from various reasons in the nests. These young were collected over several years during the course of an ecological study.

Three living owls in captivity, and a large number of living, wild ones observed and handled in the field.

All specimens studied have been collected in Sweden or Norway (14 of the skulls) and hence most likely are referable to the subspecies *Aegolius f. funereus* (Linné) (although this was not specifically checked).

## 3. Methods

Linear measurements were taken with a slide caliper that was read to the nearest 0.1 mm. The measurements taken of the external ear were rounded off to the nearest 0.5 mm before being tabulated. Where soft anatomy structures are involved in external ear measurements, great care was taken to obtain measurements with the ear slit and flaps in what were judged to be their natural positions and attitudes. No stretching of ear structures occurred during measurement. I measured only undamaged ears whose skin flaps were fresh and soft.

Ear structures whose areas were measured were drawn with the aid of a camera lucida (drawing tube) mounted on a Wild M5 dissecting microscope. A slide caliper with appropriately opened jaws was located at the object and served as a scale that was also drawn. With the aid of a polar compensating planimeter the areas were found of the drawing and of a reference square, drawn with the use of the scale. By comparison with the reference square the true area of the structure was found.

The planimeter tracer arm was so adjusted that readings containing three digits were always obtained. All areas, including those of the reference squares, were measured three times and the means were taken. By repeated drawing of test structures and measurement of areas with planimeter and by counting squares on a millimetre-grid paper, the error of the planimeter method was estimated to be less than 1 %.

Volumes of cavities were measured by injecting water with a hypodermic syringe. Where this was not feasible, volume estimates were obtained from the geometry and linear dimensions of the cavities.

The developing skulls of young owls were cleared and stained with the technique described by Evans (1948). In short, the procedure was as follows.

The skin was removed from the head which was then cleared in 2% KOH at room temperature for a few days. When the soft anatomy had become clear, the bone was stained in a solution of alizarine red (Alizarinsulfonic acid sodium salt) in 2% KOH. The dye solution should be very dilute and only lightly reddish. The best result was obtained when staining was terminated after the bone had become only light red (after about two hours). After additional clearing in KOH to destain the soft tissue that was dyed, the specimen was placed in 70% alcohol.

The result was very good with even tiny ossification centra clearly visible in their natural positions. Sutures were very obvious.

For the preparation of illustrations, the skulls were placed in 70% alcohol in a glass box and photographed normal to the box wall. The best photographs were obtained when the skulls were illuminated from behind through a white, semi-transparent Perspex plate. Drawings were then made from the photographs.

Evans (1948) recommended the use of glycerine for the final clearing and as a mounting medium. However, any stir caused serious optical diffraction in the glycerine. Hence glycerine is a highly unsuitable medium when photographs of high quality are required.

The staining technique for gross dissection of muscles devised by Bock & Shear (1972) was used for dissection of muscles of the ear folds bordering the ear aperture in the skin. Although staining the muscles only lightly and temporarily, this iodine stain proved very helpful.

The description of asymmetries was based partly on photographs (of several skulls) into which symmetry lines were drawn.

Great care was taken to attain exactitude of the illustrations. All photographs, those reproduced here and those from which drawings were made, were taken with an object-frontlens distance of 42 cm or more. Owing to this the illustrations deviate less than 5% from orthographic projection (in linear dimension). That is to say that distortion of relative linear dimensions of parts of the object nearest to and farthest from the lens is less than 5% (for figure 21 this holds only when the rostral part is excluded).

The illustrations not drawn strictly from photographs were drawn with the aid of a camera lucida on a dissecting microscope.

All illustrations are of adult specimens unless otherwise stated in the figure legends.

Information on terminology used is given in the descriptive sections.

## 4. Definitions of ear asymmetry and reference planes

*External or outer ear.* By external or outer ear is meant ear structures outside the eardrum. Parts of external ear thus are the external auditory, or acoustic, meatus, the aural skin folds or flaps bordering the ear aperture in the skin, the flat cavities between these folds and the skull, and also feathers around the ear.

*Asymmetry.* In *Aegolius* each external ear is asymmetrical in the sense that there is no way that a plane (or planes) can be oriented so as to divide the ear in two equal halves (or more than two equal parts). A more familiar, strongly asymmetrical structure of this kind is the human pinna. In the following, asymmetries within one ear, as defined above, are treated only in relation to bilateral asymmetry.

*Bilateral asymmetry.* Bilateral asymmetry of the external ears means that the two ears are geometrically dissimilar, i.e. one ear is not the mirror image of the other one. It is this kind of asymmetry that this paper is concerned with.

All symmetry questions treated henceforth are concerned with bilateral symmetry. For simplicity the word bilateral is therefore often omitted.

*The plane of the jugal bars, or the horizontal plane of the head.* For most of their length the jugal bars are straight. The plane best fitting the jugal bars is termed the plane of the jugal bars, or the horizontal plane of the head. It is a readily accessible reference plane which is well defined.

The anteriormost part of the jugal bar is dorsoventrally flattened (the proximal part of the labial process of the maxilla, cf. § 9). This flattened zone indicates the region of bending of the jugal bar upon the kinetic rotation of the upper beak about the fronto-nasal hinge. Since this compressed region is right below the fronto-nasal hinge, kinetic rotation of the upper beak does not bring about any significant change in orientation of the plane of the jugal bars.

Before using this reference plane in dead owls and in skulls, it should be ascertained that the quadrate is not dislodged from its squamosal articulation socket (which sometimes is the case in damaged skulls).

As seen from the side, the plane of the horizontal semicircular canal is parallel with the plane of the jugal bars (within the error of measurement, *ca.* 2°).

As far as could be judged, also the lines of sight are about parallel with the plane of the jugal bars. This is indicated by the fact that the vertical diameter of the anterior orifice of the sclerotic ring is about normal to this plane. It was also tested in the following way. In one living, captive owl the preaural fold was temporarily fixed in a forward position so as to expose a part of the jugal bar. The owl was then photographed from the side as it looked intently at a living mouse on the same horizontal plane as the owl's head. The line of sight thus indicated possibly was inclined somewhat upwards relative to the plane of the jugal bars, making an angle of 0–3° with this plane (see figures 5 and 29).

*Dorsoventral direction.* The dorsoventral direction of the head is defined as being perpendicular to the plane of the jugal bars.

## 5. Linear measurements of the external ear of intact owls

The following linear measurements were taken on intact owls. The linear dimensions are numbered from 1 to 13 and are defined as follows and as indicated in figures 1 and 18. Except when otherwise stated the measurements are direct ones. An 'l' after the dimension number denotes the left side, an 'r' the right side. Results are given in table 1.

1. Distance between the anteroventral terminations of the ear slits on the left and right side measured from the inside of the deflected edge of the skin fold.

2. Distance between the anterodorsal terminations of the ear slits on the left and right side measured from the inside of the deflected edge of the skin fold.

3. Distance between the lateral edges of the sclerotic rings on the left and right side.

4l and 4r. Height of the ear slit. Distance between its ventral and dorsal terminations measured from the inside of the slit.

5l. Distance on the left side from the anteroventral termination of the ear slit, inside of deflected edge, to the ventral border of the ear aperture of the skull, i.e. to the point of the

dorsal edge of the jugal bar visible just anterior to the squamoso-occipital wing when the skull is viewed from the side.

5r. Distance on the right side from the anteroventral termination of the ear slit, inside of deflected edge, to the ventral border of the ear aperture of the skull, i.e. to the most ventral point, inside the anterior edge of the squamoso-occipital wing, visible just lateral to the postorbital process when the skull is viewed from in front.

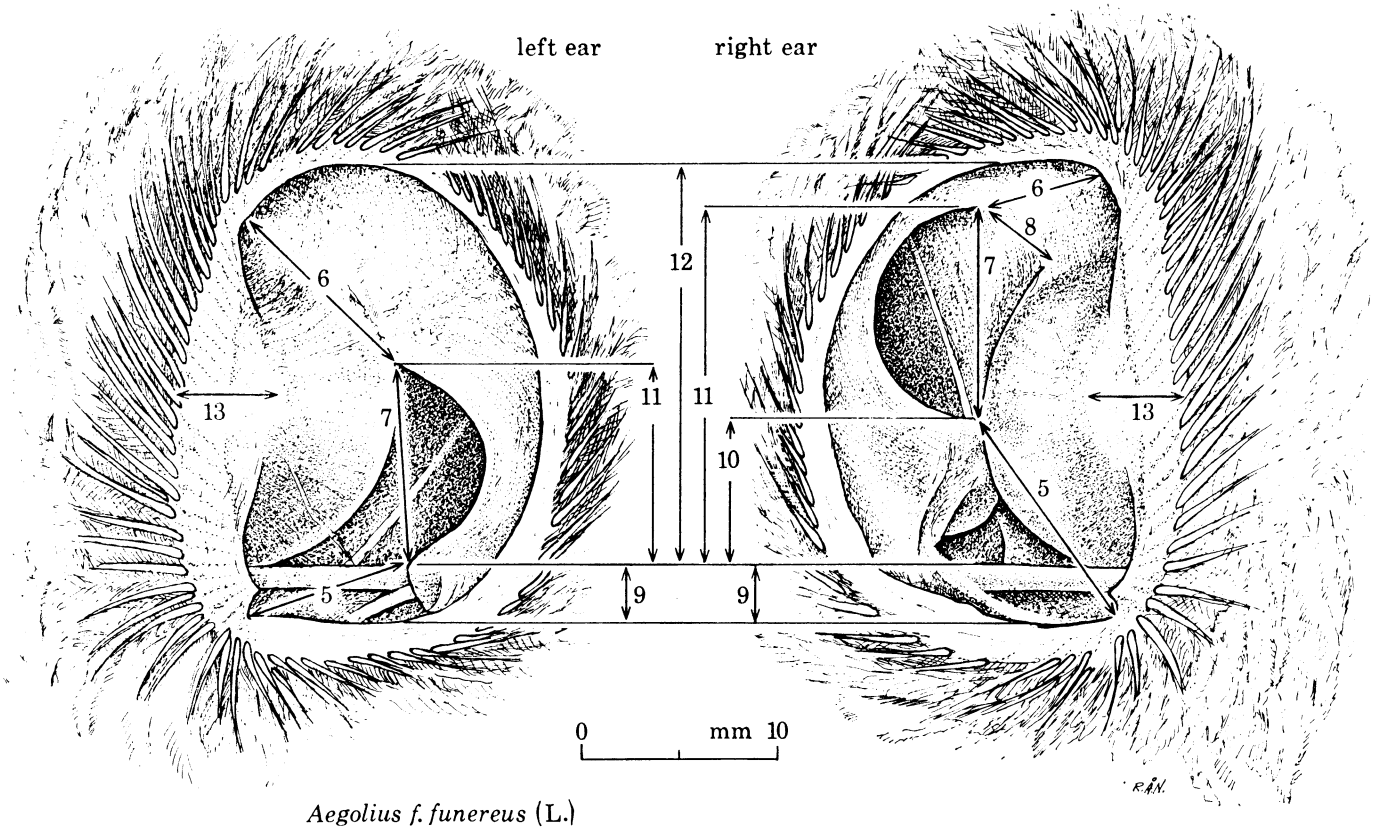


*Aegolius f. funereus* (L.)

FIGURE 1. Anterolateral views of the left and right ear of an adult *A. funereus*, showing how linear measurements of the external ears were taken. The head is oriented so that the nearest jugal bar lies in the plane of the figure and the horizontal plane of the head is perpendicular to the plane of the figure. The head and ears are intact, but the preaural flap is folded forwards and the postaural flap is displaced backwards to expose underlying structures.

6l. Distance on the left side from the anterodorsal termination of the ear slit, inside of deflected edge, to the dorsal border of the ear aperture of the skull, i.e. to the point where the anterior edge of the squamoso-occipital wing fuses with the lateral edge of the postorbital process.

6r. Distance on the right side from the anterodorsal termination of the ear slit, inside of deflected edge, to the dorsal border of the ear aperture of the skull, i.e. to the point where the anterior edge of the squamoso-occipital wing fuses with the skull.

7l. Height of the left ear aperture of the skull. Distance on the left side from the point of the dorsal edge of the jugal bar, visible just anterior to the squamoso-occipital wing when the skull is viewed from the side, to the point where the anterior edge of the squamoso-occipital wing fuses with the lateral edge of the postorbital process.

TABLE 1. LINEAR DIMENSIONS OF THE EXTERNAL EAR OF *A. FUNEREUS*

(The measurements are defined in §5 and in figures 1 and 18. One of the owls measured was a captive, living one. The others were dead but intact, and with the ear flaps fresh and soft. The owls had been kept frozen and were thawed just before the measurements were taken. All specimens are adults. Measurements taken to the nearest 0.1 mm but rounded off to the nearest 0.5 mm.)

| | measurement no. | | | | | | | | | | | | | | | | | | | |
|---|---|---|---|---|---|---|---|---|---|---|---|---|---|---|---|---|---|---|---|---|
| specimen | 1 | 2 | 3 | 4l | 4r | 5l | 5r | 6l | 6r | 7l | 7r | 8r | 9l | 9r | 10r | 11l | 11r | 12l | 12r | 13l | 13r |
| G.68-03 | | | 31 | 26 | 26 | | | | | 12 | 12 | 5½ | | | 7 | 11 | 18½ | | | | |
| G.D. | | | 32½ | | | | | | | 11 | 11 | 7 | | | 7½ | 11 | 17½ | | | | |
| S.Av.730463 ♂ | 25½ | 24½ | 32 | 24½ | 24 | 8 | 13 | 10 | 8 | 11 | 10½ | 5½ | 3½ | 3½ | 6 | 11 | 16½ | 19 | 18½ | 7 | 6½ |
| S.Av.740031 ♀ | 28 | 21 | 32 | 25 | 25 | 4½ | 12½ | 15 | 5½ | 11½ | 11 | 6 | 3 | 4 | 7 | 11½ | 17½ | 22½ | 21½ | 8½ | 8½ |
| S.Av.740032 ♂ | 27 | 24½ | 32 | 23½ | 24½ | 5 | 11½ | 12 | 9½ | 12 | 11½ | 6½ | 3 | 3 | 6½ | 12 | 16½ | 20½ | 20½ | 8 | 8 |
| N.3 | | | 32½ | 26 | 26 | 5½ | 11½ | 11½ | 5 | 10 | 10½ | 5 | | | 5½ | 9½ | 16 | | | 6 | 6 |
| N.4 | 24½ | 25 | 32 | 22½ | 22½ | 8 | 12 | 9½ | 6 | 9½ | 10½ | 5 | 3 | 2½ | 7 | 10 | 18 | 19 | 19 | 5½ | 5½ |
| N.5 | 26 | 26 | 32½ | 22½ | 22½ | 6 | 11 | 9 | 5 | 11 | 11 | 4½ | 3 | 3½ | 6½ | 11 | 17 | 19½ | 19 | 6½ | 6½ |
| N.14 | 25 | 21 | 31½ | 24½ | 24½ | 5½ | 11 | 11½ | 8 | 11½ | 12 | 7 | 3 | 3 | 6½ | 11½ | 18½ | 21 | 21 | 6 | 6 |
| N.15 | 25 | 22 | 32 | 24½ | 25 | 7 | 11½ | 10½ | 9 | 12 | 11 | 6 | 2½ | 3 | 6½ | 12 | 18 | 20½ | 20½ | 6 | 6 |
| N.1975 live ♂ | 25½ | 25½ | 32 | 24 | 23½ | 8 | 12 | 10½ | 8 | 11 | 10½ | 6½ | 3 | 3 | 7 | 11 | 17 | 19½ | 19½ | 6½ | 6½ |
| *n* | 8 | 8 | 11 | 10 | 10 | 9 | 9 | 9 | 9 | 11 | 11 | 11 | 8 | 8 | 11 | 11 | 11 | 8 | 8 | 9 | 9 |
| mean | 28.8 | 23.7 | 32.0 | 24.3 | 24.4 | 6.4 | 11.8 | 11.1 | 7.1 | 11.1 | 11.1 | 5.9 | 3.0 | 3.2 | 6.6 | 11.1 | 17.4 | 20.2 | 19.9 | 6.7 | 6.6 |
| s.d. | 1.2 | 2.0 | 0.5 | 1.2 | 1.3 | 1.4 | 0.7 | 1.8 | 1.8 | 0.8 | 0.6 | 0.8 | 0.3 | 0.5 | 0.6 | 0.8 | 0.8 | 1.2 | 1.1 | 1.0 | 1.0 |

7r. Height of the right ear aperture of the skull. Distance on the right side from the most ventral point, inside the anterior edge of the squamoso-occipital wing, visible just lateral to the postorbital process when the skull is viewed from in front, to the point where the anterior edge of the squamoso-occipital wing fuses with the skull.

8r. Distance on the right side from the point where the anterior edge of the squamoso-occipital wing fuses with the skull, to the edge of the orbit.

9l and 9r. Distance from the dorsal edge of the jugal bar to the ventral termination of the ear slit, inside of deflected edge, measured normal to the plane of the jugal bars.

10r. Distance on the right side from the dorsal edge of the jugal bar to the ventral border of the ear aperture of the skull, i.e. to the most ventral point, inside the anterior edge of the squamoso-occipital wing, visible just lateral to the postorbital process when the skull is viewed from in front, measured normal to the plane of the jugal bars.

11l. Distance on the left side from the dorsal edge of the jugal bar to the dorsal border of the ear aperture of the skull, i.e. to the point where the anterior-edge of the squamoso-occipital wing fuses with the lateral edge of the postorbital process, measured normal to the plane of the ugal bars.

11r. Distance on the right side from the dorsal edge of the jugal bar to the dorsal border of the ear aperture of the skull, i.e. to the point where the anterior edge of the squamoso-occipital wing fuses with the skull, measured normal to the plane of the jugal bars.

12l and 12r. Distance from the dorsal edge of the jugal bar to the dorsal termination of the ear slit, inside of deflected edge, measured normal to the plane of the jugal bars.

13l and 13r. Width of preaural fold at the level of the middle of the eye. Distance from bottom of the cavity between the preaural fold and sclerotic ring to the lateral edge of the preaural fold, measured parallel with the plane of the jugal bars.

## 6. Ear aperture in the skin, aural folds, and external ear cavities

(figures 1, 2, 3 and figure 5, plate 1)

### 6.1. *Ear aperture, or slit, in the skin*

The ear aperture, or slit, in the skin is bounded by the aural skin folds. Inside this slit lies the smaller ear aperture of the skull (figures 1, 2, 3 and figure 5, plate 1).

The ear slit in the skin is crescent shaped and bounded by a continuous fold of skin that forms the preaural flap, operculum, and the postaural flap. The left and right slits are of the same size, and the holes in the skin also are of the same form on the two sides. However, due to the asymmetry of the underlying skull bones, the postaural fold has a somewhat different orientation on the left and right side. As seen from in front, the ear slits therefore are skew. This distortion of symmetry of the slits is due entirely to the skull asymmetry.

Except for their somewhat different orientation due to the skull asymmetry, the left and right ear slits are symmetrically located relative to the skull. This can be clearly seen with reference to the eyes and the jugal bars (table 1, measurements 9l, 9r, 12l, 12r).

On both sides of the head the ear slit reaches ventrally approximately to the ventral edge of the lower jaw at a level *ca.* 2 mm anterior to the ventral tip of the postorbital process. Dorsally the slits reach to within *ca.* 3 mm of the level of the skull roof.

At about the middle of its height the anterior margin of the slit lies 2–3 mm anterior to the lateral edge of the postorbital process, thus exposing a 2 mm wide strip of the posterior

part of the sclerotic eye ring (posterior to the preaural skin flap). When the owl is alert, the postaural folds are drawn somewhat forwards so that the posterior margin of the slit comes to lie *ca.* 2 mm anterior to the most lateral border of the ear aperture of the skull. The dorsal and ventral corners of the ear slit curve anteromedially and almost half encircle the sclerotic eye rings.

The length of the ear slit is about 24.3 mm both on the left and right side (table 1, measurements 4l, 4r). This almost exactly equals the height of the skull which is 23.9 mm (table 2, measurement 15). In the alert owl the horizontal width of both the left and right ear slit is 4–5 mm at the level of the respective ear aperture of the skull.

### 6.2. *Preaural skin fold, or flap*

When handled, the aural folds in dead as well as in living owls are easily displaced from their natural positions. Further, the folds, particularly the postaural one, are equipped with muscles (cf. §7), and so are under the owl's control. Indeed, the position and orientation of the aural folds in *Aegolius* differ in various attitudes of the living bird.

It has been found that the position of the aural folds influences the directional sensitivity pattern of the ears (cf. §28). Therefore, the aural fold positions, pertinent to the ear function, are those seen in the owl when it is alert. The following description of the aural folds refers to conditions in the owl when attentive.

The preaural skin flap is sometimes called *operculum*. This designation is more appropriate in for instance *Tyto alba* and some *Strix* species, in which it is very large and distinct and overlaps the entire ear apertures in the skin and skull. In *Aegolius*, as in *Asio*, the fold is smoothly rounded and thus differs strikingly from the almost square flaps in some *Tyto* and *Strix* species.

In *Aegolius* the preaural flap is a feather-carrying fold of skin that originates just lateral to the eyes. It is directed posteriorly but has a laterally deflected, marginal rim.

At the eyes the inside of the preaural fold is free forwards right to the anterior edge of the sclerotic ring. Here the skin curves back and lines the sclerotic ring. The preaural flap rests loosely against the sclerotic eye ring. The flat cavities between the ear folds and the underlying skull structures, here the sclerotic ring, are termed *external ear cavities* (cf. §6.4). At the level of the middle of the eyes the width of the preaural flap, defined as the distance from its lateral edge to the bottom of the cavity underneath, is *ca.* 6.6 mm (table 1, measurement 13). Three millimetres of this distance lie on the deflected rim of the flap.

As seen from in front, the preaural flap is of about the same outline as the postorbital process. The flap is very thin and elastic. Along its periphery, however, there is a thick rim which is stiffened by feather calami of the marginal facial disk feathers. This stiffened rim is deflected laterally in the plane of the facial disk. Since carrying the peripheral facial disk feathers, this rim actually determines the facial disk plane. At the level of the eyes the marginal rim is *ca.* 3 mm wide. Towards the dorsal and ventral terminations of the ear slit, the width of the deflected rim reduces to *ca.* 2 mm. Above and below the eyes the rim of the flap curves somewhat forwards.

At the level of the middle of the eyes the laterally deflected rim of the preaural flap lies 2–3 mm anterior to the lateral edge of the postorbital process, thus exposing laterally the posterior part of the sclerotic ring. However, the ear slit is completely concealed by feathers of the facial disk and ruff.

As seen from in front the preaural flap overlaps the postorbital process, and hence the ear aperture of the skull, by *ca.* 2½ mm. Thus, as seen from in front, the preaural flap reduces the width of the ear aperture of the skull by about half.

The preaural flaps are bilaterally symmetrical.

### 6.3. *Postaural skin fold, or flap*

The feather-carrying skin covering the side of the head simply is folded back inwards behind the ear to form a postaural flap with a flat cavity underneath. The flap is directed forwards and has a laterally deflected, marginal rim.

The postaural flap is thin and pliable but not as much so as the preaural flap. Like the preaural flap, the postaural one has a thickened rim, about 2 mm wide, that is stiffened by feather calami. In the lower part of the flap, at about the level of the jugal bar, the deflected rim is wider, or *ca.* 3 mm. This rim is deflected laterally and is oriented about perpendicular to the median plane of the head. It forms the attachment of the anteriormost ones of the facial ruff feathers, and thus gives also the facial ruff an orientation perpendicular to the median plane of the head. Dorsal and ventral to the ear aperture in the skull the rim of the postaural fold turns anteromedially.

At the level of the eye, the width of the postaural fold is 5 mm, as measured from its anterolateral edge, inclusive of the deflected rim, to the bottom of the flat cavity underneath. At the bottom of the cavity the skin curves forwards and lines the skull. The postaural flap rests loosely against the skin that lines the skull.

The flap slides very easily in the anteroposterior direction. In the alert owl it is drawn forwards so that its deflected rim comes to lie *ca.* 2 mm anterior to the lateral border of the ear aperture of the skull (the anterolateral edge of the squamoso-occipital wing).

The postaural folds are bilaterally symmetrical. However, because they rest against the asymmetrical skull, the left postaural flap bulges out laterally in its ventral part, while the right one bulges out dorsally. This results in an askew appearance of the ear slits as seen from in front.

### 6.4. *External ear cavities*

Between the skin lining the skull and the continuous fold of skin that surrounds the external ear opening in the skin, there are flat cavities. At some places the skin fold lies closely against the skull, while at others there is a space in between. These flat spaces between the ear flaps and the skin that lines the skull are termed external ear cavities.

These cavities were included under the term '*the cavernum*' by Pycraft (1898, p. 259). This name, however, seems to have included also the outer part of the external auditory meatus, while the inner part of the meatus was called '*the cavernulum*'. Pycraft did not clearly define the transition zone between these parts. His division and terms will not be used here.

At the bottom of the external ear cavities the skin of the ear flaps curves back and lines the underlying skull bones. The skin over the ear structures inside the aural folds is very thin. It is not tightened but is wrinkled at places and slides easily over the skull structures below.

Dorsal to the ear aperture in the skin the cavity is *ca.* 3 mm deep, extending here dorsomedially over the skull roof.

The cavity under the preaural flap extends forwards to close to the anterior edge of the sclerotic ring and reaches a depth of *ca.* 3.6 mm.

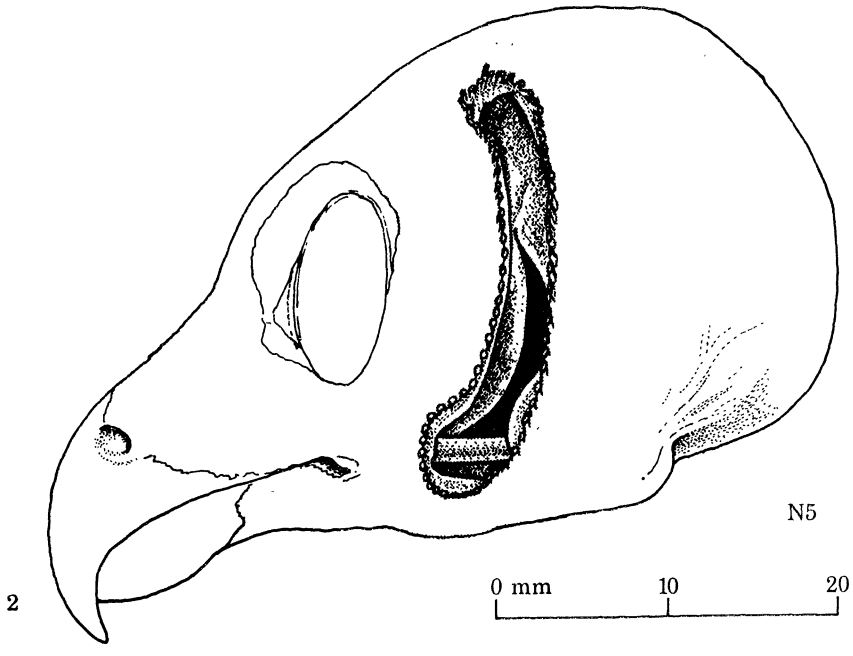


2

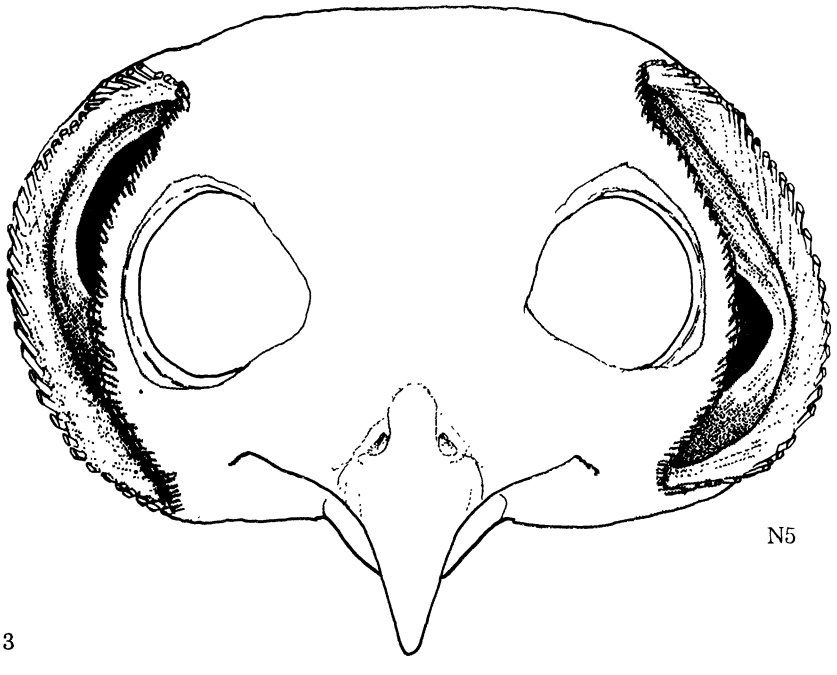


3

FIGURE 2. Lateral view of the head showing the ear slit in the skin and the extent of the external ear cavities (shaded) under the aural folds. The aural folds are drawn approximately in the positions that they are kept in the alert owl. The head is intact, but the feathers are cut. Only the cut feathers that form the edge row of the aural folds are drawn. The vertical median plane of the head is parallel with the plane of the figure. The scale is for figures 2 and 3.

FIGURE 3. Anterior view of the head. The horizontal plane of the head is normal to the plane of the figure. Otherwise as in figure 2.

Dorsal to the eye the cavity extends anteromedially right to the base of the supraorbital process that braces the dorsomedial surface of the sclerotic eye ring. The ear fold does not lie closely against the skull here, but leaves an open cavity. This is located over the concave transition area between the sclerotic ring and the frontal and orbitosphenoid bones posterodorsal to the orbit. The depth of the cavity that extends over the sclerotic ring is *ca.* 6 mm as measured anteromedially from the upper termination of the ear slit.

Ventral to the eye the cavity extends anteromedially approximately to the midline of the sclerotic ring. Here the skin curves back and lines the posterior part of the jugal bar and lower jaw, and closes the space between them. Also below the eye the cavity remains open. The depth of the cavity that extends below the eye is *ca.* 4 mm as measured anteromedially from the ventral termination of the ear opening in the skin. The cavity extends forwards to the oral angle, from which it is separated mainly by two layers of skin.

Ventral to the ear aperture in the skin the inside of the skin fold is free to just below and *medial* to the lower edge of the lower jaw. Here the skin curves back and lines the ventral and lateral aspects of the lower jaw.

The cavity under the postaural fold is *ca.* 3 mm deep. The flap is 5 mm wide, of which 2 mm comes on its deflected edge. This flap normally lies tightly against the squamoso-occipital wing and thus leaves no open cavity underneath.

The parts of the external ear cavity that are most open, and thus may be expected to be the acoustically most significant ones, are (1) the anterodorsal cavity extending above the sclerotic ring, and (2) the anteroventral cavity extending below the sclerotic ring and forwards along the jugal bar and lower jaw, right up to the oral angle.

Ventral to the right ear aperture of the skull there is a blind cavity bounded by the postorbital process, jugal bar, quadrate, and the anteroventral lobe of the squamoso-occipital wing. The cavity is *ca.* 4 mm deep. Posteriorly, and ventral to the lobe of the squamoso-occipital wing, the cavity is separated from the external auditory meatus by two layers of skin, one lining the cavity and the other the auditory meatus. This cavity is lacking on the left side of the head where the ear aperture of the skull lies immediately above the jugal bar.

The skin lining the anteroventral lobe of the left squamoso-occipital wing passes over at the ventral edge of the lobe and lines the jugal bar, lower jaw, quadrate, and the inside of the external auditory meatus.

The skin on the anteroventral lobe of the right squamoso-occipital wing passes over at the anteroventral edge of the lobe and lines the postorbital process and sclerotic ring, the inside of the external auditory meatus, and the blind cavity below the ear aperture, i.e. the postorbital process, quadrate, and jugal bar. The skin on the right lobe passes over to the postorbital process at a somewhat individually varying distance from the lateral edge of the postorbital process, depending on how close to the postorbital process the lobe lies.

Thus the skin covering the anteroventral lobe of the squamoso-occipital wing is continuous with that lining the adjacent jaw structures on the left side, and the postorbital process and sclerotic ring on the right.

## 7. Muscles of the ear folds (figure 4)

Muscles that control the ear folds originate on the skull bones or on connective tissue attached to the skull bones. The muscles are flat and passes between the skull and the overlying skin. Their insertion is in the skin, or in connective tissue attached to the skin, near the bottom of the external ear cavities.

There are numerous groups of muscle fibres under the skin at the ear slit. However, few are arranged into proper muscles. The most obvious groups of muscle fibres, and the ones that are easiest to locate, are described here.

Stellbogen (1930, p. 692) described three ear muscles in *Strix aluco* L. They differ from those in *A. funereus* in several respects. I therefore do not engage in homology questions here. The muscle designations used here are chosen in accordance with the positions of the muscles relative to the ear aperture in the skin.

### *Anterodorsal ear muscle*

*Origin.* At the posterodorsal edge of the orbit, just anterodorsal to the upper termination of the ear slit in the skin. The origin is along a *ca.* 5 mm long line oriented along the edge of the orbit, just dorsal to the sclerotic eye ring.

*Insertion.* At the bottom of the external ear cavity anterodorsal to the ear slit in the skin.

*Remarks.* This is a sheet of connective tissue containing muscle fibres. From the origin the fibres pass anterodorsally. The sheet is about 5 mm wide at the line of origin, and then widens distally towards its insertion at the bottom of the external ear cavity. It lies under the skin that covers the skull, and attaches to connective tissue at the anterodorsal corner of the external ear cavity above the sclerotic ring.

*Function.* The most dorsal part of the base of the preaural flap and the base of the ear fold anterodorsal to the ear slit in the skin are pulled posteroventrally by the muscle. Hence the muscle tends to displace the dorsal part of the slit posteroventrally.

### *Posterodorsal ear muscle*

*Origin.* On a distinct bony eminence *ca.* 3 mm posterodorsal to the orbit at the upper termination of the ear slit in the skin. This point of origin is located approximately symmetrically on the two sides. On the left side the origin is *ca.* 8 mm dorsal to the dorsal border of the ear aperture of the skull (the fusion between the anterior edges of the postorbital process and the squamoso-occipital wing). On the right side the origin is just dorsal to the ear aperture of the skull. The origin is by a short aponeurosis. The eminence for the muscle origin is further described in the developing skull (§ 9.1: 'Orbitosphenoid').

*Insertion.* Over a large area at the bottom of the external ear cavity under the postaural flap. The insertion is by fibres.

*Remarks.* This muscle is by far the largest and the best defined one of the muscles controlling the ear slit and flaps. That this is a large muscle is clearly indicated also by the distinct bony process that serves as area of origin. The muscle fibres spread fan-like posteroventrally. The area of insertion is located at the bottom of the external ear cavity under the middle part of the postaural flap. Fibres attach to the connective tissue under the overlying skin both in front of, and behind, the bottom of the cavity.

*Function.* The muscle pulls the skin behind the ear slit, and hence also the postaural flap,

anterodorsally. It thereby narrows the ear slit from behind. This is the most important muscle for the anteroposterior movements of the postaural flap.

*Posterior ear muscle*

*Origin.* In connective tissue that covers the squamoso-occipital wing. This connective tissue is tightly attached to the bone.

*Insertion.* At the bottom of the external ear cavity under the postaural flap.

*Remarks.* This is not a distinct muscle, but a group of muscle fibres passing posteriorly from their area of origin. The area of insertion is located ventral to that of the posterodorsal ear muscle.

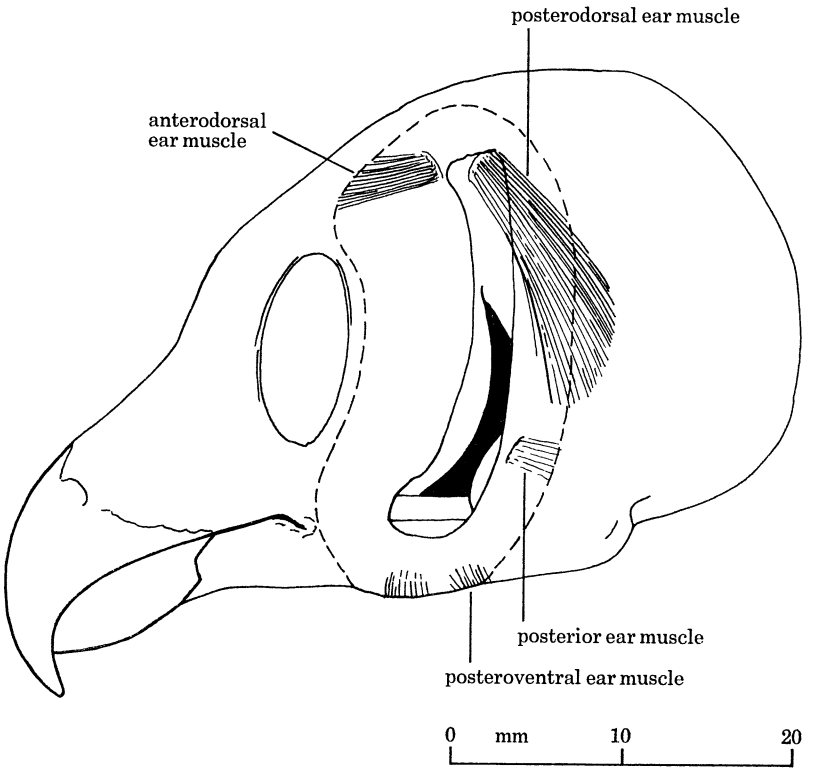


FIGURE 4. Lateral view of the head showing the largest muscles of the aural folds.

*Function.* The muscle pulls the postaural flap anteriorly, thus narrowing the ear slit from behind.

*Posteroventral ear muscle*

*Origin.* In connective tissue closely attached to the lateroventral edge of the posterior end of the lower jaw.

*Insertion.* In the bottom of the external ear cavity under the ventral part of the postaural flap.

*Remarks.* This is not a distinct muscle but sparsely distributed muscle fibres. From their origin on the lower jaw the fibres pass anterodorsally.

*Function.* The muscle fibres pull the ventral part of the postaural flap posteroventrally, and thus tend to widen the ear slit in this direction.

*Comments*

The function of the ear fold muscles is to move the ear folds. However, the movement repertoire of the flaps is very restricted. It mainly consists of relatively small movements towards or away from the ear slit in the skin, resulting in narrowing and widening of the ear opening in the skin. There seem to be no means by which the flaps could be raised. I have never seen any tendency to raising of the ear flaps. It is only when the postaural flap is pulled forwards that the facial ruff may push the peripheral feathers of the facial disk forwards, and thus slightly rise the preaural flap.

Except for the anterodorsal muscle at the dorsal base of the preaural flap, no distinct group of muscle fibres were found in connection with the preaural flap. When the preaural flap is folded forwards manually, it slowly resumes its ordinary, folded-back, position over the sclerotic ring. This seems to be due at least to a large extent to the elasticity of the flap.

Schwartzkopff (1962, p. 578) suggested that *movements* of the ear flaps might be important during the actual process of sound localization in *Asio otus* (L.).

As regards *A. funereus* I have observed three captive specimens and several wild ones in the field when they have localized sound. The observations involve normal hunting (Norberg 1970) and experiments with concealed sound sources (Norberg, unpublished). In no case have any movements been observed in the facial ruff and disk, which attach to the pre- and postaural flaps, respectively.

When localizing sound, *A. funereus* keeps the ear flaps stationary. The postaural flaps are pulled forwards so that their laterally deflected rims lie about 2 mm anterior to the lateral border of the ear aperture in the skull (cf. §6.3). In the alert owl the facial ruff becomes very prominent due to its forward position, and the face becomes very flat. The dorsal projections of the facial ruff above the head contour also become very obvious. The positions of the facial disc and ruff in the attentive owl appear from figures 5 and 6, plate 1 in this paper and from figures 1–7, on hunting owls, in Norberg (1970).

The muscles of the ear folds obviously are of importance for adjustments of the attitude of the ear folds. In this way the muscles most likely affect directional hearing. However, at least with *Aegolius*, there is no ground for thinking that the ear folds need to be moved during the actual process of localization of sound. The acoustic properties of the external ears important for directional localization thus should be evident in acoustic measurements with the ear flaps stationary.

## 8. Head plumage (figure 1 and figures 5–7, plates 1 and 2) (terminology adopted partly from Grossman & Hamlet (1964), partly from Lucas & Stettenheim (1972))

### 8.1. *Facial disk*

The facial disk is a rounded, rather flat disk of light greyish feathers set about radially dorsal, lateral, and ventral to the eye. The vanes of the feathers lie in the plane of the disk.

Dorsolateral and lateral to the eye there are about five, not very well defined, concentric rows of feathers. Ventrolateral to the eye about seven concentric rows of feathers are identifiable, some of which attach to the lower eye lid. Most of the facial disk feathers originate from the anterior surface and the laterally deflected marginal rim of the preaural flap. The calami of the peripheral disk feathers stiffen the deflected rim of the flap.

Above the eye the facial disk continues medially to about the anterodorsal termination of the ear slit. The dorsomedial margin of the facial disk is along a vertical line passing approximately through the middle of the eye when the head is seen from in front (figures 6 and 7, plates 1 and 2). The borderline is marked by a vertical, irregular strip of dark brown feathers. These belong to the facial ruff that curves down between the eye and beak. Further medially, a narrow c-shaped area of light grey feathers of the lore cover the facial ruff where it merges with the frontal tract feathers dorsolateral to the beak.

Below the eye the facial disk continues slightly farther medially than it does above the eye, and borders on the lore feathers lateral to the beak.

The facial disk feathers overlap the entire ear apertures in the skin and skull, and overlap also the facial ruff to about half its width.

The feathers in the facial disk are very specialized to be sound transparent. Their most characteristic features are that the rami are very sparsely set along the rachis, and that the radii are very short. The rami are rather long, making the feather rather wide. The rami of the facial disk feathers form a multi-layered, but delicate and sparse web in front of the ear aperture.

The feathers in the two peripheral rows of the disk are smoothly rounded in the tip. In the tip of the feathers in the third row from the rim of the flap, there are one to three fine, hairlike bristles, that are up to 11 mm long. They reach lateral to the facial ruff and lateral also to the outline of the head plumage as seen from in front. In the feathers further in on the flap these bristles become progressively shorter, as do the feathers themselves.

There is no trace of downy structures in the facial disk, not even at the base of the feathers.

### 8.2. *Lore*

The lore is the region between the beak and eye. It carries feathers that are more or less anteriorly directed, and that form a c-shaped configuration with the convex side against the beak.

The loral feathers are coarse and relatively stiff. In structure they resemble the facial disk feathers. However, the rami are much shorter and more closely set on the rachis. Hence the loral feathers are denser and narrower than the facial disk feathers.

In the feathers closest to the beak, the tip of the rachis is drawn out into a bristle, up to 6 mm long, that is coarser and stiffer than the ones in the third feather row of the preaural flap. These feathers are directed anteriorly and anterolaterally. The anterolaterally oriented ones curve forwards towards the tip. The bristles are grouped to either side of the beak like the vibrissae of a mammal. Presumably they serve the same function of tactile sense. This probably is the function also of the hairlike bristles of the facial disk feathers.

Dorsally and dorsomedially the lore feathers grade into the forehead feathers on the frontal tract. Ventrally they grade into the facial disk feathers.

The lore feathers do not seem to have any particular acoustic function.

### 8.3. *Facial ruff*

The laterally deflected anterior rim of the postaural flap carries extremely densely set feathers that form most of the facial ruff. Except for the anteriormost row, the facial ruff feathers differ strikingly from those of the facial disk. The ruff feathers are very dense and narrow.

The facial ruff feathers lie in planes that are about normal to the median plane of the head. The laterally deflected rim of the postaural flap, and the facial ruff feathers attached to it, form an anteriorly facing, concave wall.

Anteromedial to the upper termination of the ear slit in the skin the facial ruff curves sharply downwards in a direction just medial to the eye. Just above the eye a narrow brown strip of the facial ruff is visible between the facial disk and the lore feathers. It marks the dorsomedial border of the facial disk.

Dorsomedial to the eye the facial ruff grades into the forehead tract feathers. The frontal tract is a triangular area above the beak. It separates the left and right parts of the facial ruff above the beak. Hence the facial ruff is discontinuous above the beak.

Below the beak the chin feathers participate in forming the facial ruff. Hence the facial ruff parts of the left and right side are perfectly confluent below the beak.

The following description applies to the facial ruff at the level of the eyes.

On the edge of the laterally deflected rim of the postaural flap, there is a regular row of feathers that form the anteriormost layer of the facial ruff. The feathers in this first row are rather similar to the peripheral ones in the facial disk, the rami being almost as sparsely set on the rachis. However, the anteriormost feathers in the facial ruff are coarser and much stiffer than those in the facial disk.

Immediately behind this edge-row, on the posterior surface of the deflected rim of the postaural flap, there are feathers of an entirely different structure. They have much thinner rachises than the edge-row feathers. Further, the feathers are small, narrow, and very dense in structure. The rami are very closely set on the rachis, and the surface of the vane is smooth. The feathers behind the edge-row are extremely densely set. Over a 2.5 mm distance in the anteroposterior direction there are at least five (poorly defined) rows of feathers that participate in forming the anterior part of the ruff. These feathers attach mostly on the posterior surface of the laterally deflected rim of the postaural fold. Posteriorly the ruff feathers then grade into the ordinary soft, downy head feathers.

There is no trace of down in the ruff. Since the feathers in the ruff are very densely packed, and the vane of the feathers is dense and smooth with nothing of the downy structure otherwise characteristic to the owl plumage, it seems likely that the ruff reflects sound rather than absorbs it.

The very stiff but sparse feathers in the first row of the facial ruff form the most anterior feather layer in the ruff. They seem to have a function of fixing the anterior surface of the ruff and keeping the pliable ruff feathers behind in position.

The feather arrangement in the edge row along the entire fold surrounding the ear aperture in the skin (the pre- and postaural flaps included) will be described below.

---

## Description of plate 1

Figure 5. Topography of the face and external ear of *A. funereus*. Living, tame male in a moderately alert attitude. The facial disk is folded forwards to expose the ear opening and held forwards with the aid of a thread that is retouched in the figure. The owl apparently can not widen the ear slit in the skin by raising the preaural flap. 5 Jan. 1974. Photo: R. Å. Norberg.

Figure 6. (*a*) A wild *A. funereus*, in the field, immediately before striking a prey that was visible to the owl. The facial ruff is erected but kept stationary during auditory localization of prey and preparation for strike. The prey was a laboratory mouse that was released near the owl's nest (see Norberg 1970). 17 June 1968 at 23 h 50. (*b*) Frontal view of the head of *A. funereus*, showing the symmetry of the facial disks and the prominent facial ruff. A wild female in an alert attitude in the nest. 12 June 1974. Photos: R. Å. Norberg.

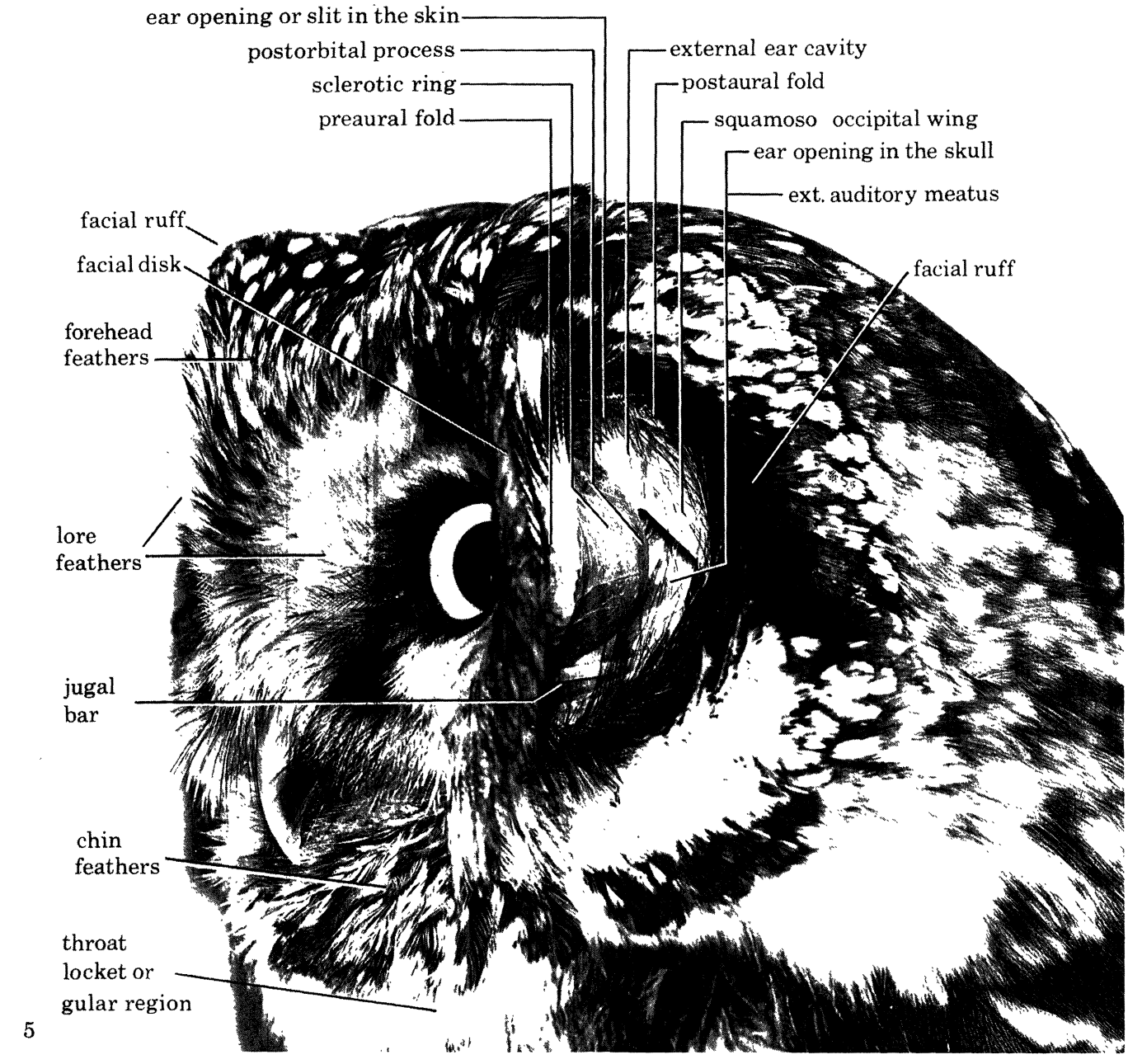


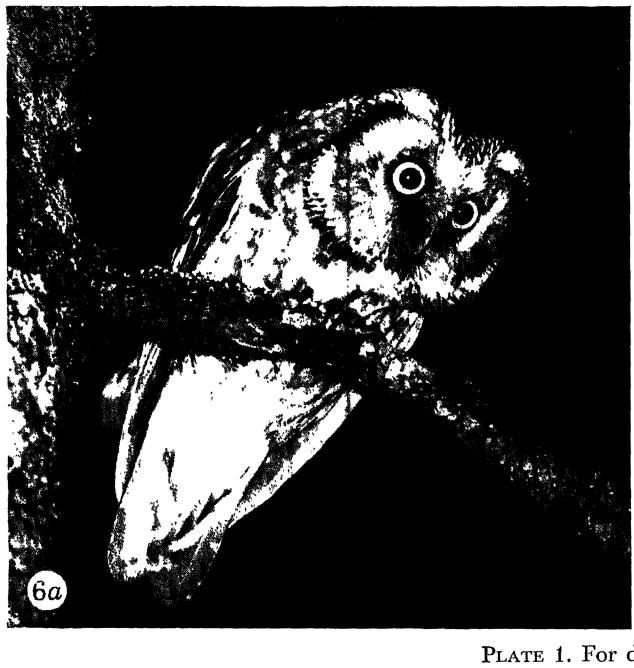


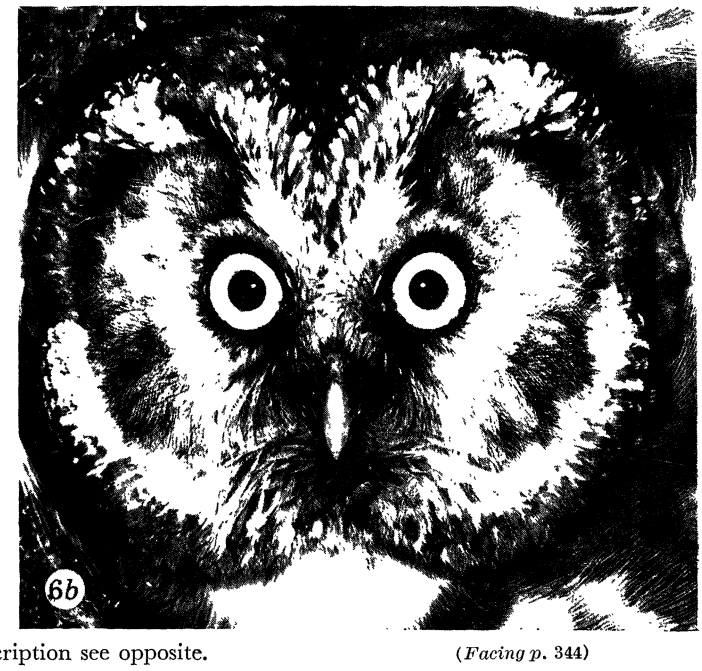


PLATE 1. For description see opposite. (*Facing p.* 344)

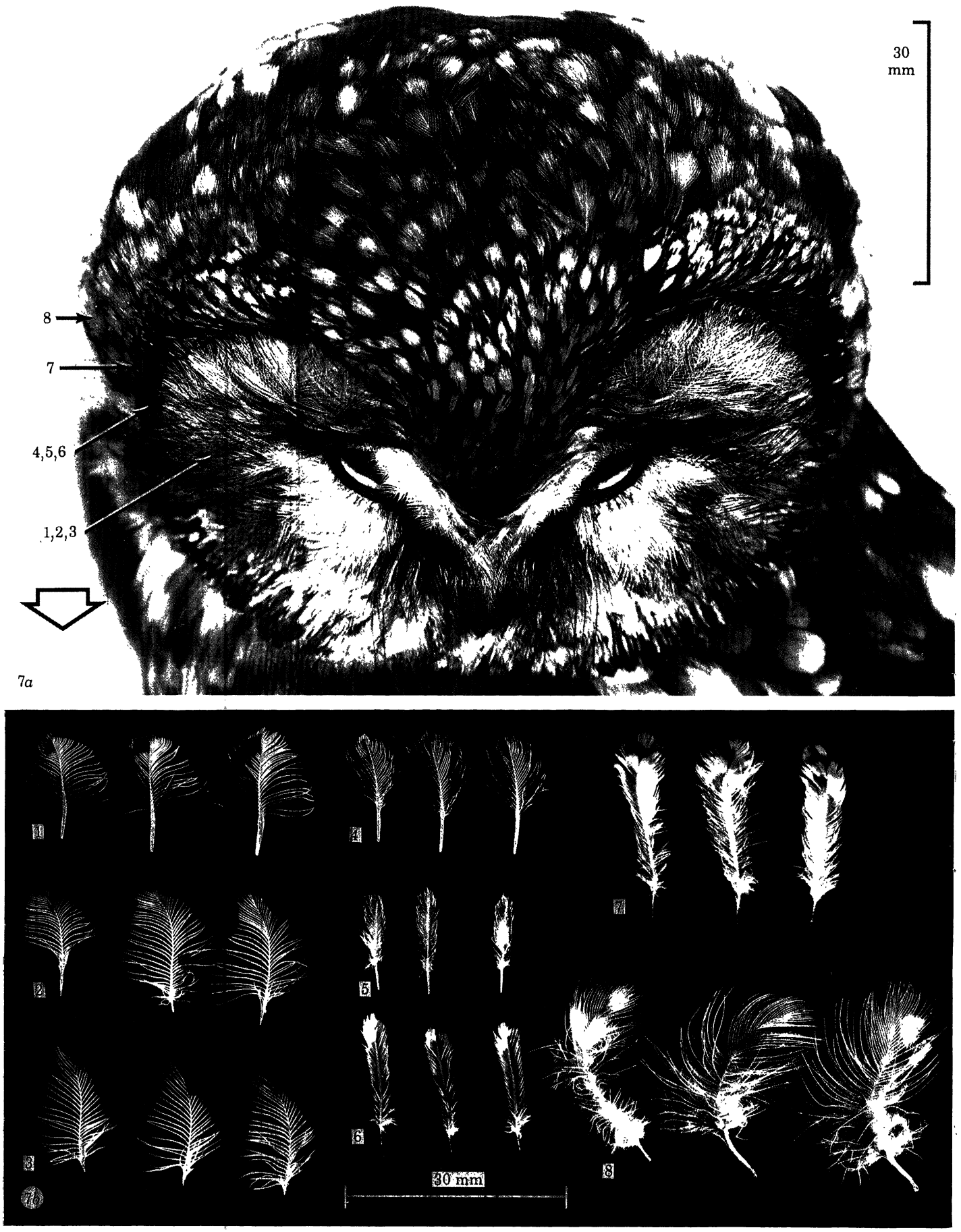


PLATE 2. For description see opposite.

The aural folds are thin but thickened and stiffened at the edge by feather calami. The feathers attached to the edge are set close together and form a regular row. Their orientation can be seen in figures 1, 5, and 6. They are directed dorsolaterally in the larger parts of both the pre- and postaural flaps. This is brought about by two changes of their angles of attachment.

1. In the preaural flap, at the level of the ventral side of the jugal bar, the feathers diverge. When the flap is folded forwards, the converging calami form a protrusion on the inside of the flap. Dorsal to this protrusion the feathers are directed dorsolaterally, and still at the dorsal part of the ear slit they keep about the same angle relative to the edge of the fold. This angle is retained also in the dorsal part of the fold's continuation behind the slit, i.e. in the postaural flap. Ventral to the protrusion at the jugal bar the feathers are directed ventrolaterally, and at the ventral part of the ear slit they keep about the same angle relative to the edge of the fold. This angle is retained in the larger part of the fold's continuation behind the slit, i.e. in the postaural flap.

2. In the postaural flap, at the level of the dorsal border of the right ear aperture of the skull, the feathers converge and cross. Ventral to this point the feathers are directed dorsolaterally, and dorsal to it they are directed posteriorly.

The facial disk feathers further in on the preaural flap are oriented in about the same way as those in the edge-row.

The facial ruff feathers behind the edge-row are oriented in essentially the same way as the edge-row feathers. However, their detailed arrangement deserves closer description.

In the lower part of the facial ruff all feathers are oriented like those in the front row, i.e. dorsolaterally, Likewise, all feathers in the dorsal part of the ruff are oriented like those in the front row, i.e. posteriorly. However, the transition zone as regards feather orientation is so constructed, that the ventral tract with dorsolaterally oriented feathers is wedge-shaped dorsally, and passes in front of the dorsal tract with posteriorly oriented feathers. The ventral tract thus tapers dorsally. Its upper termination is indicated by the most dorsal, dorsolaterally directed, edge-row feather. The dorsal tract with posteriorly directed feathers passes behind the ventral, wedge-shaped tract, and continues *ca.* 10 mm ventral to the point, where the front row feathers intersect. In the transition zone at the middle of the ruff, therefore, there are about five layers of feathers that are directed dorsolaterally, and behind these there are several layers of posterolaterally directed feathers.

Towards the tip the facial ruff feathers curve backwards, making the ruff smoothly rounded laterally.

The most dorsal part of the facial ruff is located right above the upper termination of the ear slit in the skin. When the owl is alert, this part of the ruff projects somewhat above the dorsal head contour. The left and right parts of the ruff therefore form two rounded eminences on top of the head.

---

## DESCRIPTION OF PLATE 2

FIGURE 7. (*a*) A tame male in an alert attitude with the facial ruff and disks in forward positions, making the face flat. 1973. (*b*) Feathers from the ear region of the right side. Facial disk feathers from 1. the edge row of the preaural flap, 2. the third row from the edge, and 3. the fifth row from the edge of the preaural flap (about the fourth row from the eye). Facial ruff feathers from 4. the edge row of the postaural flap, 5. the second row, and from 6. about the fifth row from the edge of the postaural flap. Figure 7*b*:7 shows feathers from the posterior part of the facial ruff and figure 7*b*:8 feathers from the side of the head, posterior to the facial ruff. Photos: R. Å Norberg.

These dorsal projections of the ruff are entirely different from the ear tufts possessed by some owls. The ear tufts are formed by modified, elongated forehead feathers. There is no trace of ear tufts in *A. funereus*.

### 8.4. *Frontal tract*

The frontal tract is a triangular feather area above the beak. It lies between the left and right parts of the facial ruff that curve down ventromedially towards the beak. The frontal tract forms a distinct break in the continuity of the facial ruff above the beak.

The frontal feathers are small and similar in outline to those in the posterior part of the facial ruff. However, they are not so dense in structure, nor as densely packed as the ruff feathers.

### 8.5. *Chin*

The chin is the area between the two branches of the lower jaw. It is densely covered with feathers that are directed ventrally. These feathers are similar to, but softer than, those in the posterior part of the facial ruff.

The chin feathers are so arranged as to make the facial ruff perfectly continuous below the beak.

## 9. The head skeleton

### 9.1. *The skull*

The extent and geometrical constellation of individual bones (as delimited embryonically) of the owl skull is known only fragmentarily and for very few species. Such information is not readily accessible, but can be ascertained from developing skulls only (with the exception of few bones).

The extent, boundaries, and positional relations of skull bones are of potential value for comparative osteology and owl classification. Therefore all skull and jaw bones, whose geometry was evident in the skulls examined, will be treated here. Special emphasis is put on clarifying which bones participate in the skull asymmetry. When no remark is made on symmetry conditions in the following bone description, this implies that no sign of bilateral asymmetry was seen.

In the young skulls examined, the asymmetry was not fully developed. Further, there is a possibility that the developing skulls examined and illustrated may have been deformed during the process of fixation, clearing, and staining. It is believed, however, that the possible deformation is slight and negligible.

The part played by various bones in the skull asymmetry is shown in illustrations of young birds, whereas the detailed asymmetry of the skull is most accurately and clearly shown in illustrations of adult birds (cf. §11). Indeed, the skull asymmetry develops gradually in the growing young and is still not completed at the age of about 30 days, when the young become fledged.

The terminology and sequence of bones follow those used by Jollie (1957), with few deviations in terminology. The few terminology questions pertaining to owls are commented upon in the respective bone description below.

*Basioccipital* (figures 8–11, plates 3 and 4)

The basioccipital is an unpaired, medial bone of a roughly triangular shape. Its ventral surface is somewhat concave. Its tapered posterior part underlies the occipital condyle. Laterally it abuts against the exoccipitals and anteriorly the basiparasphenoid. At its junction with the basiparasphenoid the basioccipital forms two eminences with their umbos spaced *ca.* 2 mm. These eminences are formed mainly by the basioccipital, the junction with basiparasphenoid lying about half way up on the anterior slope of the eminence. The tips of the cochleae lie immediately beneath these eminences.

Because the cochleae are extremely long in owls, their tips come to lie close together near the midline of the skull. Hence they are located at the junction between the basioccipital and basiparasphenoid instead of at the junction between the basioccipital and exoccipital as in birds like the chicken (*Gallus*) (Jollie 1957).

In *A. funereus* the basioccipital is rather thick in its anterior part where it abuts against the basiparasphenoid and the underlying parasphenoid, which is likewise rather thick. These bones are hollowed out to accept the medially curving tips of the cochleae that lie on the borderline between these bones and are embedded half in each of them.

The basioccipital is clearly distinguished in *ca.* 12 days old birds (figure 8, plate 3) but then fuses rapidly with surrounding bones. The sutures are virtually obliterated in 25 days old birds in which most other skull sutures are still evident.

*Exoccipital* (figures 8–14, 16, plates 3–6)

There is one exoccipital to either side of the basioccipital and foramen magnum. A pointed, medial extension of the exoccipital underlies the occipital condyle. Medially the exoccipital abuts against the basioccipital, posterolaterally against the squamosal and posterodorsally against the epiotic and supraoccipital. Ventrolaterally, the exoccipital forms a ventrally convex wing that vaults over the medial part of the tympanic membrane. Hence the exoccipital forms the terminal and medioventral walls of the external auditory meatus.

Following Lucas & Stettenheim (1972, e.g. figs 22, 24) I call this lateroventral wing of exoccipital the *paroccipital process*. This name was used by Stellbogen (1930) to designate also the *squamoso-occipital wing*. For distinctions used here see description of the latter process.

The paroccipital process gives way in the young bird to a cartilaginous wing that forms the outer wall of the external auditory meatus. This cartilaginous wing is supported also by other bones and later ossifies and is known as the *squamoso-occipital wing* (see below).

Deeper parts of the exoccipital form the posterior and ventral parts of the bony tympanic ring (supporting the tympanic membrane) (figures 10, 12) and the posterior part of the bony ridge, crossing the tympanic cavity and accommodating (in its prootic part) the internal otic process of quadrate.

The posterior air space of the middle ear extends under the lateroventral part of exoccipital, its opening lying lateral to the fenestra ovalis.

Although supporting parts of the squamoso-occipital wings that are strongly asymmetrical, there is no trace of asymmetry in the exoccipital.

*Supraoccipital* (figures 9, 10, 16, plates 3, 4 and 6)

In the youngest skull examined (figure 9) the supraoccipital forms one bone plate, and so it can not be told whether there are one or two ossification centres, a condition that seems to vary among birds (Jollie 1957, p. 396). The supraoccipital lies posterior to the foramen magnum and abuts dorsally against the parietals. Laterally, the supraoccipital leaves a wide gap to the squamosals, and here the epiotics fill in and participate in forming the posterior skull wall.

*Prootic* (*Petrosal*) (figures 10–12, plate 4)

The prootic is associated with the middle ear, the bony cochlea, and parts of the semicircular canals. It encloses the anterior part of the anterior vertical semicircular canal and the anterior part also of the horizontal canal. The fenestra ovalis, accommodating the footplate of bony stapes, lies on the boundary between the prootic and opisthotic. The prootic forms the dorsolateral rim of the fenestra ovalis, opisthotic the ventromedial rim.

The prootic also forms a part of the bony ridge that crosses the tympanic cavity. The elongated, curved articular surface against which the internal otic process of quadrate articulates, is formed by the prootic.

The entrance to the small posterior air space of the middle ear is located underneath the exoccipital and over the fenestra ovalis. The entrance thus is bounded dorsolaterally and laterally by the prootic, medially by the opisthotic.

There is a wide gap between the prootic and squamosal. This is the opening of the superior air space of the middle ear. The opening of the anterior air space is located under the tympanic ring and quadrate, and lateral to the prootic and opisthotic.

The sutures between the prootic and surrounding bones are fused in 25 days old birds.

*Opisthotic* (*Mastoid*) (figure 10, plate 4)

The opisthotic encloses parts of the posterior vertical semicircular canal. It forms the bone bridge between the fenestra ovalis and the intracochlear foramen. It thus forms the ventromedial rim of the fenestra ovalis and the dorsal boundary of the fenestra rotunda. The ventral rim of the fenestra rotunda is formed by the exoccipital (cf. §18).

*Epiotic* (figures 9, 10, 16, plates 3, 4 and 6)

One epiotic is located to either side of the supraoccipital. It encloses the posterior part of the anterior vertical semicircular canal and forms a distinct part of the external wall of the skull, lateral to the supraoccipital and posterior to the anterior vertical semicircular canal.

*Parasphenoid* (figures 8, 11, 12, plates 3 and 4)

In the youngest bird examined (*ca.* 12 days old) all ossification centres of the parasphenoid are fused except for the basiparasphenoid. The parasphenoid forms the anterior part of the skull base, the sphenoid rostrum and much of the ventral part of the interorbital septum. On its lateral sides it carries processes with articular facets against which the pterygoids articulate. These processes are well developed in 12 days old birds. The parasphenoid also forms the anteromedial part of the bony ridge that crosses the middle ear cavity. Thus it forms part of the middle ear groove into which the internal otic process of quadrate lies, the

bone flange ventromedial to this process, and also the anteroventral part of the bony tympanic ring (ventromedial to the body of quadrate). The junction between the parasphenoid and prootic lies at the tip of the internal otic process of quadrate.

The parasphenoid is hollow and thin-walled and contains the anterior air space and eustachian tube. The parasphenoid and basiparasphenoid form the carotid canal, which in its first part passes anteriorly near the bottom of the air space in the parasphenoid. The large cavity dorsal to the canal is the anterior air space, while the dorsoventrally flattened eustachian tube passes ventral to the canal and just underneath the ventral plate of the basiparasphenoid (figure 12).

The walls of the anterior air space (that extends into the sphenoid rostrum and there communicates with the contralateral air space) are formed by the parasphenoid.

The *basiparasphenoid* is clearly distinguishable in 12 days old owls but at 25 days it has fused almost completely with adjacent bones. It forms a ventral plate that covers part of the skull base. The basiparasphenoid forms the ventral wall of the eustachian tube, behind and in front of which it fuses with the parasphenoid. At its anterior fusion with the parasphenoid, the basiparasphenoid is drawn out ventrally into a narrow flange that is clearly discernible also in adult birds. Its anterior, medial tip covers the anterior, common opening of the eustachian tubes. The tips of the cochleae lie at the posterior margin of basiparasphenoid that forms the anterior fourth of the ventral eminences marking the position of the cochlea tips.

The posterolateral extension of the basiparasphenoid plate reaches to the lateroventral border of the middle ear cavity and participates in forming its bottom. The basiparasphenoid further forms a small part of the bony tympanic ring (figures 11, 12), and a small part also of the most medial bony wall of the inner part of the external auditory meatus. It bridges the gap between the parasphenoid part of the tympanic ring at the quadrate, and the anteromedial edge of the exoccipital wing (the paroccipital process) that supports part of the squamoso-occipital wing.

*Basisphenoid*

The basisphenoid forms the sella turcica, and in the specimens examined it was fused with the parasphenoid.

*Orbitosphenoid* (figures 13–15, plates 5 and 6)

In the youngest specimen examined, there is a trace of a suture between a dorsal and a ventral ossification centre.

During development the orbitosphenoid forms one narrow dorsal, and one wide ventral projection that extend anteromedially and take part in formation of the posteromedial wall of the orbit. The orbitosphenoid develops ventrally to abut against the parasphenoid, and posteriorly is somewhat overlapped by the squamosal. Posterodorsally it meets the anterior extension of the parietal and dorsally the frontal.

The orbitosphenoid forms the middle part of the posteromedial wall of the orbit and the entire postorbital process. It even continues somewhat behind the postorbital process before fusing with the squamosal. Hence the orbitosphenoid forms the dorsomedial wall of the outer part of the external auditory meatus.

*Asymmetry*. The posterodorsal parts of the orbitosphenoid are bilaterally asymmetrical.

On the left side the part of the orbitosphenoid located posterodorsal to the postorbital process, extends very markedly lateroventrally and supports the base of the anterior part of the squamoso-occipital wing. Dorsal to the squamoso-occipital wing there is a shallow depression (very obvious in some skulls, absent in others), and dorsal to this the orbitosphenoid merges smoothly with the parietal and frontal. About 3 mm posterodorsal to the orbit rim, there is a small eminence or tubercle that forms the point of origin of the posterodorsal ear muscle that moves the posterior ear flap. This eminence is located nearly symmetrically on the two sides and is formed in the region of fusion of the orbitosphenoid, squamosal, parietal and frontal (at the dorsal boundary of the fontanelle between these bones in figures 13 and 14). The tubercle is probably formed jointly by some or all of these bones.

On the right side the part of the orbitosphenoid located posterodorsal to the postorbital process, forms a laterally concave wall that is not associated with the squamoso-occipital wing. At the place where the left orbitosphenoid extends laterally to support the squamoso-occipital wing, the right orbitosphenoid forms a concave, medial wall in the outer part of the external auditory meatus. Dorsally, at its fusion with the parietal and frontal, the orbitosphenoid curves outward much more than on the left side. The region of fusion between the orbitosphenoid, parietal, and frontal forms a horizontal, very marked ridge that passes from the anterodorsal base of the squamoso-occipital wing and forwards to the orbit, which it reaches dorsal to the postorbital process. This ridge reaches farther laterally than the corresponding region on the left side. The tubercle for the posterodorsal ear muscle is located on or immediately dorsal to the anterior part of the ridge.

The asymmetry described for the orbitosphenoid is not very obvious in the young skulls examined and illustrated (figures 13–15). However, in the adult skull the asymmetry is very obvious, and the rôle played by various bones were found by comparison with their constellation and extent in young skulls.

In the skull illustrated in figures 13–14 the dorsal part of the orbitosphenoid is wider on the right side than on the left. However, in two other skulls the difference was negligible, so it is uncertain how consistent this point of the asymmetry may be.

*Squamosal* (figures 9–17, plates 3–6)

Posteroventrally the squamosal abuts against the exoccipital, posteromedially against the epiotic, posteromedially and dorsally against the parietal, and anteriorly it abuts against and slightly overlaps the orbitosphenoid. In its anteroventral part it forms an articular socket for the external otic process of quadrate. It forms the zygomatic process in front of the external otic process of quadrate, the postglenoid process behind it. The postglenoid process is slightly bifurcated, the anterior part lying against and supporting the otic process of quadrate, the posterior part curving down along the side of the body of quadrate, taking part in formation of the bony tympanic ring. The squamosal forms the dorsal part of the bony tympanic ring, from the quadrate (the posterior part of the postglenoid process) back to the exoccipital. It also forms much of the medial wall of the external auditory meatus.

The squamosal is hollow, its inner wall forming part of the braincase. The inside of the walls are strengthened by ridges and bony strands (trabeculae). This gives a characteristic, strongly reticulated appearance to the squamosal in the stained, developing skulls (figures 16, 17). The cavity inside the squamosal constitutes part of the superior air space of the middle ear. This cavity opens ventromedial to the squamosal part of the bony tympanic

ring, and dorsal to the internal otic process of quadrate and the bony ridge crossing the middle ear (prootic).

The squamosal forms, and supports, a large part of the squamoso-occipital wing as described below.

*Asymmetry.* The squamosals are strongly bilaterally asymmetrical, the asymmetry being associated with the position of the squamoso-occipital wings.

In all developing skulls examined, the squamoso-occipital wings are entirely cartilaginous. Along the base of these wings the squamosals form supporting, broad and laterally projecting ridges. The spongy, reticulated interior of the squamosals is clearly visible at these ridges, which look as if the squamosals had been cut along the base of the squamoso-occipital wing. This is clearly visible in figures 12–15 which show intact, developing skulls.

On the left side the lateral extension of the squamosal is located much lower than on the right. The lateral extension on the left side passes over to the orbitosphenoid near the dorsal base of the postorbital process. Because the squamosal curves outwards very low, this bone forms only a relatively small part of the dorsomedial wall of the external auditory meatus. This part of the wall is strongly concave.

On the right side the lateral extension of squamosal is located high. It runs in a much more dorsal direction than on the left side, and passes over to the parietal far posterodorsal to the orbitosphenoid. Hence the squamosal forms a large part of the medial wall of the right external auditory meatus. This medial wall is much less concave than in the left meatus.

Owing to the very different location and orientation of the lateral extensions of the squamosals supporting the squamoso-occipital wings, the skull becomes very skew. Its dorsolateral part is very strongly raised and laterally extended on the right side as compared to the left. Indeed, the most important, structural reason of the skull asymmetry lies with the different location and orientation of these lateral extensions of the squamosals, which form the base of the dorsal part of the squamoso-occipital wing.

The lateral extension of the squamosal is continuous, posteroventrally, with the lateral edge of the wing of the exoccipital (the paroccipital process) (figures 11–14), that supports the posteromedial and ventral part of the squamoso-occipital wing. The exoccipital part of the squamoso-occipital wing support is completely bilaterally symmetrical. The asymmetry of the wing-support is restricted to the squamosal, parietal, frontal, and orbitosphenoid bones.

*Parietal* (figures 9, 13–17, plates 3, 5 and 6)

The two parietals form the posterodorsal aspect of the skull. They fuse along the midline where a straight suture is formed in developing skulls. Posteriorly the parietal abuts against the supraoccipital and slightly overlaps the epiotic. Posterolaterally and laterally it borders on, and is overlapped by, the squamosal. Anterolaterally it meets the orbitosphenoid and anteriorly the frontal.

The parietal forms a narrow extension that passes anterolaterally between the squamosal and frontal, and contacts the dorsal part of the orbitosphenoid behind the orbit. In 25 days old birds there still remains a large fontanelle between the parietal and orbitosphenoid, bounded also by the squamosal posteriorly and the frontal anteriorly.

The anterolateral extension of the parietal is hollow and contains the anterodorsal extension of the superior air space. This penetrates farther anterodorsally on the right side than on the left.

*Asymmetry*. The parietals are bilaterally asymmetrical in their anterolateral extensions.

On the left side the anterior part of the squamoso-occipital wing attaches to the squamosal and orbitosphenoid, and thus is not associated with the parietal. The parietal participates in forming a rounded surface dorsal to the wing.

On the right side the anterior part of the base of the squamoso-occipital wing originates from the anterior part of the anterolateral extension of parietal. The lateral part of the right skull roof is raised relative to the left one and also projects farther laterally. The parietal forms the most anterolateral part of this extension. The parietal continues somewhat anterior to the dorsal base of the wing, and here participates in forming the ridge passing from the dorsal border of the ear aperture to the edge of the orbit. The ridge is formed jointly by the parietal, frontal, orbitosphenoid, and squamosal. This ridge is absent, or only weakly marked on the left side.

*Frontal* (figures 9, 13–17, plates 3, 5 and 6)

The two frontals form the dorsal and anterodorsal roof of the skull, the supraorbital rim, the dorsal part of the postorbital wall, and the dorsal part of the interorbital septum. The frontals fuse along a rather straight line on the skull's midline. Over the middle of the orbit the frontal forms a wide, lateral, supraorbital process, against which the anterodorsal aspect of the sclerotic ring lies (figures 19–24).

The frontal abuts against the orbitosphenoid posterolaterally and in the orbit, and against the parietal posteriorly. Anteriorly it overlies the mesethmoid and is overlapped by the posterior, strongly irregular edge of the nasal.

As with the parietal, the frontal is thin-walled in developing skulls, but in the adult bird is thick, multilayered, and spongy. On top of the skull roof of adult birds about five very thin bony membranes can be distinguished between the thicker outer and inner walls. They are oriented approximately parallel with the external skull wall and the brain case. All are connected via very thin bony strands. Thus the spongy skull roof consists of about six concentric layers of tiny air spaces. The small air spaces communicate laterally, whereas there is virtually no communication through the concentric layers. The frontals are very thick and spongy also in their anterior parts and here form a swollen forehead that bulges over the nasals. It is separated from the nasals by a deep horizontal notch. In developing skulls the frontals are thin and form a smooth transition with the nasals.

In the midline of the dorsal surface of the adult skull there is a longitudinal furrow that is most marked between the supraorbital processes.

*Asymmetry*. The frontals are bilaterally asymmetrical in their posterolateral parts, which are involved in formation of the lateral part of the skull roof. The part played by the frontals in the skull asymmetry is very small. It is essentially that the frontal participates in forming a lateral ridge on the right side, between the dorsal border of the ear aperture and the orbit. This ridge is absent, or nearly so, on the left side.

*Squamoso-occipital wing* (figures 8, 9, 13–16, plates 3, 5 and 6)

The squamoso-occipital wing is a thin, strongly curved bony wing that vaults over the external auditory meatus, and forms its outer wall. It is rather solid, consisting of spongy bone only in the anterior edge of its anteroventral lobe. The boundary between the squamoso-occipital wing and the bones supporting its base is defined by the zone of transition between

8

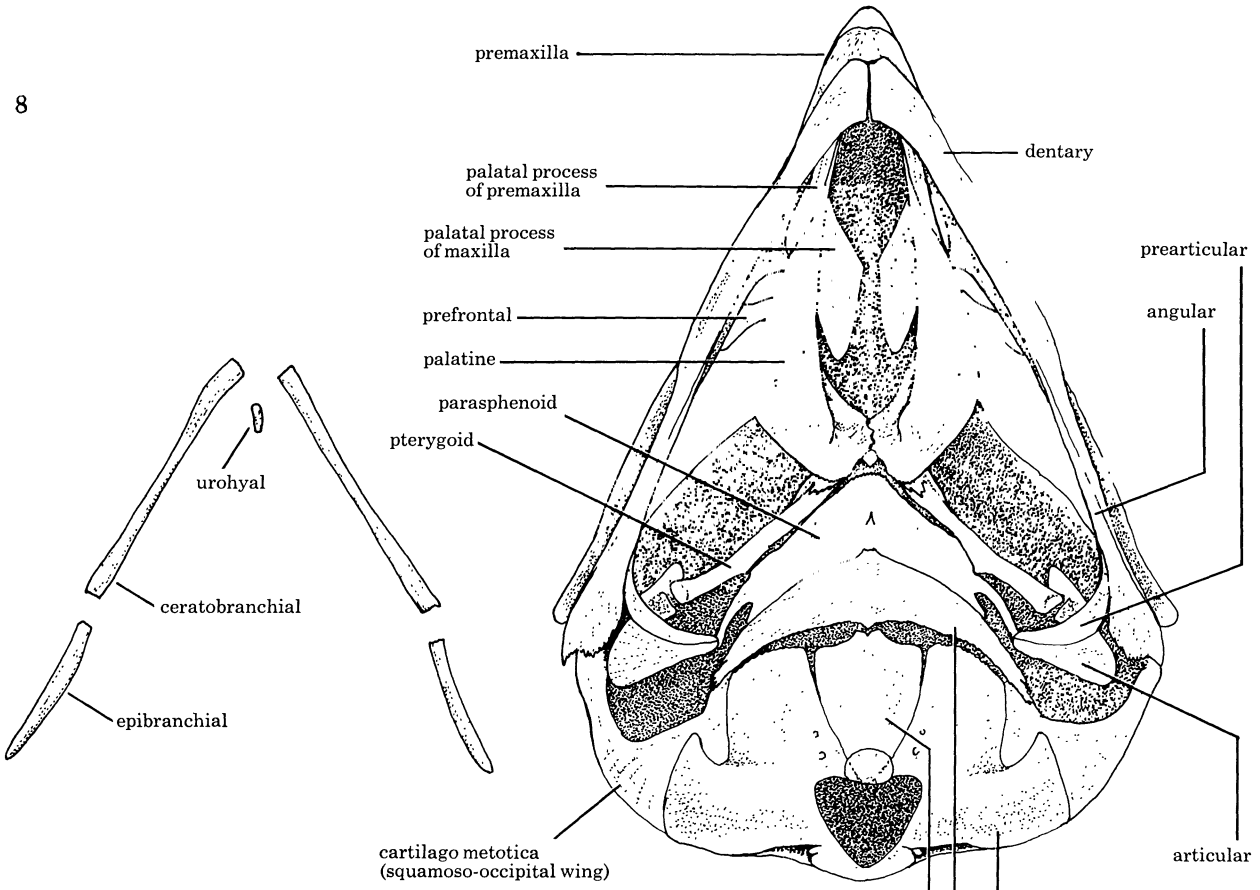


9

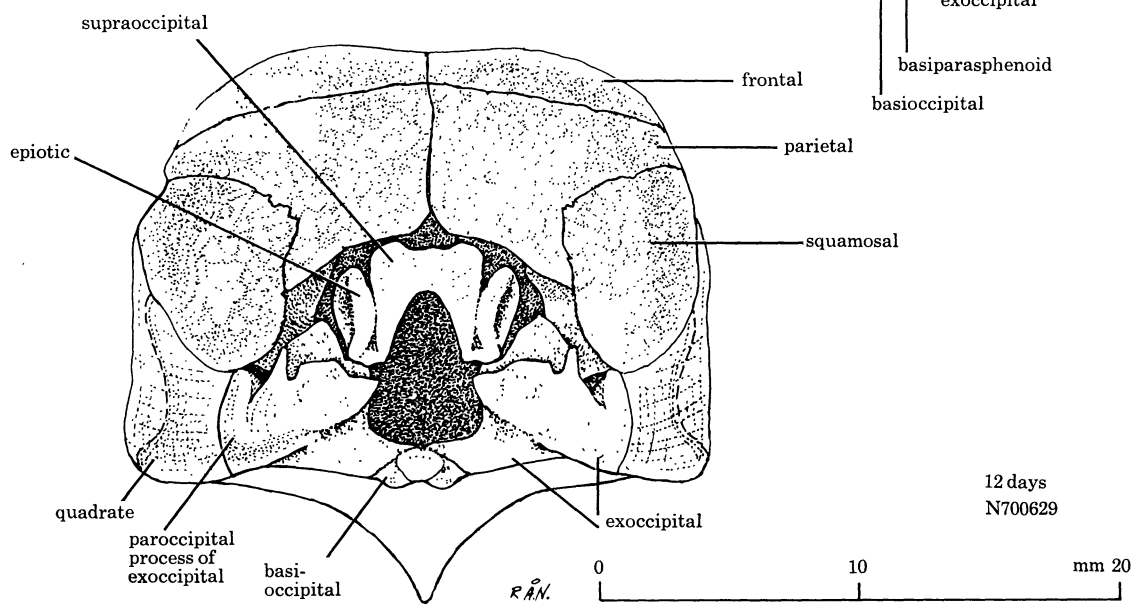


FIGURE 8. Ventral view of the skull of a *ca.* 12 days old young. The plane of the jugal bars is parallel with the plane of the figure. To the left is the hyoid apparatus. Figures 8–17 are drawn of cleared skulls stained with alizarine red.

FIGURE 9. Posterior view of the same skull as in figure 8. The plane of the jugal bars is normal to the plane of the figure. The scale is for figures 8 and 9.

(*Facing p.* 352)

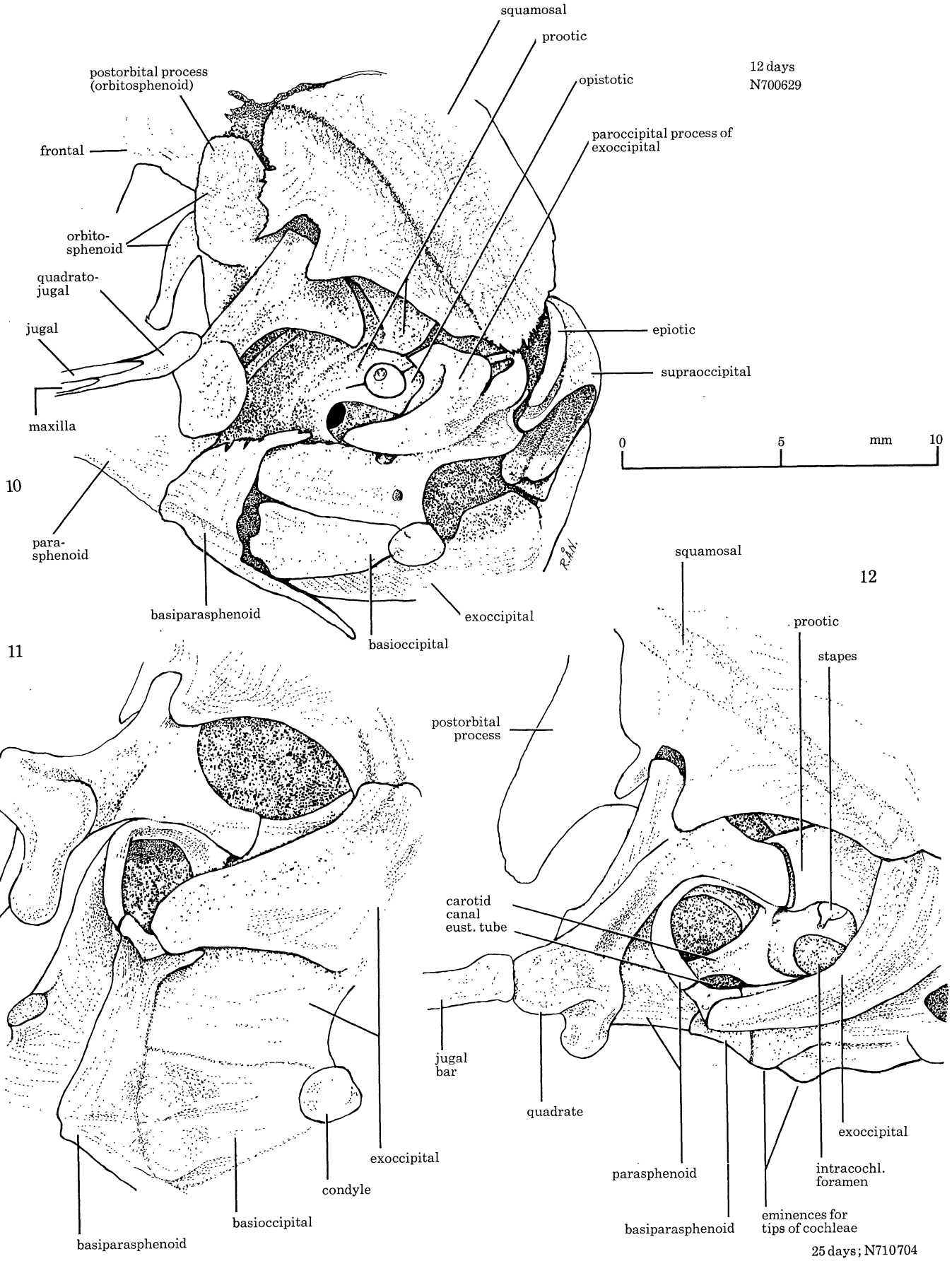


PLATE 4. For description see opposite.

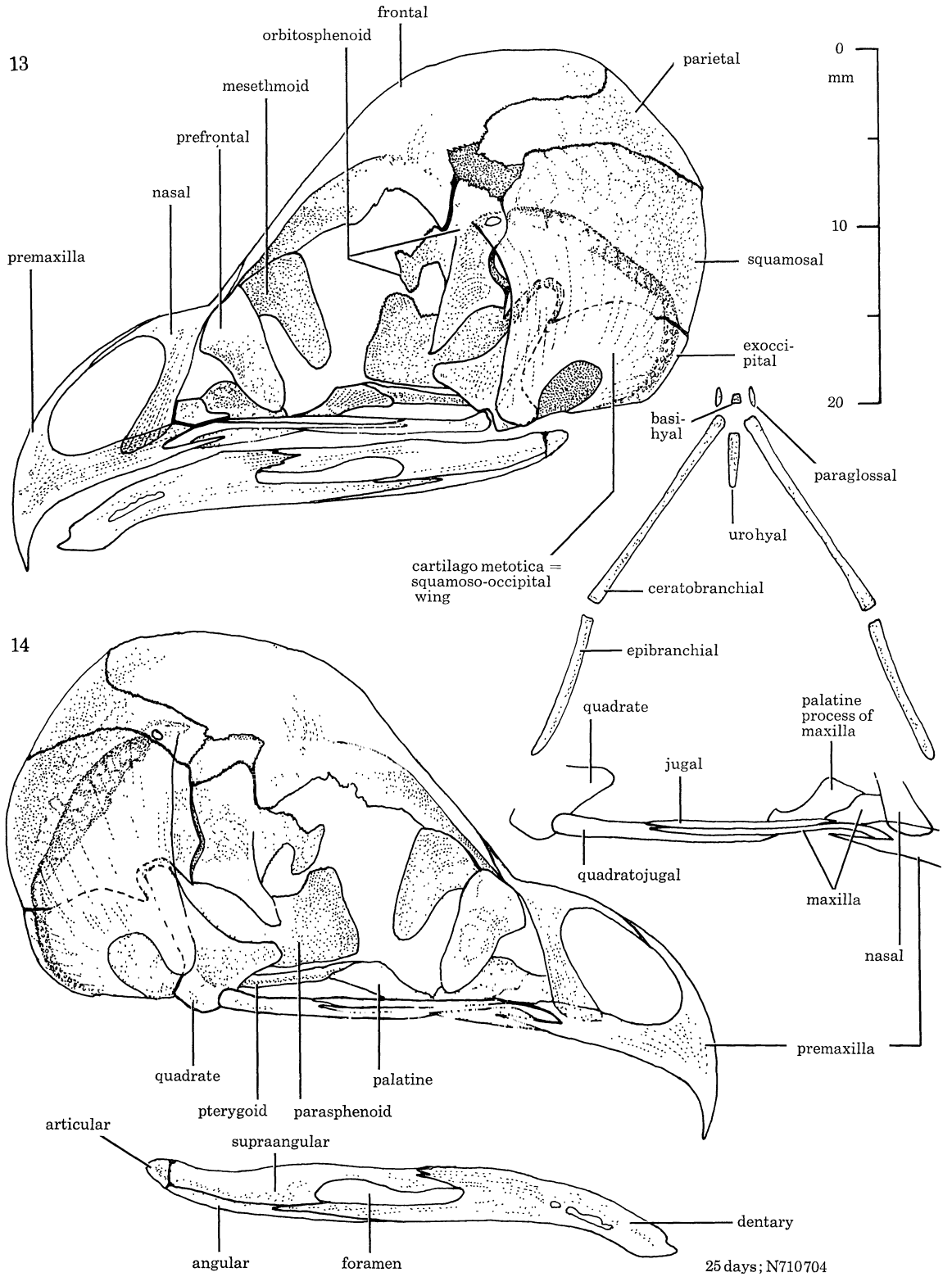


FIGURES 13 and 14. Lateral views of the skull of a *ca.* 25 days old bird. The vertical median plane of the head is parallel with the plane of the figure. The hyoid apparatus is shown in ventral view to the right. A part of the upper jaw of the right side is drawn separately to the right of the lower figure. All figures drawn to the same scale.

## DESCRIPTION OF PLATE 4

FIGURE 10. The left ear region of the skull of a *ca.* 12 days old young, seen from a lateroventral and somewhat posterior direction (the same specimen as in figures 8 and 9). The scale is for figures 10–12.

FIGURE 11. The left ear region of the skull of a *ca.* 25 days old young, seen from a lateroventral direction. This skull is seen from a more ventral direction than that in figure 10.

FIGURE 12. The left ear region of the same skull as in figure 11, seen from a lateral, and somewhat posteroventral direction.

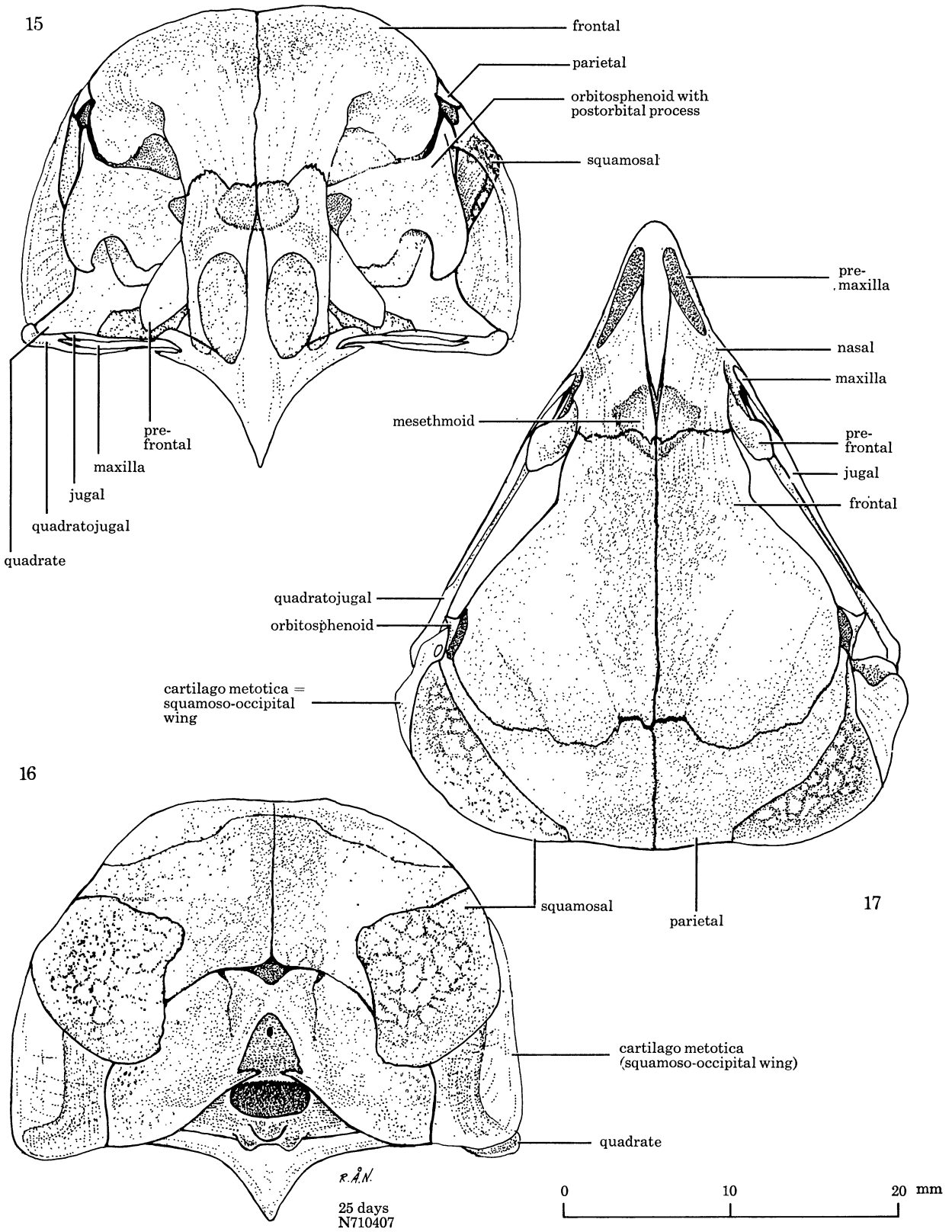


FIGURES 15–17. Skull of a *ca.* 25 days old bird (the same as in figures 13 and 14). The plane of the jugal bars is normal to the plane of the figure in figures 15 and 16, and parallel with it in figure 17. The scale is for all three figures.

the relatively solid structure of the wing and the highly pneumatized structure of the supporting bones (see below).

The term squamoso-occipital wing is adopted from Pycraft (1903, pp. 8, 44), and was used also by Lucas & Stettenheim (1972, figs 22, 24). This process, or part of it, has also been termed '*crista*' of '*os squamosum*' (Collett 1871), '*tympanic wing of the squamosal*' (Pycraft 1898, p. 274), '*tympanic wing of the exoccipital*' (Pycraft 1903, p. 3), and '*the squamoso-parietal wing*' (Pycraft 1903, p. 8). Stellbogen (1930) called the whole wing '*Processus paroccipitalis*' in adult *Strix aluco*. This term has been restricted here to mean only the lateroventral wing of the exoccipital. The boundary between the paroccipital process and the squamoso-occipital wing is taken to be the line of transition between the very pneumatized bone proximally and the relatively solid bone of the wing. Ossification is early proximal to this line, very late lateral to it.

In all developing skulls examined, the squamoso-occipital wing was entirely cartilaginous. This cartilaginous wing was called '*Cartilago metotica*' in young *Strix aluco* by Stellbogen (1930) and May (1961).

It ossifies late, and at the age of *ca.* 30 days, when the young leave the nest, the squamoso-occipital wing is still soft and somewhat flexible. When ossified, the wing bulges much farther laterally than in the developing skull, thus making the ear aperture of the skull wide.

As noted under the respective bones above, the left squamoso-occipital wing attaches to the exoccipital, squamosal, and orbitosphenoid. On the right side it attaches to the exoccipital, squamosal, and parietal.

The skull asymmetry is largest at the base of attachment of the squamoso-occipital wing. It is described further in §13.

*Nasal* (figures 13–15, 17, plates 5 and 6)

The nasal strongly overlaps the frontal posteriorly, contacts the prefrontal posterolaterally and the premaxilla anteromedially. It overlies much of the mesethmoid. It sends a latero-ventral process down behind the narial aperture. This process is laterally flattened and lies medial to the ventrolateral plate of the premaxilla and lateral to the maxilla underneath.

*Prefrontal* (figures 13–15, 17, plates 5 and 6)

The prefrontal is an elongated, swollen, highly pneumatized bone projecting down from the anterior roof of the orbit. It contacts the frontal and nasal dorsally. Ventrally it abuts against, but does not fuse with, the jugal bar and the posterolateral part of the palatal process of the maxilla. In the adult skull the posterolateral aspect of the prefrontal is concave to fit against the sclerotic ring whose ventromedial part rests firmly against it.

*Mesethmoid* (figures 13–15, 17, plates 5 and 6)

The mesethmoid lies medially in the anterior part of the orbit roof. It consists of a dorsal plate and a ventral, laterally flattened process. The dorsal aspect of the plate is parallel with the overlying, flat parts of the frontals and nasals. The tip of the narrow, posterior extension of the premaxilla overlaps the anterior part of the mesethmoid plate. In developing skulls a part of the mesethmoid plate is exposed dorsally through the wide sutures between the two nasals and the premaxilla. However, the entire plate is clearly visible through the thin, membraneous overlying bones in developing skulls. In the adult skull this region is partly

covered by the swollen forehead (frontal). The ventral process is laterally flattened and lies medially, forming part of the interorbital septum.

*Premaxilla* (figures 8, 13–15, 17, plates 3, 5 and 6)

In the developing skulls examined, the premaxillae had already fused medially. They form one posteriorly pointed process along the culmen of the beak (the nasal or frontal process). It passes between the nasals and overlaps the anterior part of the dorsal plate of mesethmoid. Below the narial aperture it sends a laterally flattened labial process backwards. It passes lateral to the nasal and maxilla. Posteriorly this process splits into a dorsal and a ventral part clasping the jugal bar. Medial to the labial process the elongated, dorsoventrally flattened palatine process projects backwards and contacts the anterolateral side of palatine. The palatine process is fused with the palatine and maxilla in adult birds.

*Maxilla* (figures 8, 13–15, 17, plates 3, 5 and 6)

The maxilla is a bone of complex shape. It forms one mass of spongy bone just medial to the lateroventral process of the nasal, behind the narial aperture. Its palatine process lies dorsal to the palatine and extends medial to it where it forms a ventrally flattened plate. The medial edges of the palatine processes are parallel and spaced *ca.* 0.5 mm. The palatine process of maxilla remains dorsal to the palatine and separated from it, except for its anterolateral end which is fused with the palatine in adult birds. The posterolateral part of the palatine process (dorsal to the palatine) is swollen and highly pneumatized. It makes broad contact with, and braces the medioventral aspect of the prefrontal. The maxilla also sends a long slender labial process backwards. It participates in forming the jugal bar. The process is dorsoventrally flattened anteriorly and here forms most of the jugal bar. The process tapers posteriorly and there lies lateral to the quadratojugal and ventral to the jugal.

*Jugal* (figures 10, 13–15, 17, plates 4–6)

The jugal is a distinct but thin splint of bone lying against the dorsolateral aspect of the quadratojugal and making contact ventrally with the labial process of maxilla.

*Quadratojugal* (figures 10, 13–15, 17, plates 4–6)

The quadratojugal makes up the largest part of the jugal bar and alone forms the posterior part of this bar with the articulation with the quadrate. It extends anteriorly to the level of the frontonasal hinge.

The labial process of maxilla, the jugal, and the quadratojugal are fused in the adult skull and form the *jugal bar* (also called the *labial*, *zygomatic*, *suborbital* and *quadratojugal arch*). The jugal bar is laterally compressed along most of its length, its dorsal edge lying somewhat lateral to its ventral. In its most anterior part, however, at its fusion with the main part of the maxilla, the jugal bar is strongly dorsoventrally flattened. This part is formed by the labial process of maxilla and lies ventral to the frontonasal hinge.

The dorsoventral compression of the jugal bar facilitates the kinetic rotation of the upper beak by allowing elastic deformation of the anterior part of the jugal bar when the upper jaw rotates about the frontonasal hinge.

*Quadrate* (figures 10–15, plates 4–6, and figures 35, 37, 38, 40, 41)

The quadrate articulates lateroventrally with the jugal bar, ventrally with the lower jaw, and medioventrally, at the base of its orbital process, with the pterygoid. The orbital process projects into the bottom of the orbit. The upper termination of the body of quadrate forms the external otic process that articulates in a socket of the squamosal (figure 38). The slender internal otic process juts out normal to the posteromedial aspect of the body of quadrate. It lies in a groove in the middle ear and with its apex articulates with the elongated articular surface (of prootic) terminating the groove posteriorly (figures 10–12, 38, 39). The articulations of the two otic processes thus are widely separated. The external one lies just in front of the eardrum in the medial wall of the external auditory meatus, the internal one in the middle ear cavity. The quadrate is pneumatic, its air space communicating with the middle ear via a foramen, located ventral to the base of the internal otic process.

*Pterygoid* (figures 8, 13, 14, plates 3 and 5)

From its articulation with the posterior end of the palatine the pterygoid extends posterolaterally. Its other end articulates with the quadrate at the base of the orbital process of quadrate. Near the middle of its length there is a distinct, medial process with an articular surface. This articulates against the articular surface of the articular process for the pterygoid on the lateral side of the sphenoid rostrum (parasphenoid).

*Palatine* (figures 8, 13, 14, plates 3 and 5)

The two dorsoventrally flattened palatines fuse medially along their posteromedial ends below the interorbital septum. The palatine extends forwards and lies ventral to the palatine process of maxilla with which it makes contact anteriorly. In the adult bird the anterior part of the palatine is fused with the most anterior part of the palatine process of maxilla and with the medial edge of the palatal process of premaxilla.

*Vomer*

The vomer is rudimentary. In the adult bird it forms a medial, membraneous, small bony sheet. Its posterior part lies ventral to the posteromedial fusion between the two palatines. It extends forwards between the palatines.

*Sclerotic eye ring*

The two rings of one skull (G 7910) were composed of 15 and 16 plates respectively.

The dorsomedial surface of the sclerotic eye ring lies against the ventral side of the superior orbital process and the roof of the orbit. The ventromedial surface rests against the prefrontal. The posterior rim of the ring rests ventromedially against the anterolateral edge of the lateral process of the interorbital septum, dorsally against the orbit roof, and laterally against the lateral margin of the postorbital process. All the skeletal structures associated with, and supporting the sclerotic eye rings exhibit bilateral symmetry.

### 9.2. *The lower jaw*

*Articular* (figures 8, 13, 14, plates 3 and 5)

The articular is a dorsoventrally flattened, triangular, and ventrally convex plate that forms the lower jaw's articulation with the quadrate. The articular forms the posterior margin

of the lower jaw and alone constitutes the retroarticular process, without support from the angular and supraangular (figure 8).

The medial process of the articular reaches with its tip *ca.* 2 mm anteromedial to the anteromedial rim of the bony tympanic ring. On the dorsal side of the process, *ca.* 2 mm from its tip, there is a small foramen to the interior cavity of the pneumatized posterior part of the lower jaw. This foramen lies just underneath a small foramen in the anteromedial rim of the bony tympanic ring. A tube of connective tissue (no ossification noted) connects these foramina, and so the lower jaw cavity communicates with the middle ear.

*Angular* (figures 8, 13, 14, plates 3 and 5)

The angular forms the ventral margin of the posterior part of the lower jaw. Posteriorly it is widened to a plate that contacts the prearticular and articular posteromedially. It tapers anteriorly and passes along the ventromedial edge of the jaw, on to the level of the anterior rim of the jaw fenestra. This anterior part is wedged between the dentary (lying laterally) and the splenial (lying medially).

*Supraangular* (figures 13, 14, plate 5)

The supraangular forms the dorsal margin of the posterior part of the lower jaw. It contacts the angular posteroventrally and lies medial to the posterior tip of the lateroventral process of the dentary. Anterodorsally it is wedged between the lateral plate and the dorsomedial process of the dentary. An elongated fenestra (the anterior mandibular, or lower jaw, fenestra) is formed between the anterior part of the supraangular and the dentary.

*Dentary* (figures 8, 13, 14, plates 3 and 5)

The dentary forms the anterior part of the lower jaw. Posteroventrally it forms the ventral border of the jaw fenestra and lies lateral to the angular and supraangular. Posterodorsally it forms a lateral plate and a medial process with the anterior part of the supraangular in between. The medial symphysis between the left and right dentary is distinct in 12 days old birds but almost obliterated already at 25 days of age.

*Prearticular* (figure 8, plate 3)

The prearticular is a small but distinct bone in the posteromedial part of the lower jaw. It covers part of the medial aspect of the jaw behind its fenestra. It contacts the angular ventrally and the supraangular dorsomedially. Posteriorly it curves medially and forms a thin plate that covers the anterior part of the articular and its medial process.

The prearticular was reported as missing in owls by Marinelli (1936), following Stresemann (1934) (cited from Jollie 1957, p. 429).

*Splenial*

The splenial forms a thin sheet of bone covering the medial aspect of the dentary anterior to the lower jaw fenestra. It sends a short process posteriorly above the fenestra and a long one below it, thus forming the anterior and ventral margins of the fenestra. The long ventral process lies mediodorsal to the angular and reaches to the posterior margin of the jaw fenestra.

*Coronoid*

I found no trace of a coronoid.

### 9.3. *The branchial skeleton*

*Bony stapes* (figure 10, plate 4)

The bony stapes is ossified in the youngest bird examined (12 days). It is described further in §19.

*The hyoid apparatus*

The terminology followed is that used by Lucas & Stettenheim (1972) in their figs 7, 9, and 24.

*Paraglossal* (figure 13, plate 5)

There is no trace of ossification of the paraglossal in 12 days old birds. At the age of 25 days there is one small ossification centre to each side of the basihyal.

*Basihyal* (figure 13, plate 5)

As with the paraglossal, the basihyal begins to ossify between the 12th and 25th day. It eventually articulates with the ceratobranchials and urohyal posteriorly, and with the paraglossals anteriorly.

*Ceratobranchial* (figures 8, 13, plates 3 and 5)

The ceratobranchial is well ossified at 12 days of age. It articulates with the epibranchial posteriorly, and eventually with the urohyal and basihyal anteriorly.

*Epibranchial* (figures 8, 13, plates 3 and 5)

The epibranchial is well ossified at 12 days of age. It articulates with the ceratobranchial anteriorly.

*Urohyal* (figures 8, 13, plates 3 and 5)

The urohyal has begun to ossify in 12 days old birds. It lies medially and posterior to the anterior ends of the ceratobranchials.

## 10. Linear measurements of skulls

The following linear measurements were taken on intact skulls. The linear dimensions are numbered 7, 8, 10, 11, and 14–19. They are defined as follows and as indicated in figures 1 and 18. Except when otherwise stated, the measurements are direct ones. An 'l' after the dimension number denotes the left side, an 'r' the right side. Results are given in table 2.

7l, 7r, 8r, 10r, 11l, and 11r are taken in the same way as those with the same numbers taken on intact ears as described in §5 and figure 1. The measurements with these numbers taken on intact ears (with soft parts intact) are given in table 1, while those taken on skulls are given in table 2. The skin lining the skeletal parts involved in measurements is very thin and therefore makes very little difference to the results.

14l. Distance on the left side from the most ventral part of the squamoso-occipital wing

(bottom of skull) to the dorsal border of the ear aperture of the skull, i.e. to the point where the anterior edge of the squamoso-occipital wing fuses with the lateral edge of the postorbital process, measured normal to the plane of the jugal bars. 'The most ventral part of the squamoso-occipital wing' refers to its ventral, vaulted part, not to the anteroventral edge of the wing that in some skulls is deflected ventrally and may reach somewhat farther ventrally than the vaulted part.

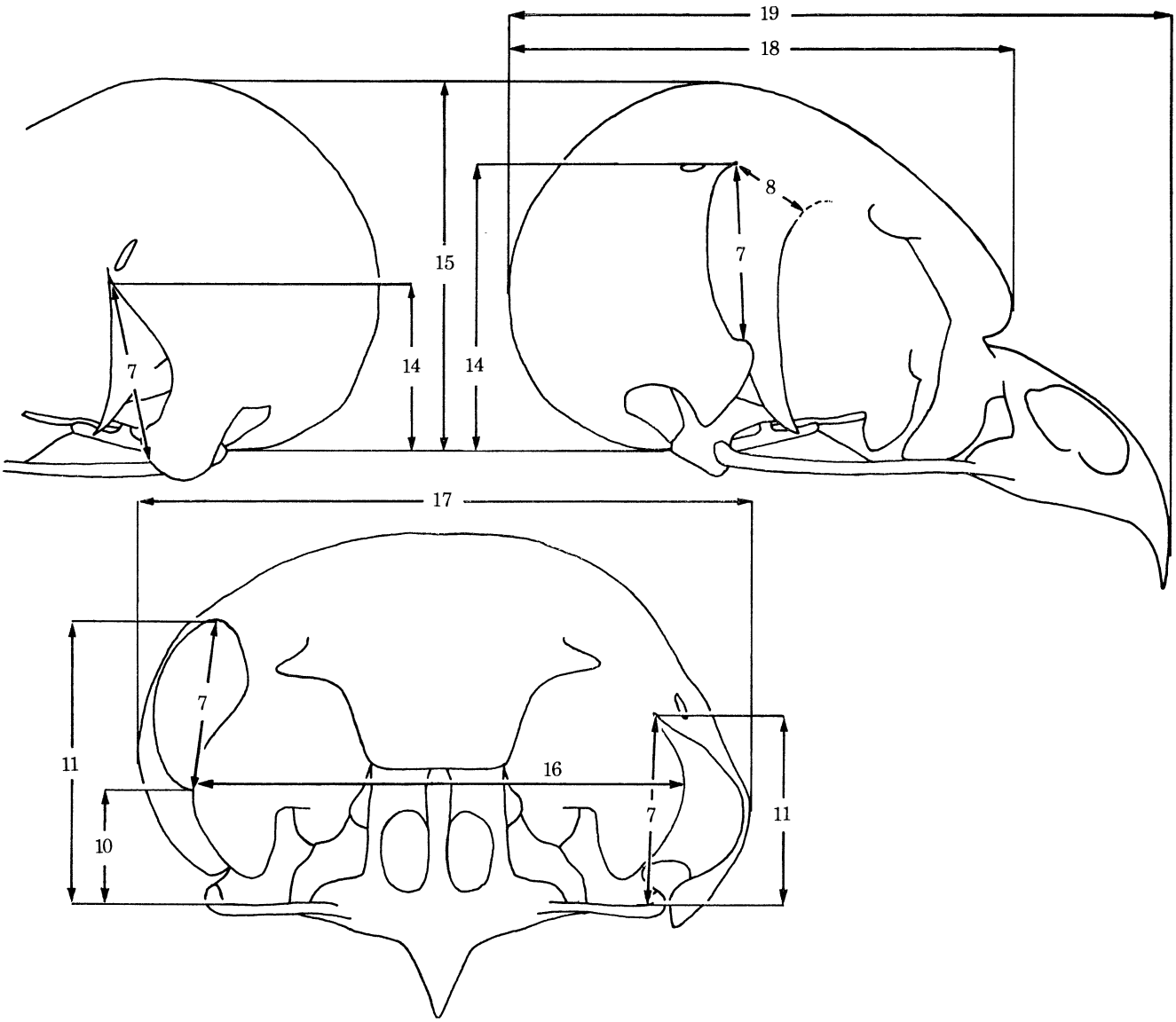


FIGURE 18. Illustrations showing how linear measurements were taken of skulls. Cf. §10.

14r. Distance on the right side from the most ventral part of the squamoso-occipital wing (bottom of skull as defined under 14l) to the dorsal border of the ear aperture of the skull, i.e. to the point where the anterior edge of the squamoso-occipital wing fuses with the skull, measured normal to the plane of the jugal bars.

15. Height of the skull. Distance from the most ventral part of the squamoso-occipital wing

(bottom of skull as defined under 14l) to the most dorsal point of the skull, measured normal to the plane of the jugal bars.

16. Distance between the most lateral points of the postorbital processes, measured parallel with the plane of the jugal bars.

17. Width of the skull. Distance between the most lateral points of the squamoso-occipital wings, measured parallel with the plane of the jugal bars.

18. Length of the skull, the rostral parts excluded, measured parallel with the plane of the jugal bars.

19. Length of the skull, the rostral parts included (rhamphotheca excluded) measured parallel with the plane of the jugal bars.

TABLE 2. LINEAR DIMENSIONS OF SKULLS OF *A. FUNEREUS*

(The measurements are defined in §§ 5 and 10, and in figures 1 and 18. Measurements in mm.)

(The sample size, minimum, maximum, and mean values, the standard deviation of measurements, and coefficients of variation (in percentage of the means) refer to skulls of adult owls. Some specimens were sexed, while most were not, and all are pooled in the table. At the bottom of the table, measurements are given for one adult owl (G 7910, included also in the statistics in the upper part of the table) and for two young owls (nestlings; 12 and 25 days post-hatching respectively). All three were used in making several of the illustrations. (In Norberg 1968, p. 185, I referred to measurements no. 3, 4, 9, and 10 in this table. These measurement numbers have been changed here to no. 17, 16, 8, and 7, respectively).)

| | number of dimension | | | | | | | | | | | | |
|---|---|---|---|---|---|---|---|---|---|---|---|---|---|
| | 7l | 7r | 8r | 10r | 11l | 11r | 14l | 14r | 15 | 16 | 17 | 18 | 19 |
| *n* | 30 | 31 | 35 | 27 | 30 | 30 | 31 | 32 | 32 | 30 | 34 | 34 | 25 |
| min. | 10½ | 10 | 4½ | 5 | 10 | 16½ | 10 | 16 | 23 | 30½ | 38 | 32 | 41½ |
| max. | 13 | 13 | 7½ | 8 | 13 | 19 | 11½ | 18½ | 25 | 33 | 42 | 34½ | 46 |
| mean | 11.6 | 11.0 | 6.1 | 6.8 | 11.4 | 17.4 | 10.9 | 17.1 | 23.9 | 31.7 | 39.9 | 32.9 | 43.8 |
| s.d. | 0.74 | 0.78 | 0.79 | 0.67 | 0.62 | 0.76 | 0.52 | 0.65 | 0.59 | 0.74 | 1.12 | 0.78 | 1.22 |
| coeff. of variation | 6.4 | 7.1 | 13.0 | 9.9 | 5.4 | 4.4 | 4.8 | 3.8 | 2.5 | 2.3 | 2.8 | 2.4 | 2.8 |
| specimen: | | | | | | | | | | | | | |
| adult G 7910 | 12 | 11 | 7 | 7½ | 12½ | 18½ | 11½ | 18½ | 25 | 33 | 41 | 33½ | 45½ |
| young N 70-06-29 | 8½ | | 4 | | 8½ | 11 | 9½ | 12 | 17 | 22 | 23½ | | 34½ |
| young N 71-07-04 | 10 | | 5 | | 10 | 12 | 11 | 13 | 21 | 26 | 29 | | 40 |

## 11. SIZE AND EXTERNAL FORM OF THE ADULT SKULL

Mean length of the skull is 43.8 mm, mean length with the rostral parts excluded 32.9 mm, mean width 39.9 mm, and mean height 23.9 mm (table 2).

The skull thus is exceptionally wide, having a width:length ratio of 0.91 with rostral parts included, and 1.21 with rostral parts excluded.

The most ventral parts of the skull (the anteroventral lobe of the squamoso-occipital wing on the left side, the quadrate, and the rostral parts excluded) are formed by the squamoso-occipital wings at their fusion with the lateroventral edge of the paroccipital processes (of the exoccipitals). These wings form one rounded, ventral eminence on either side of the skull base (i.e. the basioccipital and the medial parts of the exoccipitals). Measurements from the most ventral parts of the skull are taken from these ventral eminences below the terminal part of the external auditory meatus (measurements 14 and 15). In some skulls the edge of the squamoso-occipital wing anterior to the ventral eminence is deflected downwards and

reaches further ventrally. In these cases, however, measurements are still taken from the ventral eminences.

The rostral parts, jugal bars, quadrates, and all other parts of the skull anterior to the postorbital processes exhibit complete bilateral symmetry.

The postorbital processes are pneumatic in their proximal parts. The cavity is continuous with the superior air space. The anterior surface of the process is concave. The lateral edge is entire and lacks processes. The mean distance between the most lateral points of the postorbital processes is 31.7 mm (table 2:16), which approximately equals the horizontal distance between the ear apertures of the skull (figures 18, 21, plate 8).

The free part of the postorbital process on the left side is a mirror image of the corresponding part on the right side (figures 21, 27, 28). The lateral free edge of the postorbital process continues farther dorsally in the right process than in the left, this being the only bilateral asymmetry of these processes.

Posterior to the postorbital processes the lateral parts of the skull are extremely asymmetrical.

On the left side the lateral parts of the skull roof posterior to the orbit are rounded off smoothly downwards. At the dorsal base of the squamoso-occipital wing that juts out relatively low on the left side, a straight or somewhat concave contour is formed when the skull is viewed from in front or from behind (figures 21, 26). On the left side the dorsal part of the squamoso-occipital wing is displaced anteroventrally, and its anterior edge fuses with the lateral edge of the postorbital process. The distance from the most ventral point of the skull to the dorsal border of the left ear aperture is 10.9 mm (table 2:14l). The distance from the dorsal edge of the jugal bar to the dorsal border of the left ear aperture is 11.4 mm (table 2:11l).

On the right side the lateral parts of the skull roof posterior to the orbit are raised relative to those of the left side. At the dorsal base of the squamoso-occipital wing that juts out high on the right side, a smooth convex contour is formed when the skull is viewed from in front or from behind (figures 21, 26). On the right side the dorsal part of the squamoso-occipital wing is displaced posterodorsally and fuses with the skull 6.1 mm posterior to the edge of the orbit (table 2:8). The distance from the most ventral point of the skull to the dorsal border of the right ear aperture is 17.1 mm (table 2:14r). The distance from the dorsal edge of the jugal bar to the dorsal border of the right ear aperture is 17.4 mm (table 2:11r).

The anterior edge of the squamoso-occipital wing, i.e. the dorsal border of the ear aperture, juts out on the average 6.2 mm higher on the right side than on the left, as measured from the most ventral parts of the skull (the difference between measurements 14r and 14l in table 2). As measured from the dorsal edge of the jugal bar, the anterior edge of the squamoso-occipital wing juts out on the average 6.0 mm higher on the right side than on the left (the difference between measurements 11r and 11l in table 2).

In some skulls the difference between the measurements 14r and 14l is slightly larger than the difference between 11r and 11l, while in others the reverse is the case. The close agreement between the mean differences (6.2 and 6.0 mm, respectively) demonstrates that the ventral, rounded eminence of the squamoso-occipital wing reaches equally far ventrally on the left and right side with respect to the plane of the jugal bars.

At the dorsal base of the squamoso-occipital wings, between 1 and 3 mm behind the anterior edge, there is a foramen, about 1 by 2 mm in size. Its long axis is oriented approximately

along the line of fusion between the skull and the squamoso-occipital wing. Aponeurosis 1 of M. adductor mandibulae externus passes through this foramen. From this foramen and posteromedially there is a shallow furrow, the *temporal fossa*. This furrow lies near to, or partly coincides with the line of fusion between the squamosal and the parietal. The fossa accommodates the temporal part of the aponeurosis 1 portion of the M. adductor mandibulae externus. Because of the bilateral asymmetry of the squamosals, this foramen, and hence the bend in the aponeurosis passing through it, are located about 6 mm higher and 6 mm farther posteriorly on the right side than on the left.

The anteroventral part of the squamoso-occipital wing is drawn out to a lobe, the shape of which is rather similar on both sides of the head. The anterior edge of the lobe is thickened (figures 21, 23, plates 8 and 9). The difference in position of the lobe on the left and right sides is dependent mainly on differences in origin and orientation of the proximal parts of the squamoso-occipital wings.

On the left side, the lobe of the squamoso-occipital wing overhangs the articulation between the quadratojugal, quadrate, and the lower jaw. Opposite to this articulation there is a distinct, oval, flat or somewhat concave articular surface, *ca.* 2.5 mm long, on the lobe (figure 23, plate 9).

The articular surface on the anteroventral lobe of the left squamoso-occipital wing lies lateral to, and very near, or in contact with, the articulation between the quadrate and jugal bar. The posterolateral part of the lower jaw (angular) does not extend as far laterally as does the quadrate-quadratojugal articulation. Therefore the lower jaw does not contact the articular surface on the squamoso-occipital wing.

The lobe of the squamoso-occipital wing braces against, and gets support from, the quadrate-quadratojugal articulation (rather than the reverse). The articular surface of the lobe lies in a sagittal plane and apparently is developed because of the fore and aft streptostylic movements of the quadrate-quadratojugal joint.

The anteroventral lobe of the right squamoso-occipital wing is bent inwards. Therefore parts of it lie behind the postorbital process at a distance from this of 0.5 mm or less. In some of the skulls examined (G 1542, G 2054, G 3677, S 1153, S 'Skansen', O 6013, and O 7161) the lobe lies very near, or in contact with the posterior surface of the postorbital process. In these cases the anterior aspect of the lobe is modified and flattened nearest to the postorbital process (the lengths of the flattened edge being 3.5, 1.5, 4, 3, 3, 4, 4, and 5 mm, respectively). Further, the right lobe may be bent more or less inwards. When much bent (as for instance in skull G 7910, figures 20–24, plates 7–10), the anterior edge of the lobe lies relatively far behind the lateral edge of the postorbital process, however, still *ca.* 0.5 mm (or less) from its posterior surface that is convex (figure 20, plate 7).

Posteroventral to these lobes the squamoso-occipital wings are hollowed out, the recess being of about the same shape on both sides. Through these recesses parts of the quadrate, tympanic ring, and the middle ear cavity are visible. This recess is closed mainly by the M. depressor mandibulae that originates from the squamoso-occipital wing and inserts on the posterior end of the lower jaw.

The ventromedial part of the squamoso-occipital wing vaults regularly over the entrance to the middle ear (the eardrum) and forms the most ventral parts of the skull (the anteroventral lobe of the left squamoso-occipital wing, the quadrates, and the rostral parts excluded). A line connecting the ventral eminence of the left and right squamoso-occipital wing (lateral

to the foramen magnum) is parallel with, and approximately coincident with the plane of the jugal bars. This appears from table 2 where measurements 14l and 14r approximately coincide with 11l and 11r, respectively. It can also be seen in figure 22 where the posterior ends of the jugal bars are visible lateral to the quadrates.

There is complete bilateral symmetry in the ventral eminences of the squamoso-occipital wings and in the skull parts medial to these, i.e. the sphenoid rostrum, basiparasphenoid, basioccipital, and the exoccipital bones (figures 8, 9, 16, 22, 24, 25, 28).

TABLE 3. DIMENSIONS OF THE EAR APERTURE OF THE SKULL AND THE EXTERNAL AUDITORY MEATUS

(Linear dimensions in mm, areas in mm², and volumes in mm³.)

| | number of dimension | | | | | | | | |
|---|---|---|---|---|---|---|---|---|---|
| | 20 area of aperture | | 21 short length of meatus | | 22 great length of meatus | | 23 volume of blind cavity | 24 volume of meatus | |
| specimen | left | right | left | right | left | right | right | left | right |
| G.68–03 | 41 | 49 | | | | | | 800 | |
| G.D. | 47 | 61 | | | | | 50 | | |
| S.Av.730463 ♂ | 54 | 54 | | | | | 50 | 800 | 750 |
| S.Av.740031 ♀ | 47 | 57 | | | | | 60 | 890 | 880 |
| S.Av.740032 ♂ | 42 | 65 | | | | | 30 | 790 | 830 |
| G.B.B. | 52 | 63 | | | | | 30 | | |
| N.3 | 40 | 48 | | | | | | | |
| N.4 | 41 | 50 | | | | | 50 | 860 | 950 |
| N.5 (cast) | 41 | 55 | 13 | 15 | 17 | 20 | 40 | 780 | 840 |
| N.6 | | | 15 | | 17½ | | | | |
| N.8 | | | | | 17 | | | | |
| N.9 (cast) | 51 | 58 | 14 | 15 | 17 | 20 | | 820 | 820 |
| N.11 | 49 | 50 | | | | | 40 | | 730 |
| N.12 | 58 | 62 | | | | | | | |
| N.13 | 53 | 64 | | | | | 40 | 840 | 930 |
| N.14 | 44 | 59 | | | | | 40 | | 800 |
| N.15 | 56 | 68 | | | | | 50 | 800 | 890 |
| *n* | 15 | 15 | 3 | 2 | 4 | 2 | 11 | 9 | 10 |
| mean | 48 | 58 | 14 | 15 | 17 | 20 | 44 | 820 | 842 |

## 12. MEASUREMENTS OF THE EAR APERTURE AND EXTERNAL AUDITORY MEATUS

Below is a description of measurements taken on ear apertures and external auditory meatuses. The dimensions are numbered from 20 to 24. An 'l' after the dimension number denotes the left side, an 'r' the right side. Results are given in table 3.

20l and 20r. Area of the ear aperture of the skull. Measurement taken in the plane best fitting the borders of the ear aperture. Measurements taken only of ears with soft parts intact.

21l and 21r. Shortest direct length of the external auditory meatus. Distance from the ventromedial corner (at the lateral edge of the postorbital process) of the ear aperture of the skull to the inner termination of the meatus at the process (in the tympanic ring) for the

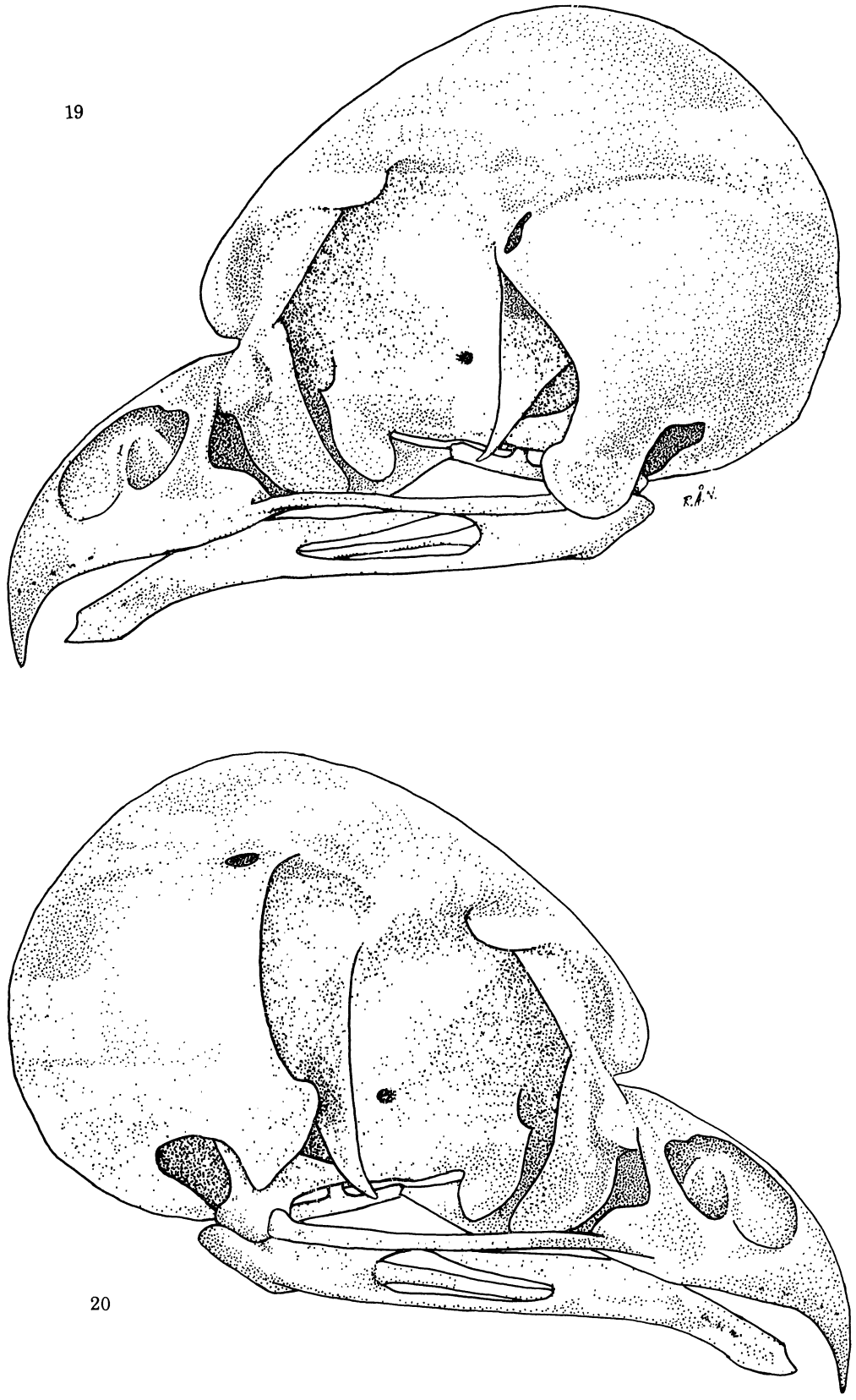


PLATE 7. For description see plate 9.

(*Facing p.* 362)

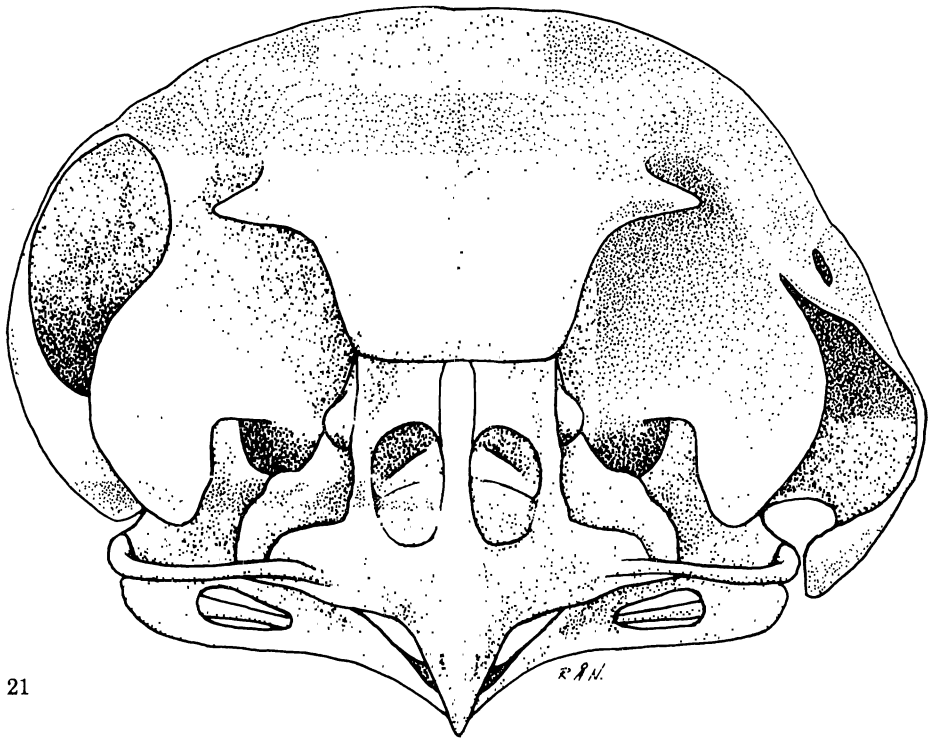

21

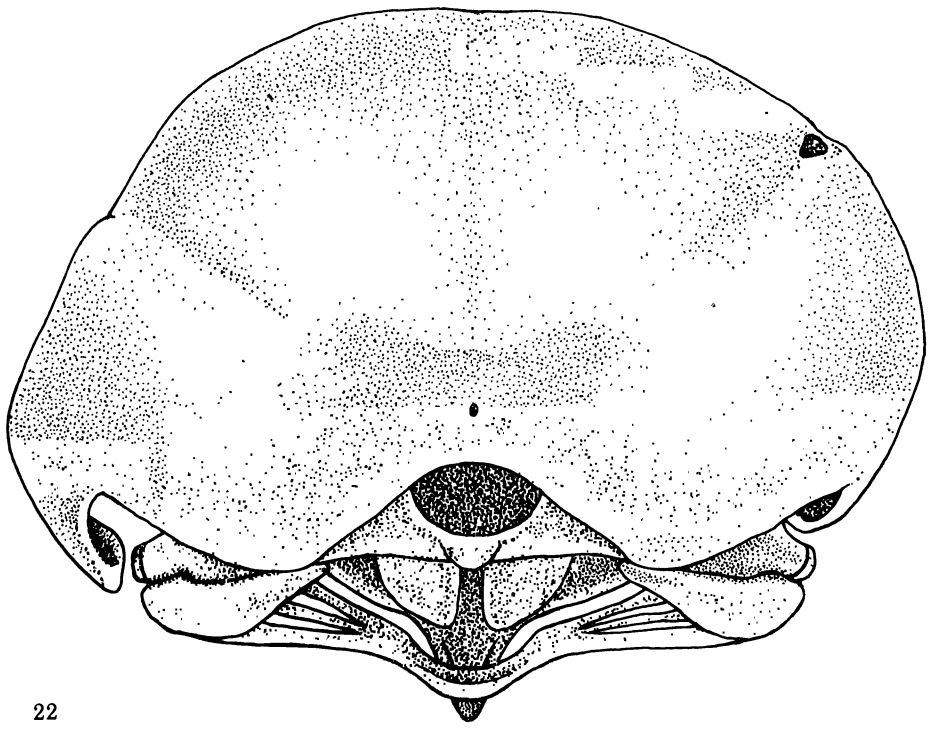

22

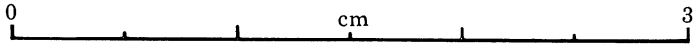


PLATE 8. For description see opposite.

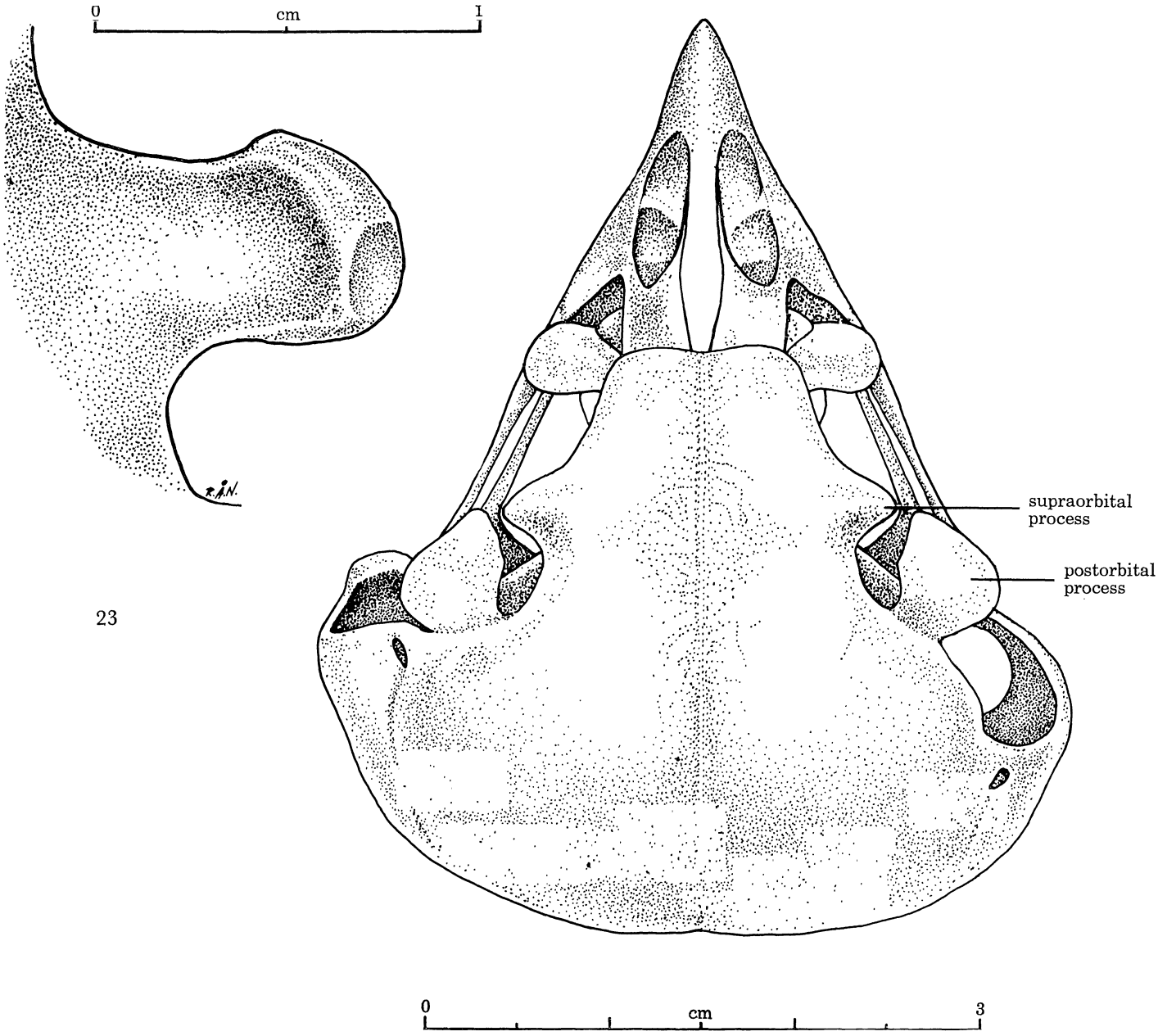


## Description of plates 7–10

Figures 19–24. The skull of an adult owl (specimen G 7910). The sclerotic eye rings and the rhamphotheca are removed. In figures 19 and 20 the vertical median plane of the head is parallel with the plane of the figure. In figures 21 and 22 the median plane of the head and the plane of the jugal bars are normal to the plane of the figure. In figures 23 and 24 the head is oriented with its median plane normal to the plane of the figure, and such that a plane through the distal points of the supraorbital processes and the postorbital processes is also normal to the plane of the figure. The plane of the jugal bars therefore is inclined *ca.* 20° to the plane of the figure in figures 23 and 24.

The inset figure to the left in figure 23 shows the anteroventral lobe of the left squamoso-occipital wing as seen from a dorsomedial direction. On the part of the lobe that lies just lateral to the quadrate-quadratojugal articulation, there is an articular surface that is oriented approximately in a sagittal plane to the head (specimen G 7910).

Figure 25. The skull base. The skull is oriented as in figure 24. A part of the ventral plate of the basiparasphenoid, covering the eustachian tube, is removed on the left side. Based on a camera lucida drawing of one skull (GB) and two photos of another skull (G 7910; one photo of the intact skull and one of the skull with the basiparasphenoid opened).

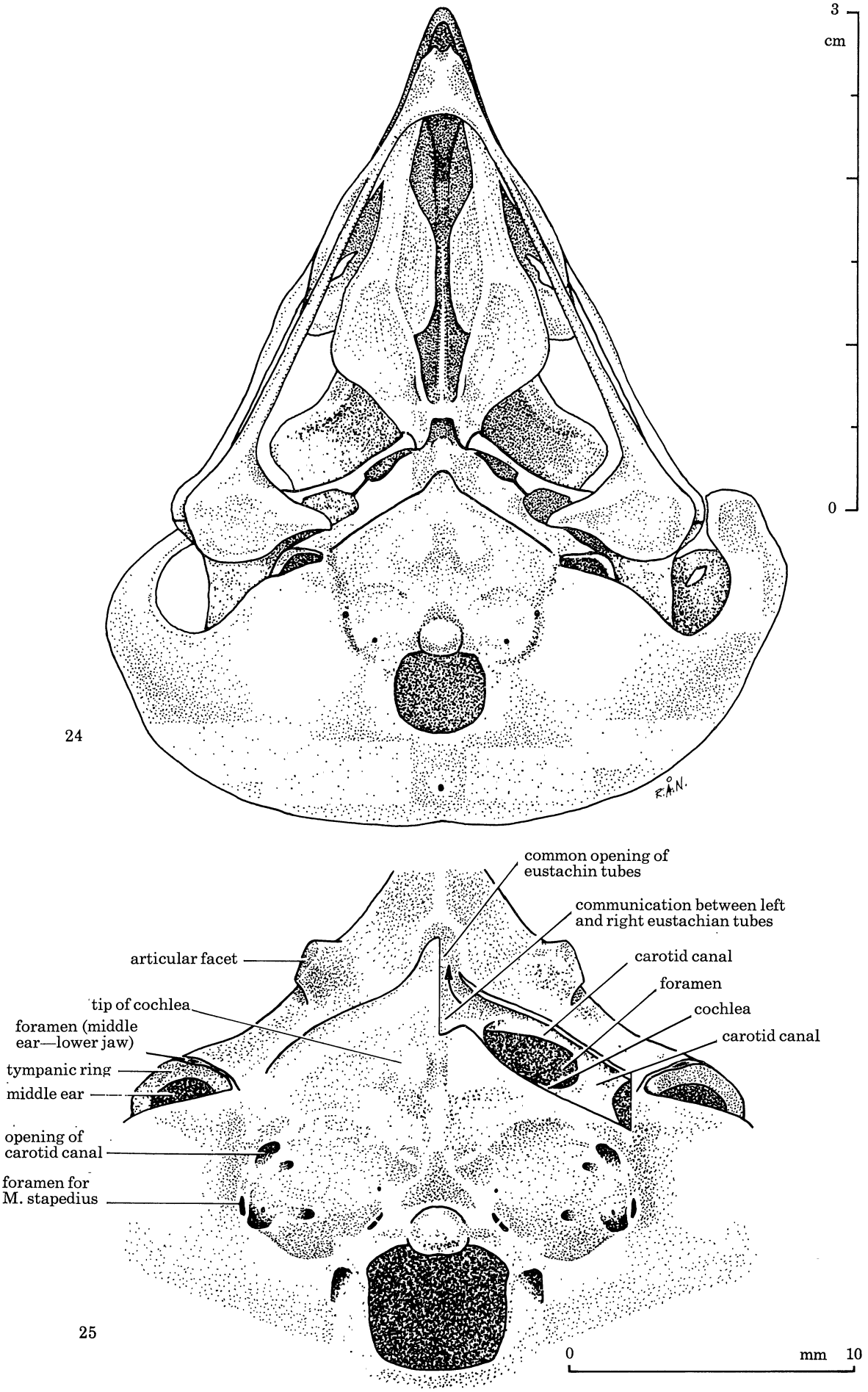


PLATE 10. For description see plate 9.

Ligamentum ascendens. Measurements taken of casts of the auditory meatus with soft parts intact, of dissected ears with soft parts intact, or of dissected skulls.

22l and 22r. Greatest direct length of the external auditory meatus. Distance from the dorsomedial corner (at the lateral edge of the orbit) of the ear aperture of the skull to the inner termination of the meatus at the process (in the tympanic ring) for the Ligamentum ascendens. Measurements taken of casts of the auditory meatus with soft parts intact, of dissected ears with the soft parts intact, or of dissected skulls.

23r. Volume of the blind cavity below the right ear aperture of the skull. Measurements taken on ears with soft parts intact.

24l and 24r. Volume of external auditory meatus (out to the lateral edge of the postorbital process and the anterior edge of the squamoso-occipital wing). Measurements taken of intact ears or of casts thereof.

## 13. Ear aperture of the skull

### 13.1. *Position and orientation*

The squamoso-occipital wing forms the lateral, and posteriorly also the ventral wall of the external auditory meatus. This process extends extremely far anteriorly and reaches to the level of the postorbital process. Owing to the remarkable development of the squamoso-occipital wings the entire ear apertures of the skull are visible when the skull is viewed from in front.

The left ear aperture is bounded by the postorbital process and the squamoso-occipital wing, and ventrally by the jugal bar. The right ear aperture is bounded only by the postorbital process and the squamoso-occipital wing (figures 1, 19–21, plates 7 and 8).

The horizontal distance between the centres of the ear apertures of the skull approximately equals the distance between the most lateral points of the postorbital processes, which is 31.7 mm (table 2:16).

The dorsal border of the left ear aperture is at the postorbital process (the lateral rim of the orbit), 10.9 mm above the most ventral parts of the skull (table 2:14l) and 11.4 mm above the dorsal edge of the jugal bar (table 2:11l).

The dorsal border of the right ear aperture lies 6.1 mm posterodorsal to the lateral rim of the orbit (table 2:8), 17.1 mm above the most ventral parts of the skull (table 2:14r) and 17.4 mm above the dorsal edge of the jugal bar (table 2:11r).

The dorsal border of the right ear aperture lies 6.2 mm higher than that of the left aperture, as measured from the most ventral parts of the skull (table 2:14l, 14r), and 6.0 mm higher as measured from the dorsal edge of the jugal bar (table 2:11l, 11r). An average value of the difference in vertical level between the dorsal border of the left and right ear aperture of the skull thus is 6.1 mm.

The jugal bar lies in the bottom of the left ear aperture. The ventral border of the right aperture is formed by the anteroventral lobe of the squamoso-occipital wing, and lies 6.8 mm above the dorsal edge of the jugal bar (table 2:10).

Viewed from in front a line connecting the centres of the ear apertures deviates *ca.* 12° from the horizontal (i.e. the plane of the jugal bars). This angle is calculated from mean values of measurements in table 2.

Because of the large difference between the two sides, the ear apertures of the skull not

only are located at different vertical levels, but also face in different vertical directions. However, the orientation of the ear aperture is not easy to define and measure. This is because the medial border of the aperture is formed by the bilaterally symmetrical postorbital processes and sclerotic rings, whereas the lateral border is formed by the highly asymmetrical squamoso-occipital wings. On the whole, however, the left ear aperture usually faces somewhat ventrally relative to the plane of the jugal bars, while the right aperture faces somewhat dorsally. Further, the right aperture usually faces more laterally than does the left one.

Approximate values on the vertical orientation of the ear apertures may be obtained as follows. On lateral-view illustrations of a skull, a line is drawn between the dorsal and ventral borders of the ear aperture, i.e. between the anterior edge of the squamoso-occipital wing at its anterodorsal origin, and the anterior edge of the anteroventral lobe of the wing. Then a perpendicular to this line is drawn forwards. These perpendiculars of the two ears are taken to indicate the vertical directions in which the apertures are facing. Taking the skull illustrated in figures 19–24 as an example, the left ear aperture thus faces *ca.* 12° downwards relative to the plane of the jugal bars, and the right aperture *ca.* 7° upwards. This gives a vertical divergence of *ca.* 19°. As can be seen in figure 26, there is rather large individual variation in orientation of the apertures.

### 13.2. *Linear dimensions*

The height of the ear aperture in the skull is 11.6 mm for the left ear and 11.0 for the right one (table 2:7l, 7r). Thus the height of the ear apertures of the skull is about half the height of the ear slits in the skin (table 1:4l, 4r) and about half the height also of the skull (table 2:15).

The maximum horizontal width of the ear aperture of the skull is poorly defined and is at different vertical levels in different skulls. Therefore the width was measured at about half the height of the aperture. It is defined as the horizontal, direct distance from the lateral edge of the postorbital process to the inside of the anterior edge of the squamoso-occipital wing. Due to differences in form between the ears, the line of measurement in the two ears forms different angles with the median plane of the head.

The width thus defined was 4.8 mm in the left ear ($n$ = 21, min. = 4, max. = $5\frac{1}{2}$, s.d. = 0.46) and 6.5 in the right ($n$ = 20, min. = 5, max. = $7\frac{1}{2}$, s.d. = 0.62).

### 13.3. *Area*

There are large individual variations in shape and size of the ear apertures in the skull (figure 26).

Areas of the ear apertures of the skull were measured as follows. The head, with the soft anatomy of the external ears intact, was oriented under a dissecting microscope so that the plane of the ear aperture under examination was horizontal, i.e. approximately normal to the microscope's optical axis. The borders of the ear aperture of the skull do not lie strictly on one plane, but the head was oriented to give the best fit with a horizontal plane. The outline of the opening was then drawn with the aid of a camera lucida. In intact heads the left ear aperture is well delimited ventromedially by soft tissue. The dorsomedial border of the right aperture is marked more or less distinctly by a bone ridge. Areas of the drawings were found with a planimeter.

The areas thus obtained were 48 mm² for the left ear aperture of the skull and 58 mm² for the right one (table 3:20).

Areas were measured in 15 owls. In all of them the area of the right aperture was larger than that of the left.

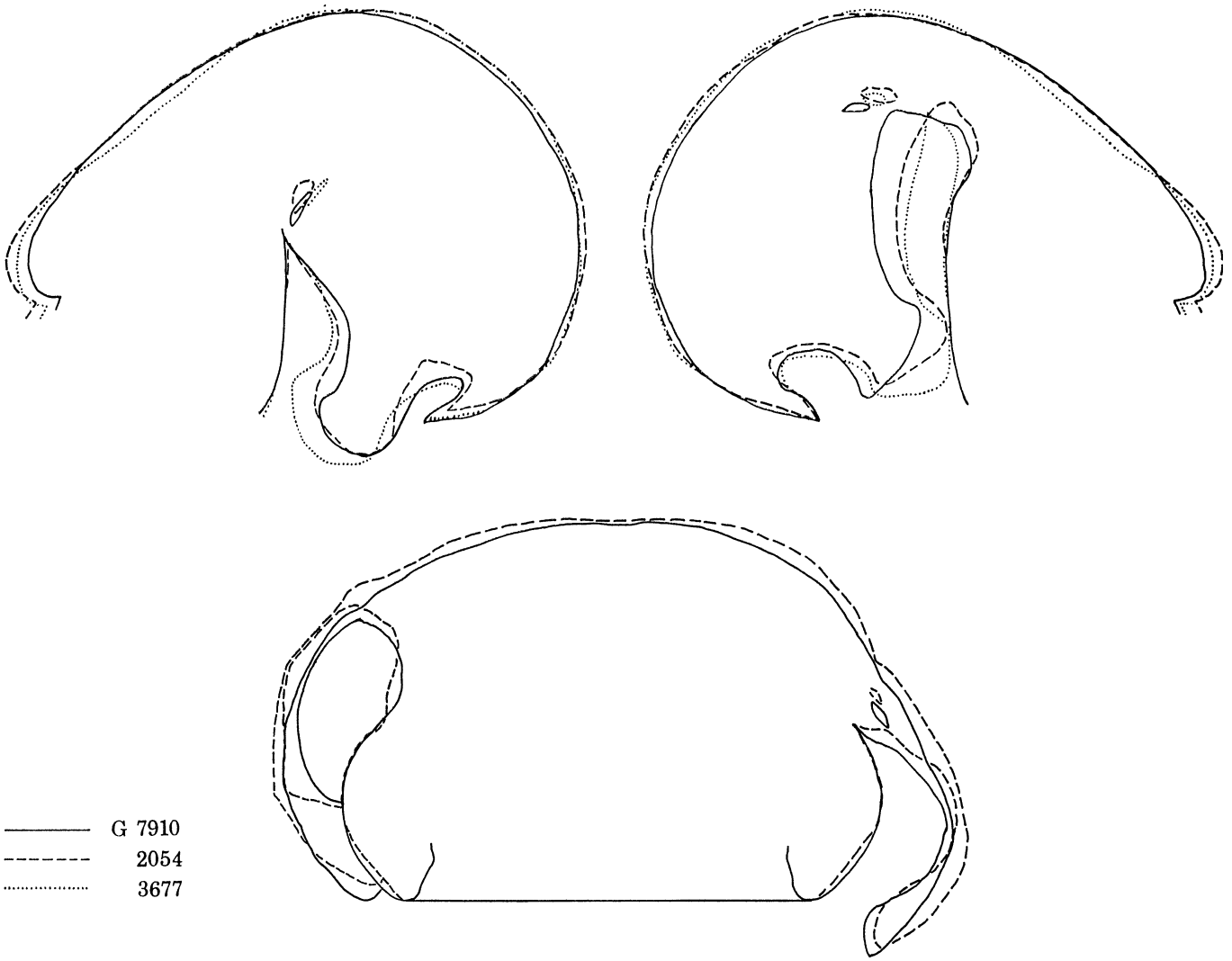


FIGURE 26. Skulls drawn to approximately the same size (i.e. to somewhat different scales) to show individual differences in shape of the ear apertures. The drawings are so adjusted that the lateral edges of the postorbital processes coincide within each composite figure. Skulls with relatively large differences in shape of the ear apertures were selected for these figures.

## 14. EXTERNAL AUDITORY MEATUS

### 14.1. *Form* (figures 29–31, 35)

Just inside the aperture both external auditory meatuses are most spacious. They extend *ca.* 2 mm medially behind the postorbital processes and here reach their maximum horizontal width that amounts to *ca.* 8 mm. The left meatus extends *ca.* 2 mm dorsally behind the anterior edges of the postorbital process and the squamoso-occipital wing. The right meatus extends ventrally behind the postorbital process and the anteroventral lobe of the squamoso-occipital wing.

27

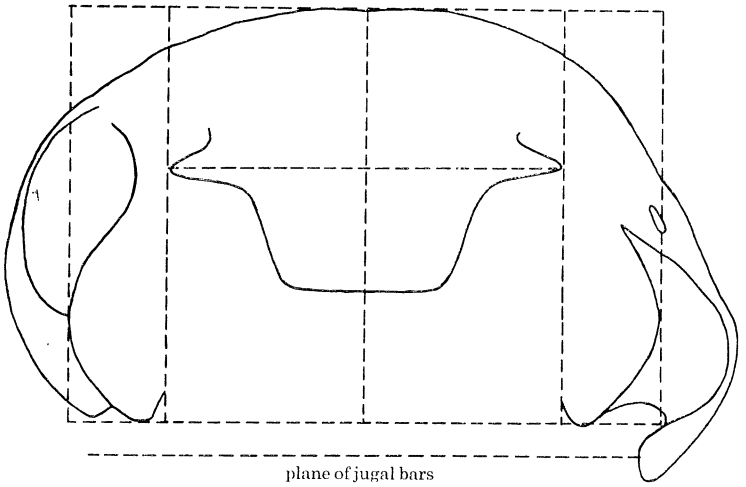


28

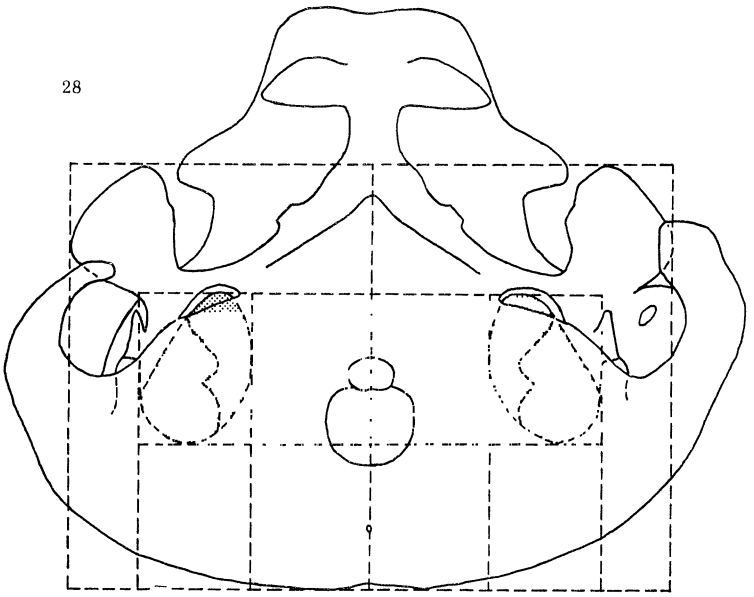

FIGURE 27. Anterior view of the skull (G 7910). The skull is oriented as in figure 21. Symmetry lines are laid into the figure. The position and orientation of a plane through the dorsal edge of the jugal bars are indicated. A line connecting the most ventral parts of the left and right squamoso-occipital wing, lateral to the foramen magnum, is parallel with, and approximately coincident with the plane of the jugal bars. This can be seen in figure 22, where the posterior ends of the jugal bars are visible lateral to the quadrates.

FIGURE 28. Ventral view of the skull. The skull is oriented as in figure 24. The quadrates and the rostral parts removed. The positions of the tympanic rings are indicated in broken lines. Symmetry lines are laid into the figure. Drawn from two photos (of skull G 7910; one photo of the skull with the quadrates and rostral parts removed, and one photo of the skull with the tympanic rings made visible by removal of the squamoso-occipital wings).

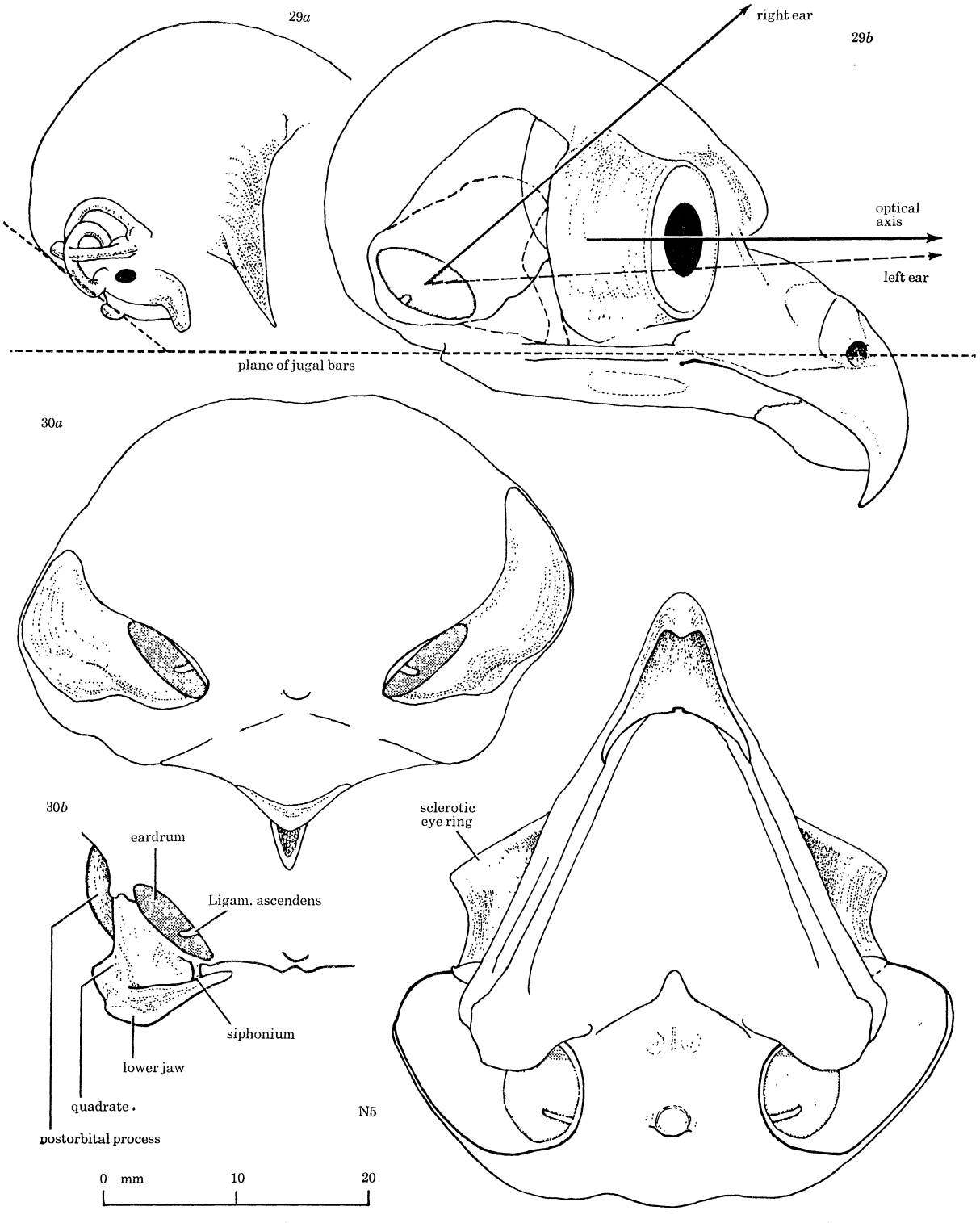


FIGURES 29–31. Lateral, posterior, and ventral view of the head with the skin removed, and with the left and right eardrum and external auditory meatus indicated. The drawings are based on several photos showing, respectively, (1) the head with the skin removed, head otherwise intact, (2) the head with casts of the external auditory meatuses in situ and with the covering squamoso-occipital wings removed, and (3) the head with the casts removed so that the eardrums were visible. Figure 29*a* is based on a photograph of skull G 7910; all the other figures are based on photographs of skull N5. The scale is for all figures.

FIGURE 29*a* and *b*. The skulls are oriented in the same way in both figures and the median plane of the head is parallel with the plane of the figures. It can be seen (29*a*) that the horizontal semicircular canal lies in a plane about parallel with that of the jugal bars. The plane of the foramen magnum (indicated with broken line in 29*a*) forms *ca.* 38° with the plane of the jugal bars. In figure 29*b* the external auditory meatus and ear aperture of the skull are indicated for both ears (broken line for the left ear). In figure 30*a* and *b* the median plane of the head and the plane of the jugal bars are normal to the plane of the figures. The external auditory meatuses are shaded (figure 30*a*) as if they were solid; a rendition of the casts of the meatuses. Figure 30*b* is a detail of figure 30*a*, showing the tympanic ring and lower jaw and the connective tissue tube, the siphonium, uniting them. In figure 31 the plane of the jugal bars is parallel with the plane of the figure.

The medial wall of the meatuses is concave, especially in the left ear where it curves laterally at a low level to support the squamoso-occipital wing. Posteriorly the meatuses curve ventrally and at the lateral edge of the body of quadrate become laterally compressed and narrow. Both meatuses here reach only 3.5–4 mm in horizontal width. The lateral edge of the body of quadrate juts into the external auditory meatus just anterior to the eardrum. Here the external otic process of quadrate articulates in a socket between the zygomatic and postglenoid processes dorsolateral to the eardrum. These articulations and processes exhibit complete symmetry between the left and right side of the skull (figure 28).

Since the anterior part of the external auditory meatus is located farther dorsally on the right side than on the left, the quadrate does not jut as far into the right meatus as into the left one. The articulation between the quadrate and the quadratojugal lies in the bottom of the meatus on the left side, entirely outside the meatus on the right (figures 19, 20).

Posterior to the quadrates the meatuses curve medially towards the ventral side of the skull, where they are flattened and extended over the eardrums. The height of this flattened cavity is *ca.* 4 mm as measured from, and normal to, the plane of the tympanic ring. This posteroventral part of the meatus, extended over the eardrum, is of the same shape in both ears.

Ventrally, and posterior to the quadrate, there is a recess in the squamoso-occipital wing, exposing parts of the auditory meatus and the tympanic cavity. The recesses are of the same shape on the left and right side. The anteroventral wing lobe in front of it, however, is oriented in different ways in the two ears. In the intact head these recesses are closed by soft tissue. Hence the inner anteroventral part of the external auditory meatus, extended over the eardrum, is bounded ventrally essentially by the M. depressor mandibulae.

The terminal, medial, part of the meatus curves anteromedially, posteromedial to the quadrate, and continues *ca.* 2 mm anterior to the anteriormost part of the tympanic ring. It here extends dorsal to the medial process of the lower jaw. The anteromedial end of the inner part of the meatus is at the siphonium, a tube of connective tissue that connects the pneumatic foramen in the medial process of the lower jaw with the foramen in the anteromedial part of the tympanic ring (figures 25, 30). The body of quadrate forms the anterolateral wall of the innermost, flattened cavity of the meatus, while the eardrum forms its dorsomedial wall.

The eardrum spans an oval tympanic ring. The tympanic rings are bilaterally symmetrically located (figures 28–31).

The bilateral asymmetry of the skull and of the external auditory meatuses reaches its maximum at the ear apertures. The asymmetry then decreases towards the posterior parts of the meatuses. In the parts of the meatuses posterior to the lateral edge of the body of quadrate, i.e. in the flattened parts over the eardrums, complete bilateral symmetry prevails.

As projected on the vertical median plane of the head, an axis through the centre of the eardrum and the centre of the ear aperture (in the skull) of one ear gives an angle of vertical divergence of *ca.* 40° to the corresponding, projected axis of the other ear (figure 29*b*).

### 14.2. *Geometric and functional lengths and volumes*

The part of the external auditory meatus farthest from the ear aperture of the skull is posteromedially in the meatus, and almost exactly at the process for the Ligamentum ascendens.

The point of origin of the Ligamentum ascendens on the bony tympanic ring thus is defined as the inner termination of the external auditory meatus.

The distance from the ventral border of the ear aperture of the skull to the termination of the meatus is *ca.* 15 mm in both ears (table 3:21). The distance from the dorsal border of the aperture to the termination of the meatus is *ca.* 17 mm in the left ear and *ca.* 20 mm in the right (table 3:22).

External auditory meatus resonance occurs when one-fourth of the wavelength $\lambda$ of the sound equals the length of the meatus (Wiener & Ross 1946, p. 405; Wever & Lawrence 1954, p. 52; Shaw & Teranishi 1968, p. 246).

Resonance occurred at *ca.* 5000 Hz in the right external auditory meatus of an artificial head of *A. funereus* used for acoustic measurements (Norberg 1968, p. 190). At this frequency, $\frac{1}{4}\lambda = 17.3$ mm (sound velocity 345 m $s^{-1}$), showing this to be the functional length of the right meatus. This agrees well with the morphological length of this particular meatus which is 15 mm as measured from the ventral border of the ear aperture, and 20 mm as measured from the dorsal border(table 3:N9 (cast)).

Mean volume is 820 $mm^3$ for the left external auditory meatus and 842 $mm^3$ for the right one (table 3:24). Volumes were measured of both ears in eight owls. In five of these the right meatus was larger than the left one, in two the left meatus was the largest, and in one owl both meatuses were equally large.

The blind cavity below the right ear aperture of the skull has an average volume of 44 $mm^3$.

## 15. Jaw muscles associated with the external ear

This section contains a brief description of only the superficial jaw muscles that are associated with the external auditory meatus.

The division and terminology of muscles are adopted from Starck & Barnikol (1954). Their paper contains descriptions of jaw muscles of several bird species, including four owls, namely *Tyto alba*, *Athene noctua*, *Strix aluco*, and *Asio otus*.

The superficial muscles treated below are M. depressor mandibulae and the complex M. adductor mandibulae externus. Owing to the skull asymmetry in *A. funereus*, the M. depressor mandibulae and the aponeurosis 1 portion of M. adductor mandibulae externus exhibit pronounced bilateral asymmetry.

The several other deeper jaw muscles are left outside this treatment. None of them is directly related to the ear, nor to skull parts involved in asymmetry. Hence these deep muscles exhibit bilateral symmetry.

*M. depressor mandibulae* (figure 32)

*Origin.* On the edge formed by the squamoso-occipital wing around its ventral recess posterior to the quadrate, and on the outer surface of the squamoso-occipital wing on a margin area bordering the recess. Fleshy origin.

*Insertion.* On the posterior and posteroventral surface of the articular end of the lower jaw and on its medial process. Insertion by aponeurosis and fibres.

*Remarks.* The muscle is wide and flat and unipinnate with the fibres running about parallelly. Together with the outward skin and the skin lining the meatus, the muscle closes the ventral recess in the squamoso-occipital wing, i.e. the opening between the posterior end of the

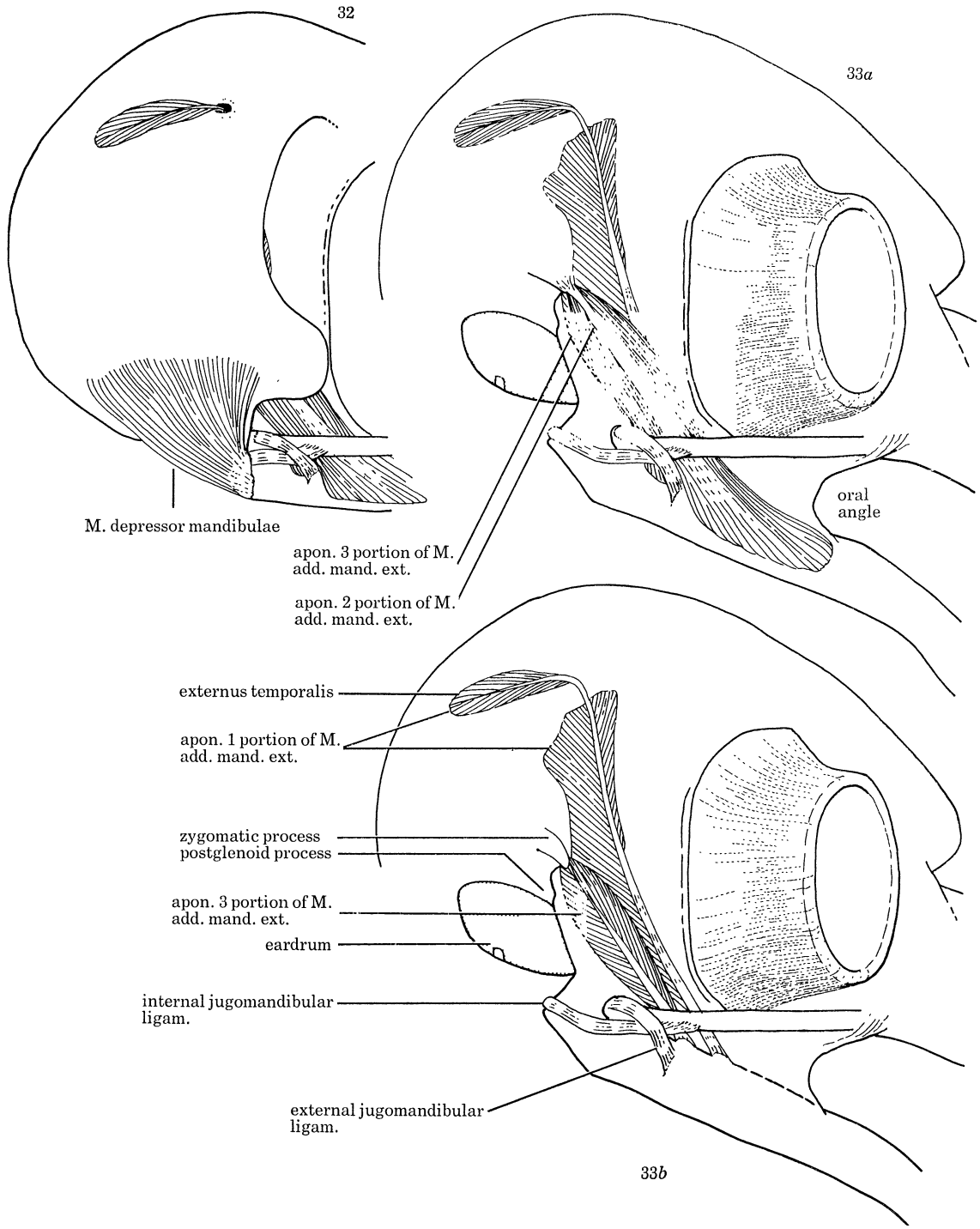


FIGURES 32–34. Illustrations showing the superficial jaw muscles.

FIGURE 32. The skull is intact and all jaw muscles are present.

FIGURE 33 (*a*). The squamoso-occipital wing and M. depressor mandibulae are removed to expose underlying jaw muscles.

FIGURE 33 (*b*). The squamoso-occipital wing and the aponeurosis 2 portion of M. adductor mandibulae externus are removed.

lower jaw and the squamoso-occipital wing. Hence it forms the anteroventral wall of the inner, medial part of the external auditory meatus. The anteromedial part of the meatus continues *ca.* 1 mm further anteriorly, just dorsal to the medial process of the lower jaw.

*Function.* The muscle opens the beak by depressing the lower jaw.

*Asymmetry.* The anteroventral lobe of the squamoso-occipital wing is located on different vertical levels and is oriented in different ways on the left and right side of the head. Those muscle fibres of M. depressor mandibulae that originate lateral and anterolateral to the recess of the squamoso-occipital wing therefore come to be bilaterally asymmetrically arranged. In particular, the distance from the lower jaw to the anteroventral lobe of the squamoso-occipital wing is longer on the right side than on the left one, thereby necessitating a longer aponeurosis and/or longer muscle fibres on the right side.

*M. adductor mandibulae externus* (figures 32–34)

This is a complex muscle composed of several portions. Its function is to close the bill by raising the lower jaw.

Starck & Barnikol (1954, p. 11) divided it according to the three aponeuroses involved.

*Aponeurosis* 1 *portion of M. a. m. e.* (figures 1, 32–34)

*Origin.* On the outer surface of the skull, along the temporal fossa dorsal to the squamoso-occipital wing (*temporal part* of the aponeurosis 1 portion of M. adductor mandibulae externus); fleshy origin; and on an elongated area in the medial wall of the external auditory meatus anterodorsal to the quadrate and zygomatic process; fleshy origin.

*Insertion.* Insertion by the aponeurosis 1 on the anterior one of the two small coronoid processes on the dorsal edge of the lower jaw, i.e. on the supraangular.

*Remarks.* The aponeurosis is a distal one of insertion. The muscle has two discrete fibre masses, one temporal part (*externus temporalis*) originating on the external wall of the skull, dorsal to the squamoso-occipital wing, and one portion originating on the medial wall of the external auditory meatus. The latter one has a much larger fibre mass than has the temporal part.

The temporal part is a bipinnate, very thin and sheet-like muscle that spreads over the region of fusion between the squamosal and the parietal. In the region of fusion there is a shallow depression in the skull (the *temporal fossa*), with an outline corresponding to that of the muscle. The depression narrows anteriorly to form a marked furrow in which the tendon of the temporal part of the muscle lies. The tendon passes through a foramen in the anterior end of the furrow at the base of the squamoso-occipital wing. It then passes anteroventrally along the medial wall of the external auditory meatus.

Immediately inside the external ear aperture, muscle fibres originate from the medial wall of the auditory meatus and join the tendon from a posterodorsal direction, in the right ear also from an anterodorsal direction. The tendon lies against the posterior surface of the base of the postorbital process and is forced to curve in passing ventrally along the process. The muscle fibres originating on the medial wall of the auditory meatus form a thin sheet over the bony wall of the meatus. The fibre mass lies close to the medial wall of the meatus, and ventrally passes closely behind the base of the postorbital process.

At about the level of the middle of the eye the tendon widens into an aponeurosis. Further distally (anteroventrally) the aponeurosis 1 muscle lies deep (medial) to, and is entirely covered externally by, the aponeurosis 2 muscle. Here the muscle parts exchange fibres.

*Asymmetry.* The temporal part of the muscle is of about the same size and shape on both sides of the head.

The anterodorsal base of the squamoso-occipital wing is located 6.1 mm higher on the right side than on the left (cf. §13.1; table 2:11, 14). Since the tendon of the temporal part of the muscle passes through a foramen in the anterodorsal base of the wing, the part of the tendon-aponeurosis running between this foramen in the meatus roof and the lower jaw insertion, is correspondingly longer on the right side. Further, due to the much more posterior location of the foramen in the meatus roof on the right side, the tendon passes farther posterior to the postorbital process on the right side than on the left. The tendon therefore curves only slightly behind the ventral part of the right postorbital process, whereas on the left side the tendon is forced to curve strongly behind this process.

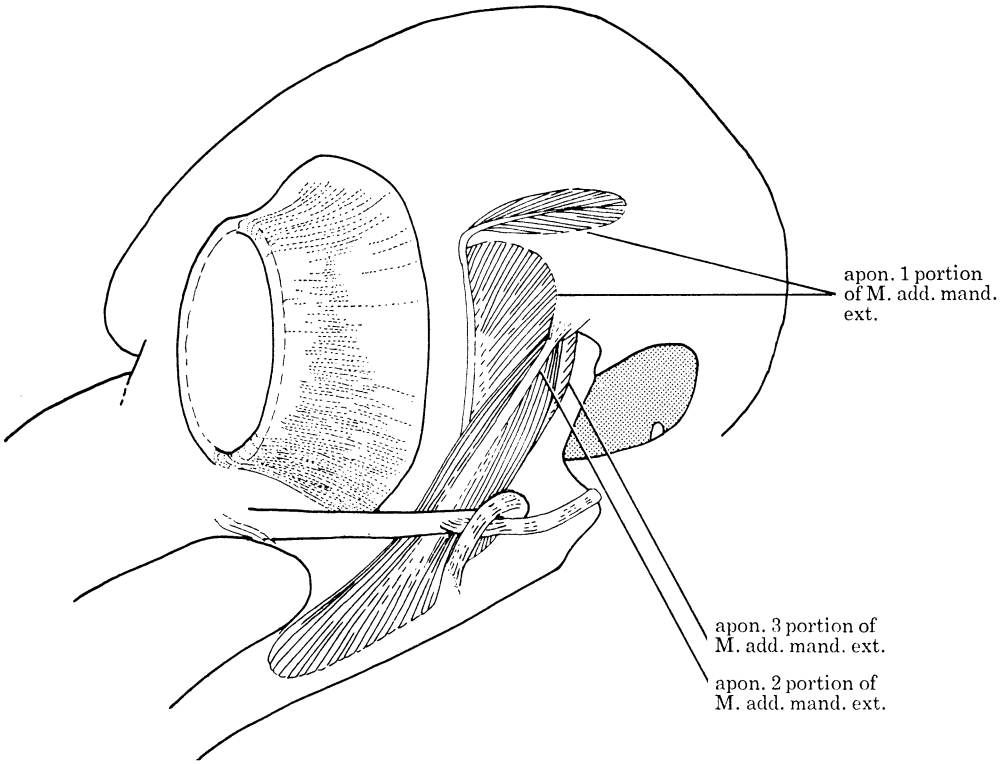


FIGURE 34. The squamoso-occipital wing and M. depressor mandibulae are removed. The strong bilateral asymmetry of the aponeurosis 1 portion of M. adductor mandibulae externus is visible in figures 33 and 34.

In the intact ear the aponeuroses 1 and 2 are clearly visible through the thin skin that covers the medial wall of the external auditory meatus. In the left ear it is the aponeurosis 2 that is best visible (figure 1). The aponeurosis 1 passes closely behind the postorbital process. In the right ear the aponeurosis-tendon 1 is clearly visible (figure 1), whereas the aponeurosis 2 is largely concealed by the anteroventral lobe of the squamoso-occipital wing.

The configuration of muscle fibres originating from the medial wall of the external auditory meatus differs between the left and right ear. In the left ear the fibres join the tendon from a posterodorsal direction and form a wide sheet that covers much of the medial wall of the meatus anterior to the zygomatic process. In the right ear the tendon lies much farther posteriorly, and fibres join the tendon both from a posterodorsal and an anterodorsal direction.

The muscle sheet is more elongated in the dorsoventral direction in the left ear than in the right one, but less extended in the anteroposterior direction. Because the medial wall curves more strongly laterally towards the meatus roof in the left ear than in the right, the tendon, near its passage through the foramen in the meatus roof, comes to be lifted farther away from the medial wall in the left ear than in the right one. The skin lining the anterodorsal wall of the meatus therefore adheres more closely to the bone wall in the right ear than in the left.

TABLE 4. DIMENSIONS OF THE EARDRUM AND THE FOOTPLATE OF STAPES

(Lengths in mm, areas in mm². (Area ratios eardrum/footplate of stapes were calculated with figures containing three digits; before rounding off.))

| specimen: | N.6 | N.8 | G 7910 | | An.1 | N.5 | | *n* | mean |
|---|---|---|---|---|---|---|---|---|---|
| | left | left | left | right | right | left | right | | |
| eardrum | | | | | | | | | |
| 25. longest diameter | 8.6 | 8.2 | | | 8.5 | 8.6 | 8.7 | 5 | 8.5 |
| 26. short diameter | 6.5 | 6.1 | | | 6.4 | 6.5 | 6.6 | 5 | 6.4 |
| 27. height of cone | | | | | | 1.5 | 1.4 | 2 | 1.5 |
| 28. area | 45 | 40 | | | 44 | 43 | 43 | 5 | 43 |
| footplate of stapes | | | | | | | | | |
| 29. longest diameter | | | 1.5 | 1.5 | 1.5 | | | 3 | 1.5 |
| 30. short diameter | | | 1.0 | 1.0 | 1.0 | | | 3 | 1.0 |
| 31. area | | | 1.2 | 1.2 | 1.3 | | | 3 | 1.2 |
| area ratio | | | | | | | | | |
| 32. eardrum/footplate | | | | | 35.1 | | | | 35.3 |

*Aponeurosis 2 portion of M. a. m. e.* (figures 1, 32–34)

*Origin.* On the zygomatic process, by aponeurosis.

*Insertion.* Fibres insert on the dorsal edge and the lateral side of the lower jaw.

*Remarks.* The aponeurosis is a proximal one of origin. The aponeurosis widens distally and covers much of the lateral aspect of the muscle. The muscle spreads distally and attaches to a large area along the dorsal edge and lateral side of the lower jaw, and completely covers the lower jaw fenestra. The attachment is from just anterior to the lower jaw-quadrate articulation and *ca.* 12 mm anteriorly, on to the anterior border of the lower jaw fenestra. This is somewhat anterior to the oral angle and just behind the lower jaw rhamphotheca. On the posterior part of the lower jaw the muscle attachment is dorsomedial to the external jugomandibular ligament.

The muscle exchanges fibres extensively with the aponeurosis 1 and 2 portions which it partly overlies. The aponeurosis 2 portion overlies and covers only the ventral half of the aponeurosis 1 muscle portion that lies in the external auditory meatus, whereas it covers the aponeurosis 3 portion almost entirely. Only a narrow, proximal strip of portion 3 is visible ventral to the zygomatic process.

The aponeurosis 2 portion exhibits bilateral symmetry. Because of the asymmetry of the squamoso-occipital wings, however, the aponeurosis 2 is clearly visible through the skin in the left ear in the intact owl, but in the right ear it is concealed by the anteroventral lobe of the squamoso-occipital wing.

*Aponeurosis 3 portion of M. a. m. e.* (figures 32–34)

*Origin.* On a large area of the anterolateral surface of the dorsal part of the body of quadrate, and on its external otic process (that is just the dorsal continuation of the body of quadrate). Origin by fibres.

*Insertion.* On the posterior coronoid process on the dorsal edge of the lower jaw, i.e. on the supraangular, just dorsal to the insertion of the external jugomandibular ligament. Insertion by aponeurosis.

*Remarks.* The aponeurosis is a distal one of insertion. The aponeurosis 3 portion lies underneath the aponeurosis 2 portion. With all muscles intact, only a narrow strip of the aponeurosis 3 portion is visible near its origin, just ventral to the proximal part of the aponeurosis 2 portion. The aponeurosis 3 runs parallel with the ventral part of the aponeurosis 1 and inserts on the posterior coronoid process. This is located *ca.* 2 mm behind the anterior one on which the aponeurosis 1 inserts. The aponeurosis 3 muscle portion exchanges fibres with the overlying aponeurosis 2 portion.

## 16. Measurements of the eardrum and the footplate of stapes

Below follow a listing and a description of measurements taken on the eardrum and the footplate of stapes. The dimensions are numbered from 25 to 31. Besides, one area ratio is calculated and numbered 32. Results are given in table 4.

25. Length of the longest diameter of the tympanic ring.

26. Length of the tympanic ring diameter normal to the longest, measured at the widest part. The ligament that supports the tympanic membrane across the quadrate is considered part of the tympanic ring, and its width therefore is excluded from the diameter.

27. Height of the cone formed by the eardrum, i.e. the outward displacement of the umbo relative to the plane of the tympanic ring.

28. Area enclosed by the tympanic ring. This equals the base area of the tympanic membrane.

29. Longest diameter of the footplate of stapes.

30. Short diameter of the footplate of stapes, normal to the longest.

31. Area of the footplate of stapes.

32. Area ratio between the tympanic membrane (base area) and the footplate of stapes.

## 17. The eardrum (figures 10–12, 28–31, 35, 36, 38–43)

### 17.1. *Attachment and form*

The eardrum forms a flat, oblique cone, with umbo directed outwards into the external auditory meatus. The eardrums are bilaterally symmetrical to form as well as to position.

The eardrum is spanned in an oval opening, the tympanic ring, that is formed by the squamosal dorsolaterally, the exoccipital posteriorly and posteroventrally, the basiparasphenoid anteroventrally, parasphenoid anteriorly, and the body of quadrate anterodorsally (figures 10–12). Except for the quadrate, the bones supporting the membrane are fused to form a ring. The bony ring is incomplete at the quadrate where it leaves a gap, *ca.* 2.2 mm wide. The eardrum is supported across this gap by a stout ligament that extends between the bony ring ends and also attaches in its whole length to the body of quadrate. The ring end dorsal to the gap is formed by the medial part of the slightly bifurcated postglenoid process of the

squamosal (figures 35, 38–41). This process part curves down behind the body of quadrate and supports the tympanic membrane over part of the quadrate. The ring end ventral to the gap at the quadrate is formed by the parasphenoid. This bone forms a tiny, pointed process, *ca.* 0.3 mm long, that projects in the direction of, and supports the ligament spanning the gap in the bony tympanic ring (figures 35, 40).

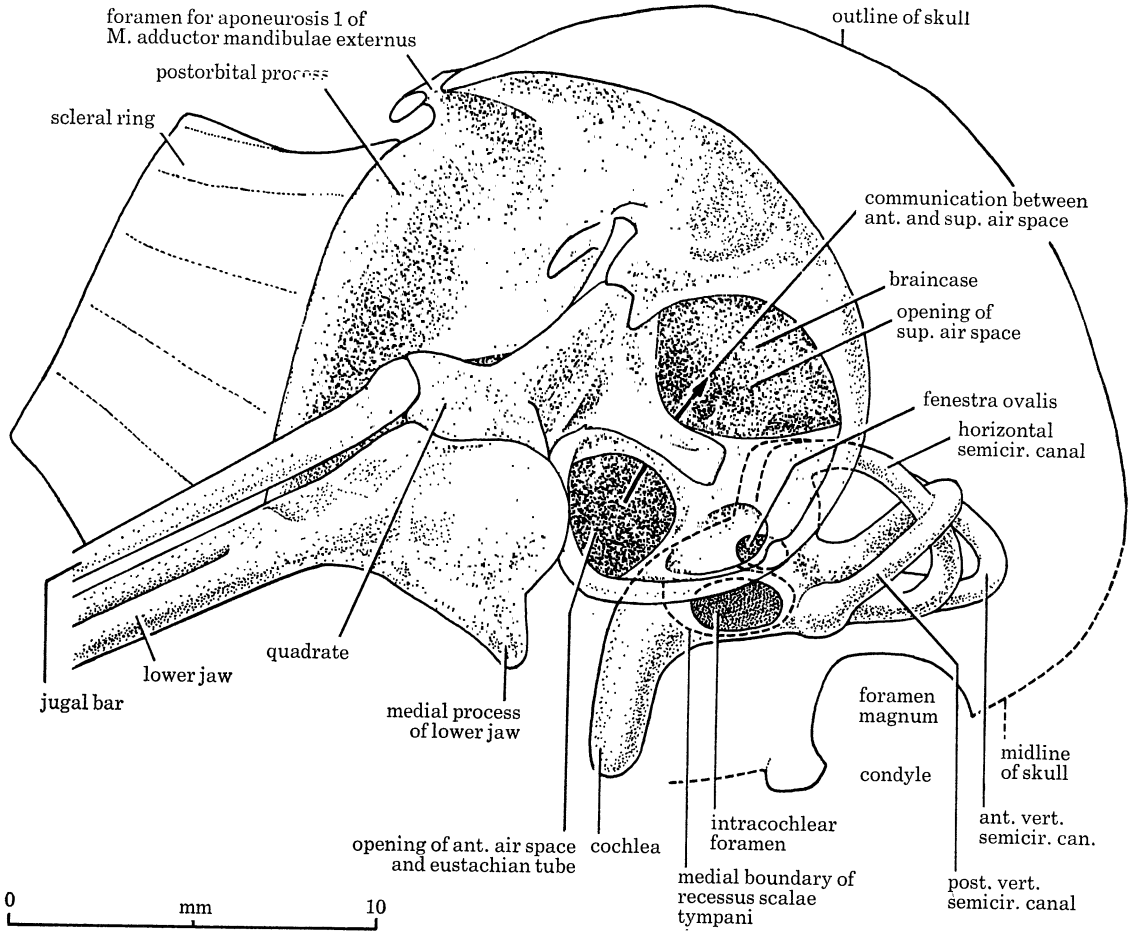


FIGURE 35. Lateroventral view of the skull (N6) with the squamoso-occipital wing removed (cut along the base), thus exposing the medial wall of the left external auditory meatus and the middle ear cavity. The bony cochlea and the bony semicircular canals are dissected partly free. The tympanic ring lies in the plane of the figure. Drawn from photo.

The attachment of the ligament to the quadrate occurs lateral to the pneumatic foramen of the quadrate (figures 37, 38, 41). This foramen thus comes to open into the middle ear cavity.

In the adult skulls examined, there was no trace of ossification of this ligament that bridges the gap in the bony tympanic ring.

### 17.2. *Dimensions*

The longest diameter of the tympanic ring, and thus also of the base surface of the cone formed by the tympanic membrane, is *ca.* 8.5 mm. The diameter normal to this is *ca.* 6.4 mm. The diameter of the tympanic ring along the line of the Ligamentum ascendens is *ca.* 7.1 mm.

The height of the cone, i.e. the outward displacement of umbo, is *ca.* 1.5 mm. The area enclosed by the tympanic ring, i.e. the base area of the eardrum, is 43 mm² (table 4).

### 17.3. *Ligaments of the eardrum*

*Terminology*

In *A. funereus* there are four ligaments that are associated directly with the eardrum.

One ligament spans the gap in the bony tympanic ring and supports the margin of the tympanic membrane across the gap. This ligament was treated in §17.1 and is not further commented upon here.

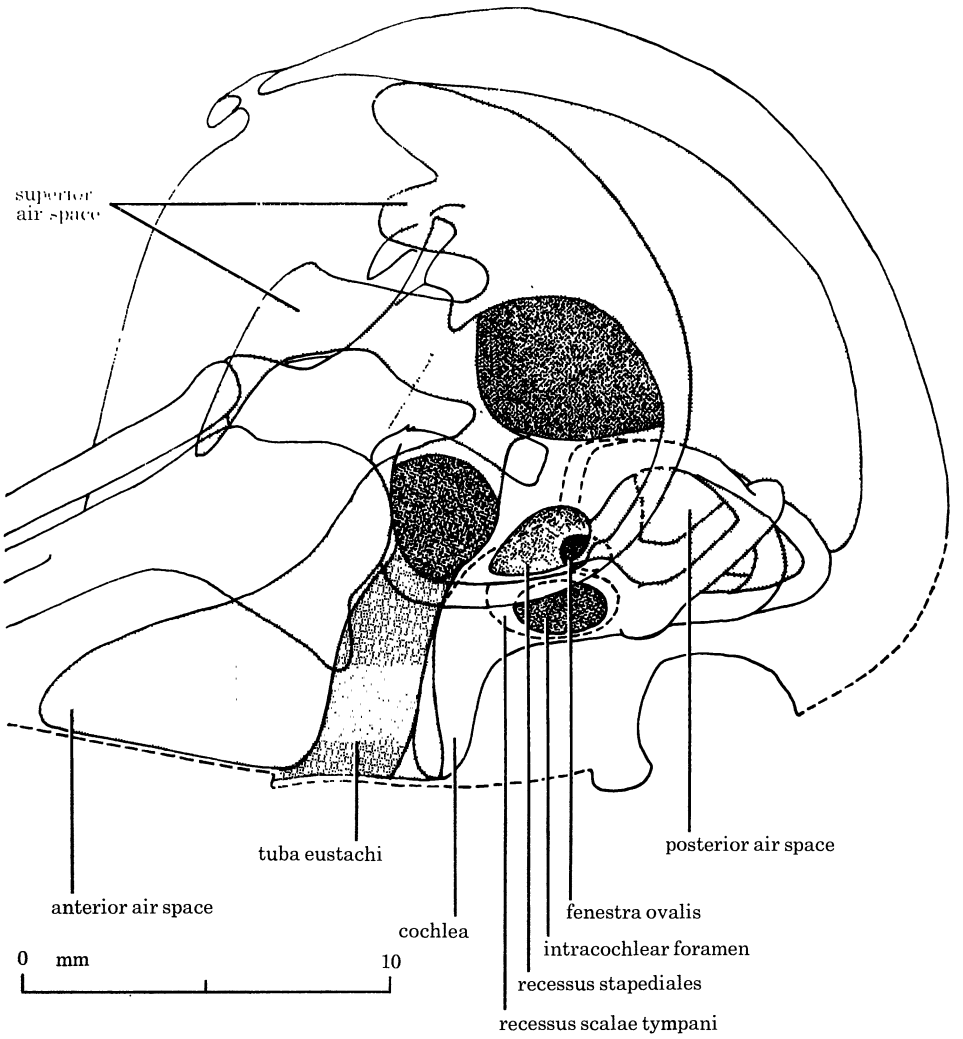


FIGURE 36. Schematic figure, based on figure 35, showing the extent of the eustachian tube and the air spaces communicating with the middle ear cavity.

The largest ligament of the remaining three is the *Ligamentum ascendens* that is located in the posteroventral part of the eardrum and is associated structurally and functionally also with the stapedial complex. This name was used by Dombrowsky (1925, p. 31) who homologized this ligament in birds with the *Ligamentum superius* ('*Sehne der Extracolumella*, Versluys') of the Lacertilia.

Stellbogen (1930, p. 715) treated this ligament in *Strix aluco* under the name '*Sehne der Extracolumella*', while Freye-Zumpfe (1952/53, p. 446) used the name *Ligamentum ascendens*. Werner (1960, p. 219) variously called it '*Ligamentum posterius des Trommelfelles*' and '*Ligament der Trommelfellfläche*'.

In the anterior part of the eardrum in *A. funereus* there are one simple and one bifurcated band of connective tissue that originate on or close to the tympanic ring, inside the eardrum, and that pass along the inner surface of the eardrum and insert on it. They are termed here respectively the *anterior* and the *anteroventral ligament of the eardrum.*

Stellbogen (1930, p. 718) made a note of a band attaching to the anteroventral part of the eardrum in *Strix aluco* and termed it '*Bandmasse*'. Freye-Zumpfe (1952/53, pp. 451, 452) described one similar, probably identical structure associated with the rostral part of the eardrum in *Tyto alba* and *Strix aluco*, and termed it *Septum rostralis.*

In the chicken (*Gallus*) Pohlman (1921, p. 243) described three eardrum ligaments which are associated with the eustachian tube and therefore were named the superior, middle, and inferior *drum-tubal ligament.* They were not illustrated, but their courses seem to deviate from those of the similar eardrum ligaments in *Aegolius.*

In the following description no attempt is made to homologize these two ligaments in *Aegolius* with those described in other birds.

*Ligamentum ascendens* (figures 42–44)

*Origin.* On a flat, rounded bony process on the edge of the tympanic ring in its posteromedial part. The process is very small, jutting out only *ca.* 0.3 mm from the tympanic ring. However, in the skull it clearly indicates the origin of the Ligamentum ascendens and hence the position of the extracolumella.

*Insertion.* The Ligamentum ascendens is attached in its entire length to the middle layer (the *membrana propria*) of the eardrum. The outer epithelial layer of the eardrum, however, is free from the ligament. The ligament is attached also to two processes of the extracolumella. Hence the outer end of the Processus extracolumellaris is attached to the inner surface of the ligament near its apex. Further, the Processus mediocolumellaris attaches to the ligament via a small curved extension. This penetrates into the lateral edge (posterodorsally) of the ligament about halfway from base to apex, and reaches to the midline of the ligament.

*Remarks.* The Ligamentum ascendens is *ca.* 2.9 mm long and 0.5 mm broad and flattened in the plane of the eardrum. It is directed approximately towards the centre of the eardrum. The ligament forms a flat band that is straight except for the apex which bends slightly anteriorly. The apex is smoothly rounded. As projected on the plane of the tympanic ring (i.e. the base plane of the tympanic membrane) the ligament reaches only *ca.* 2.6 mm, or *ca.* 35% of the length of the tympanic ring diameter along the line of the ligament.

The ligament is flexible. However, it is tautened between its process of origin on the rim of the bony tympanic ring and the outer end of the Processus extracolumellaris of the extracolumella. Further, the Processus mediocolumellaris supports the middle part of the ligament. The ligament therefore is rather tense and straight.

The extracolumella is relatively stiff and raises the ligament so that it forms an angle of *ca.* 30° with the base plane of the eardrum. The apex of the ligament supports the tip of the oblique cone that the eardrum thus comes to form.

The outward displacement of the eardrum is due primarily to the stapedial complex and

only secondarily to the Ligamentum ascendens that is flexible and held in position by the extracolumella.

*Function.* The Ligamentum ascendens forms one functional unit together with the extracolumella. This unit picks up vibrations from the eardrum and is the functional equivalent of the mammalian ear ossicles malleus and incus. Functionally the Ligamentum ascendens corresponds to the manubrium of the mammalian malleus (cf. §25).

*Anterior ligament of the eardrum* (figure 42)

*Origin.* The ligament originates from a tiny bony process, only *ca.* 0.2 mm long, on the parasphenoid just where it curves posteromedially below the gap, at the quadrate, in the bony tympanic ring (figures 35, 40). This process lies immediately (*ca.* 0.3 mm) inside the inner edge of the tympanic ring and hence just inside the eardrum. This process also lies immediately (0.3 mm) medial to the tiny process that supports the anteriomedial end of the ligament that spans the gap in the bony tympanic ring (cf. §17.1).

*Insertion.* The ligament inserts in the anterior part of the tympanic membrane along a line, *ca.* 1.5 mm long.

*Remarks.* The ligament is *ca.* 1.5 mm long and wider than either arm of the anteroventral ligament. It inserts in its whole length along a line that runs from the ligament's origin below the gap in the tympanic ring and posterodorsally along the eardrum, just posterior to the quadrate.

*Function.* The ligament probably keeps the anterodorsal part of the eardrum taut. Due to its position and orientation behind the gap in the bony tympanic ring it may also tend to relieve the eardrum from strains caused by streptostylic rotating movements of the quadrate.

*Anteroventral ligament of the eardrum* (figure 42)

*Origin.* The ligament originates from the inner side of the anteroventral part of the bony tympanic ring, *ca.* 0.5 mm from the inner rim of the ring. The point of origin lies *ca.* 0.5 mm posteromedial to the inner foramen of the canal, through which the middle ear cavity communicates with the lower jaw via the siphonium. The point of origin also lies in the bottom of the entrance to the tuba eustachii.

*Insertion.* The ligament inserts into the anteroventral part of the eardrum. The insertion is along two lines, each *ca.* 2 mm long, that diverge at the margin of the eardrum and form an almost right angle with each other. After *ca.* 2 mm the ligament branches dwindle into nothing.

*Function.* The ligament probably keeps the anteromedial part of the eardrum taut.

## 18. The middle ear cavity and associated air spaces (figures 25, 35–43)

When looking into the middle ear through the tympanic ring, three distinct subcavities of the middle ear cavity are visible. A heavy bony ridge crosses the middle ear approximately along the short diameter of the tympanic ring. Dorsolateral to this ridge is one large opening, and ventromedial to it are two smaller openings that are separated by a small, narrow ridge.

The large bony ridge traverses the middle ear from the gap in the anterolateral part of the bony tympanic ring, on to the posteromedial rim of the ring. The anterolateral half of his ridge is made up of the internal otic process of quadrate, and of a thin flange of the

parasphenoid lying ventral to, and supporting the quadrate process. This process lies in a groove that hollows out the underlying bone (figure 39). In the posteromedial, terminal end of this groove there is an elongated, concave articular facet. A portion of the articular facet lies in the bottom of the groove and via a narrow central part continues into a posterior portion that terminates the groove (figure 39).

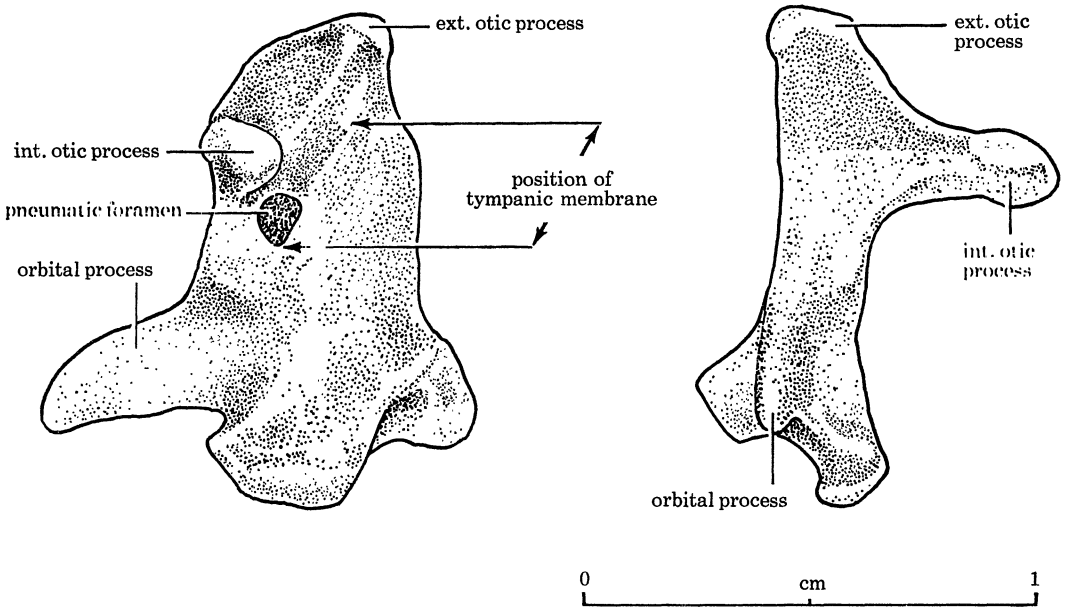


FIGURE 37. The quadrate of the right side (G 7910). Left: The long axis of the body of quadrate and its orbital process lie in the plane of the figure. Right: The long axis of the body of quadrate and its internal otic process lie in the plane of the figure.

The internal otic process juts out perpendicularly to the body of the quadrate and extends into the middle ear somewhat farther than half the short diameter of the tympanic ring (figures 35, 37). On the medial side of the distal end of this process there is an elongated, convex articular facet that continues to and covers the apex of the process. It fits against the corresponding articular surface that terminates the groove.

For most of its length the middle ear ridge lies well internal to the plane of the tympanic ring. But near the centre of the tympanic ring the apex of the internal otic process of quadrate, and adjacent parts of the ridge, reach out to the plane of the tympanic ring, i.e. to the base plane of the tympanic membrane (figures 41, 43).

As described in §9.1 the anterolateral part of the ridge, forming the groove for the internal otic process of quadrate and the flange ventral to this process, is formed by the parasphenoid (figures 11, 12). A large segment of the posteromedial part of the bony ridge, including the articular facet that terminates the groove, is formed by the prootic (figure 10). The most posteromedial part of the ridge is formed by the exoccipital.

The external otic process of quadrate is a rectilinear continuation of the body of quadrate and articulates in a socket in the squamosal anterodorsal to the eardrum. Dorsal and posterior to the articular socket the squamosal forms a very thin wall between the external auditory meatus and the underlying superior air space and middle ear cavity. The anterolateral aspect of the external otic process faces outwards into the external auditory meatus while the posteromedial

aspect is inside the thin squamosal wall and lies in the anterior part of the dorsal subcavity of the middle ear (figure 35).

The opening dorsal to the heavy ridge occupies almost half the area enclosed by the tympanic ring. It is the entrance of the superior air space.

Below the ridge containing the internal otic process of quadrate there is a less pronounced ridge that is set at about right angles to the first. It passes from the region of the apex of the

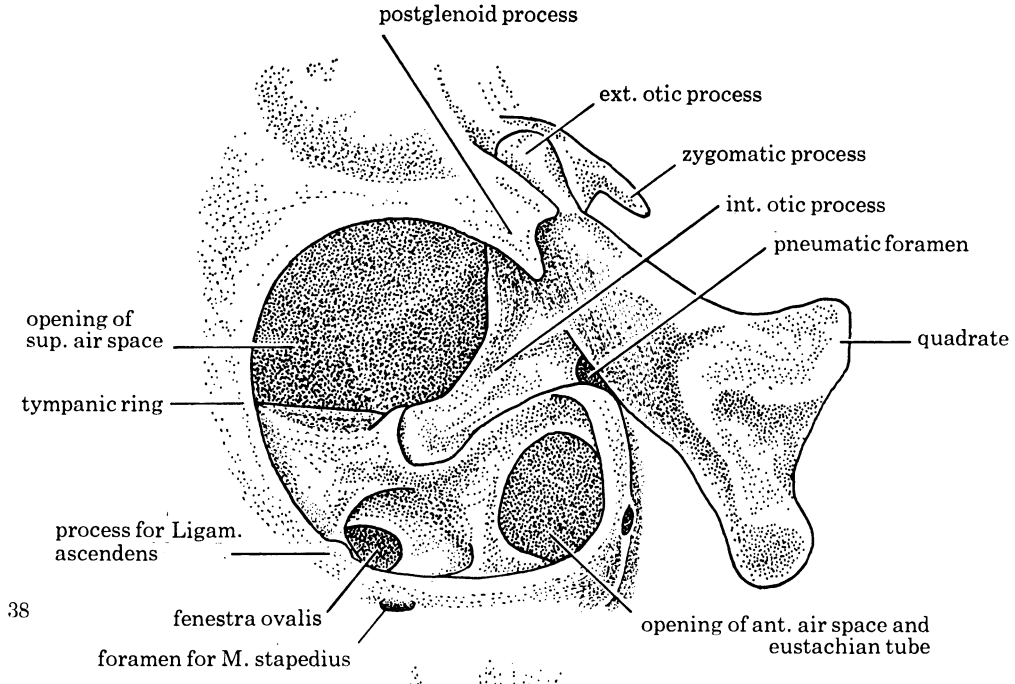


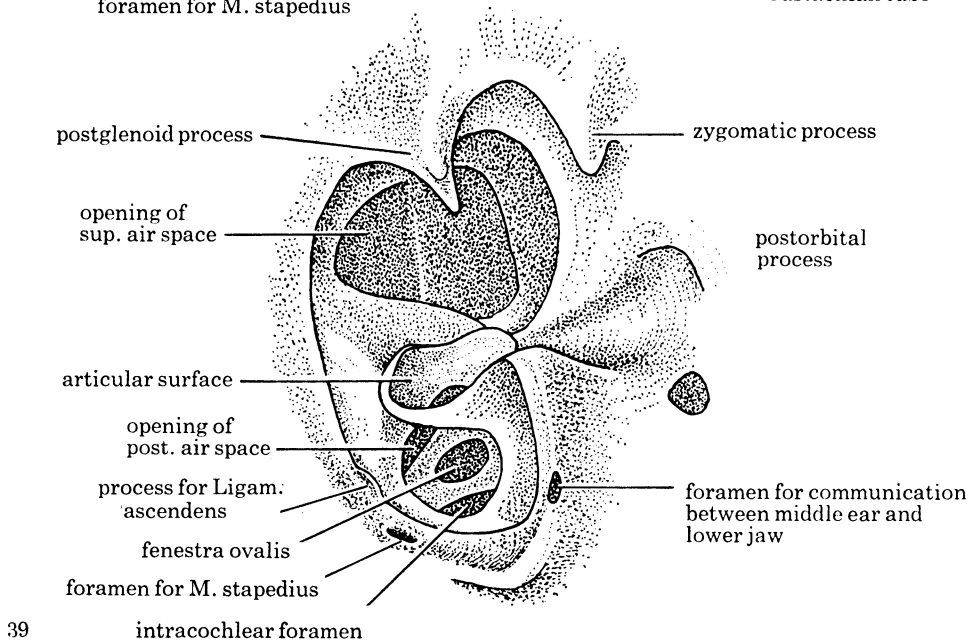


FIGURE 38. The quadrate and middle ear cavity on the right side (G 7910). The tympanic ring is in the plane of the figure.

FIGURE 39. Anterolateral view of the middle ear cavity on the right side (G 7910). The quadrate is removed.

internal otic process of quadrate and anteroventrally on to the ventromedial rim of the tympanic ring.

The cavity anterior to this almost vertical ridge communicates with the dorsal cavity via an opening in the parasphenoid underneath the middle part of the internal otic process of quadrate (figures 35, 36, 43). The anteroventral subcavity of the middle ear is the opening of the anterior air space and the eustachian tube. Via the siphonium it also communicates with the space in the lower jaw.

The posterior one of the two ventromedial subcavities is termed the recessus stapediales (cf. below). It is the site of the stapedial complex, the fenestra ovalis and fenestra rotunda. It is also the opening of the posterior air space.

The middle ear cavity and all associated air spaces except for the superior one are symmetrically developed on the two sides. The superior air space occupies much of the interior of the squamosal and hence is affected by its asymmetry.

The various air spaces communicating with the middle ear, and the recessus stapediales will be described in turn below.

In the intact head the bones bounding the middle ear and associated air cavities are lined with epithelia (mucous membrane). The soft anatomy does not affect significantly the extent and form of the cavities as seen in the skull. The description below is from the intact head.

*The superior air space*

From the wide opening in the dorsal half of the middle ear cavity the superior air space extends anteriorly, dorsally, and posteriorly.

The superior air space sends a narrow extension anteriorly on to the ventral part of the base of the postorbital process, the basal part of which it invades. The opening from the middle ear to this forward extension is *ca.* 3 by $1\frac{1}{2}$ mm wide and lies dorsomedial to the proximal part of the internal otic process of quadrate (figures 36, 40). The proximal, pneumatic part of the postorbital process thus communicates with the middle ear.

Anterodorsally the superior air space extends between the medial wall of the external auditory meatus and the braincase. It further extends dorsally and posteriorly lateral to the braincase and dorsal to the horizontal and the posterior vertical semicircular canal. The anterior vertical canal lies in the medial wall of the superior air space which here bulges into the posteromedial part of the braincase to accommodate the canal. The anterior vertical canal lies at the circumference of the bulge into the braincase.

The braincase wall medial to the superior air space and also the wall separating the superior air space from the external auditory meatus are very thin. Only towards the dorsal and posterior flat parts of the superior air space do bony strands and thin septa connect the medial and lateral walls of the air space. Further medially the bone becomes spongy, and there is no communication between the superior air space on the left and right side.

The superior air space communicates with the anterior air space via a $1\frac{1}{2}$ mm wide opening underneath the middle part of the internal otic process of quadrate (figures 36, 43).

*Asymmetry.* The medial wall of the external auditory meatus curves strongly outwards dorsally on the left side, whereas it continues farther dorsally, and hence is flatter, on the right side where the ear opening of the skull is located higher. Owing to this asymmetry the superior air space on the left side comes to extend anterodorsally on to *ca.* 2 mm behind the dorsal base of the postorbital process, whereas on the right side it terminates *ca.* 6 mm

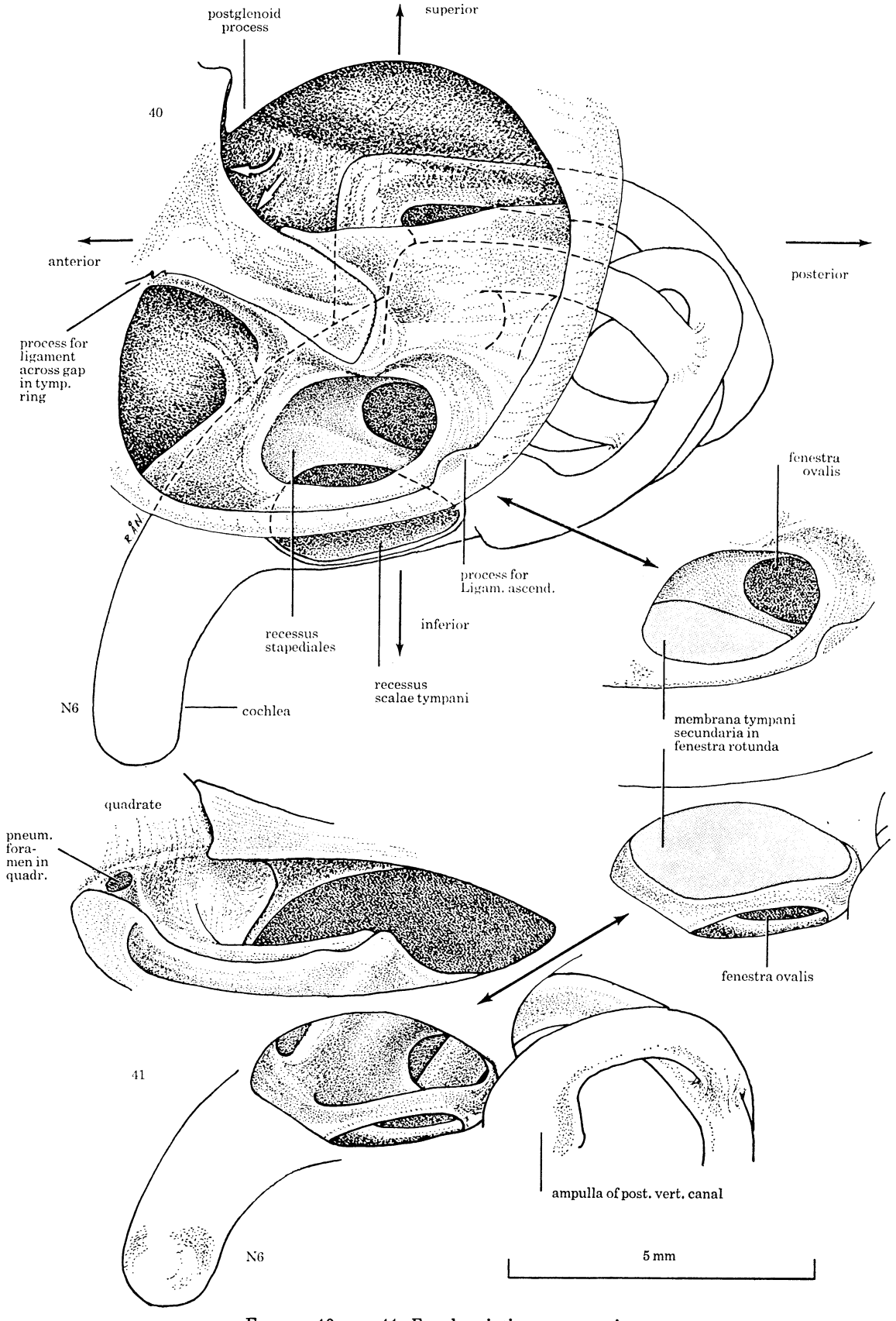


FIGURES 40 AND 41. For description see opposite.

behind the dorsal base of the postorbital process. Further, the left superior air space extends farther laterally over the external auditory meatus than does the flatter right cavity. Finally, the left superior air space does not extend as far dorsally as does the right one.

*The anterior air space*

The anteroventral subcavity of the middle ear is the opening of the anterior air space and eustachian tube. From the middle ear the anterior air space extends anteromedially and lies anteroventral to the braincase. In its narrowest part, where leaving the middle ear, it is almost circular in cross section and with a diameter of *ca.* 3 mm.

The anterior air space is bounded posteromedially by the braincase and the bony cochlea. It extends forwards into the whole of the sphenoid rostrum and the ventral half of the interorbital septum. The interorbital septum is hollow in its ventral half, and its walls are rather thin. The septum is not fenestrated. The cavity in the interorbital septum is continuous with that in the sphenoid rostrum.

The left and right anterior air space, and hence the left and right middle ear cavities, communicate widely in the sphenoid rostrum and interorbital septum, from the level of the apex of the cochlea and anteriorly on to the level of the lateral process of the interorbital septum. This medial communication opening has a length of *ca.* 8 mm along the sphenoid rostrum and a greatest height of *ca.* 4 mm as measured normal to the rostrum. The only minor obstruction in this communication opening is formed by the ascending bony tube of the carotid canals. They unite medially in the cavity of the sphenoid rostrum and ascend *ca.* $2\frac{1}{2}$ mm anterior to the tips of the cochlae.

*The eustachian tube*

From the anteroventral subcavity of the middle ear the eustachian tube runs anteromedially and in its whole extent lies ventral to the anterior air space. It passes along the anterior surface of the bony cochlea distal to the bend in the cochlea, and is covered ventrally by the ventral plate of the basiparasphenoid. In the skull's midline the left and right eustachian tubes fuse and open anteriorly in a common aperture (figures 25, 36).

The eustachian tube is separated from the anterior air space by an anteriorly running part of the carotid canal laterally, and by an almost horizontal bony partition wall medially (figures 12, 25).

From the outer opening of the carotid canal in the exoccipital (figure 25) the bony carotid canal runs anterodorsally and fuses with the lateral wall of the bony cochlear proximal to its

---

FIGURE 40. The middle ear cavity, the bony cochlea, and the bony semicircular canals of the left side (N 6). The tympanic ring is not in the plane of the figure. Oblique view; the anterodorsal part of the tympanic ring, i.e. the part at the postglenoid process, is somewhat closer than the rest of the ring. The view therefore is somewhat in underneath the ventromedial rim of the tympanic ring.

The inset figure below and to the right of figure 40 shows the recessus stapediales, in the same orientation and scale as in figure 40, but with the membrana tympani secundaria indicated in the fenestra rotunda.

FIGURE 41. As figure 40 (N.6), but the middle ear seen from a ventral direction. The ventral wall of the recessus scalae tympani (of the cochlea) is removed to expose the bottom of the recessus stapediales. The bony bridge between the fenestrae rotunda and ovalis is seen in the bottom of the recessus stapediales (the horizontal bar), and the fenestra ovalis is seen from inside the cochlea.

The inset figure at bottom right shows the recessus stapediales in the same orientation and scale as in figure 41, but with the membrana tympani secundaria indicated in the fenestra rotuda. The scale is for figures 40, 41 and inset figures.

curvature. At the bend of the cochlea the carotid canal separates from the cochlea *ca.* 1 mm dorsal to the ventral wall of the eustachian tube (the basiparasphenoid plate) and passes *ca.* 1½ mm anteriorly, thus separating the eustachian tube from the anterior air space. The carotid canal then turns anteromedially, fuses with the ventral wall of the parasphenoid, underneath and approximately along the anteromedially running flange of the basiparasphenoid, and thereby forms the anterior boundary of the middle part of the eustachian tube (figure 25). Near the skull's midline the carotid canal turns dorsally, fuses with the contralateral carotid canal, and then enters the braincase via a common, medial, ascending bony tube.

Medially the horizontal partition wall, separating the tuba eustachii from the dorsal to it lying anterior air space, connects the bony tube for the carotid canals with the distal 1½ mm of the bony cochleae. Between the tips of the cochleae and posterior to the eustachian tubes, the horizontal partition wall fuses with the ventral plate of the basiparasphenoid.

Medially, the left and right eustachian tubes communicate via a dorsoventrally compressed passage between the horizontal partition wall dorsally, and the ventral plate of the basiparasphenoid ventrally. The cross-section area measures *ca.* ½ by 2 mm. This communication passage between the middle ear cavities thus is much smaller than that of the anterior air space in the sphenoid rostrum and interorbital septum.

In the skull's midline the fused eustachian tubes open anteriorly via a dorsoventrally compressed aperture, *ca.* 1½ by ½ mm large. The opening is covered ventrally by a flange drawn out anteriorly from the ventral plate of the basiparasphenoid.

The eustachian tube and anterior air space communicate via a foramen, *ca.* 1½ by 3 mm large, bounded laterally and anteriorly by the carotid canal, medially by the horizontal partition wall, and posteriorly by the bony cochlea. Distal to its bend the cochlea lies on the borderline between the eustachian tube and the anterior air space (figure 25).

*The posterior air space*

The posteroventral subcavity of the middle ear, the recessus stapediales, is the entrance to the small posterior air space. The opening is over the fenestra ovalis and under the posteromedial rim of the tympanic ring. It also extends under the posterior part of the heavy bony ridge that crosses the middle ear in an anterolateral-posteromedial direction. The opening measures *ca.* 1 by 2 mm. This opening leads in ventral to the horizontal semicircular canal and anterior to the posterior vertical canal (figures 35, 36, 39–41).

The posterior air space is contained in the space between the horizontal and the posterior vertical semicircular canal. The two dorsal openings between these canals, the posteroventral and the anteroventral opening, except for the passage to the recessus stapediales, are closed by four irregular bony walls. These walls and the canal parts they connect form the boundary of the posterior air space.

*The quadrate air space*

The quadrate is hollow. On the posterior aspect of the body of quadrate, close to the base of the internal otic process of quadrate, there is a pneumatic foramen *ca.* 0.9 by 1.4 mm in size (figures 37, 38, 41). This foramen is located just inside the eardrum, i.e. just medial to the band of connective tissue that attaches to the quadrate and supports the tympanic membrane across the gap in the bony tympanic ring at the quadrate. The foramen thus does not

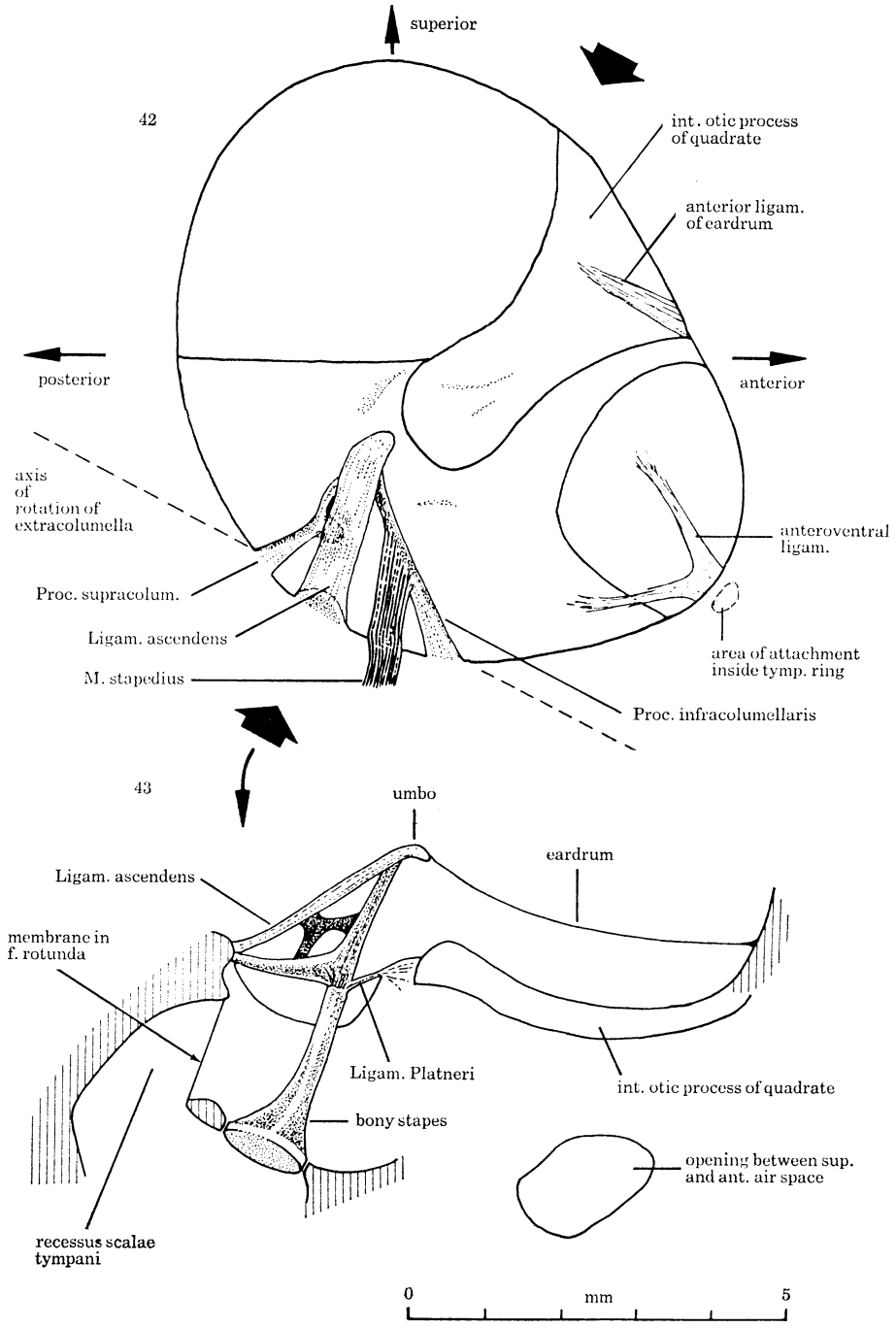


FIGURE 42. The tympanic ring and stapedial complex of the right side. The tympanic ring is in the plane of the figure. The stapedial complex is in its natural position.

FIGURE 43. Anterior view of the right middle ear cavity (the same as in figure 42) with the stapedial complex and the eardrum in natural positions. The plane of the tympanic ring and the axis of rotation of the extracolumella are normal to the plane of the figure. Hatched areas denote cut bone. The scale is for figures 42 and 43.

open into any of the three subcavities of the middle ear, but is located over the anterolateral base of the heavy bony ridge that crosses the middle ear cavity (figure 41).

*The lower jaw air space*

The posterior, extended part of the lower jaw, and the medial process of the lower jaw contain a strongly dorsoventrally flattened, tiny air space.

The medial process of the lower jaw has a small pneumatic foramen, *ca.* 0.4 by 0.7 mm in size, on its dorsal side *ca.* 1½ mm from the apex. A tube of connective tissue, the *siphonium*, *ca.* 1.8 mm long, 0.6 mm internal diameter, passes from this foramen to a foramen in the anteromedial part of the tympanic ring (figures 30, 39). The foramen in the tympanic ring is *ca.* 0.4 by 0.6 mm in size. Through these foramina and the tube, the cavity in the pneumatized posterior part of the lower jaw communicates with the middle ear cavity.

*The recessus stapediales*

Following Freye-Zumpfe (1952/53, p. 446) and Stresemann (1934, p. 129) the posteroventral subcavity of the middle ear is termed the recessus stapediales. The opening leading in to this subcavity is bounded posteriorly, dorsally, and anteriorly by the two bony ridges of the middle ear. The ventral rim of the opening is formed by a bone flange extending inwards from the ventral part of the tympanic ring.

Posteriorly the recessus stapediales communicates with the posterior air space that extends in between the horizontal and the posterior vertical semicircular canal. In the bottom of the recessus stapediales lies the fenestra ovalis. When the middle ear cavity is viewed normal to the plane of the tympanic ring only the anterior half of the fenestra ovalis is visible (figure 35). The posterior half lies underneath the posterolateral rim of the tympanic ring.

When the middle ear is viewed normal to the plane of the tympanic ring, the process (on the edge of the ring) for the Ligamentum ascendens is located right over the fenestra ovalis.

The membrane closing the fenestra rotunda, the *membrana tympani secundaria* (see for example, Pohlman 1921, p. 249), forms the ventromedial boundary of the recessus stapediales. The posterior, dorsomedial, and anterior lines of attachment of this membrane are poorly indicated in the skeleton.

Posteriorly the membrane attaches to a bone wall that passes between the posteromedial part of the tympanic ring and the wall of the bony cochlea just anterior to the ampulla of the posterior vertical semicircular canal (figures 40, 41). Dorsomedially, the membrane attaches to the bony bar that separates the fenestrae ovalis and rotunda. The outward surface of this bar is slightly angled, the faint ridge marking the line of attachment (figures 40, 41). Anteriorly the membrane attaches to the posterior wall of the almost vertically oriented bony ridge of the middle ear. Ventrolaterally, finally, the membrane attaches to the edge of the narrow bony flange that extends inwards from the ventromedial part of the tympanic ring and forms the ventromedial rim of the opening to the recessus stapediales.

Internal to the fenestra rotunda membrane the recessus scalae tympani is widened into a chamber that opens into the cochlea via a large oval aperture, the intracochlear foramen (figures 35, 39–41).

*Volumes*

No direct volume measurements by means of fluid injection could be done on the middle ear cavity and associated cavities. Therefore volume estimates were made through calculations based on linear dimensions and geometry of the cavities.

For volume estimation, the extent of the middle ear cavity is defined as follows. The cavity is delimited laterally by the tympanic ring and its inward projection normal to the plane it is lying in. The inner boundary is formed by the various bony structures in the bottom of the cavity. Externally it is delimited by the conical tympanic membrane. The volume of this cavity is *ca.* 170 $mm^3$.

The volume of the left superior air space, the dorsal subcavity of the middle ear cavity excluded, is *ca.* 372 $mm^3$. Although of somewhat different shape, the right superior air space is of roughly the same volume.

The volumes of the anterior air space and eustachian tube, up to the median plane of the head, and with the anteroventral subcavity of the middle ear excluded, are *ca.* 143 $mm^3$ and 14 $mm^3$, respectively.

The posterior air space, the recessus stapediales excluded, has a volume of *ca.* 33 $mm^3$.

The volume of the quadrate air space is *ca.* 25 $mm^3$, and that of the lower jaw air space *ca.* 2 $mm^3$.

The volume of the recessus stapediales was included in the middle ear cavity volume above.

The combined volume of the middle ear cavity and of the air spaces communicating freely with it via relatively large openings, namely the superior, anterior, and posterior air space and the eustachian tube, amounts to *ca.* 730 $mm^3$. In the above sum, the volumes of the anterior air space and the eustachian tube of one side only are included (although the left and right ones of these two cavities communicate in the sphenoid rostrum).

The middle ear cavity and associated air spaces thus are very spacious and those of one ear have a combined volume almost as large as that of one external auditory meatus (*ca.* 730 $mm^3$ and *ca.* 830 $mm^3$ respectively).

## 19. The stapedial complex and associated structures

The *stapedial complex*, or *Columella auris*, consists of an inner bony *stapes* and an outer cartilaginous *extracolumella*. The extracolumella is composed of several processes that fix the stapedial complex to the tympanic ring and the eardrum.

The terminology above is decided upon from the variety of prevalent sets of terms, with a mixing of names that tends to confuse. Thus Romer (1962, pp. 489, 490) called the whole stapedial complex the *stapes* or *columella*, while the bony stapes was termed *stapes proper* or *columella*. Olson (1966, pp. 400, 401, on reptiles) and Bellairs & Jenkin (1960, pp. 281, 282, on birds) equate *extracolumella* with *extrastapes* and *columella* with *stapes*.

The terminology used for the extracolumellar parts is adopted from Stellbogen (1930) and Freye-Zumpfe (1952/53).

The *Ligamentum ascendens* is closely associated with the stapedial complex both structurally and functionally. However, it is described in §17.3, and will be treated here only in connection with other structures attached to it.

Although strictly not parts of the stapedial complex, one other ligament, the *Ligamentum platneri*, and one muscle, the *Musculus stapedius*, will be described in this section.

Both structures are closely related to the stapedial complex both structurally and functionally. The entire stapedial complex of the left and right ear exhibits complete bilateral symmetry.

*The axis of rotation of the extracolumella*

In the following description of the stapedial complex spatial relations are sometimes given relative to the *axis of rotation* or *fulcral axis* of the extracolumella. This axis is functionally founded and is defined as the line that lies in the plane of the tympanic ring and passes through the end of the Processi infracolumellaris and supracolumellaris that attach to the rim of the tympanic ring. This axis comes to pass also through the base of the Ligamentum ascendens just at its attachment to the bony process for this ligament on the rim of the tympanic ring. In response to impringing sound the whole extracolumella rotates about this axis. Hence it is functionally relevant to relate spatial descriptions to it.

*The bony stapes*

The bony stapes is *ca.* 2.5 mm long and composed of a shaft with an expanded footplate fitted into the fenestra ovalis. The shaft and foot are hollow and extremely thin-walled. The footplate is oval and *ca.* 1.0 by 1.5 mm (table 4). The surface of the footplate abutting against the perilymph of the internal ear has a very slight eminence near the centre and thus is almost flat. The footplate sits eccentrically on the shaft. The central axis of the shaft intersects the long diameter of the footplate at a point *ca.* 30 % of the diameter from the anterior margin of the footplate. Towards the footplate the shaft widens gradually thus forming a funnel-shaped connection. In this widened part there are a few pneumatic foramina, the number and size of which vary between specimens.

Near the footplate the cross-section of the shaft is almost circular. Towards the outer end that fuses with the extracolumella, the shaft, and also the end of the Processus extracolumellaris fused with it, are strongly flattened and markedly laterally widened. The plane of compression of the joint between the shaft of stapes and the Processus extracolumellaris deviates *ca.* 30° from the short diameter of the footplate and is parallel with the fulcral axis of the extracolumella.

The shaft of the stapes is fused completely with the Processus extracolumellaris, the joint being a synarthrosis. Since the extracolumella is cartilaginous, the union may be specified as a synchrondrosis.

Because of its strong compression, the joint between the shaft of stapes and the Processus extracolumellaris is permissive of flexion by deformation of the cartilage. The line about which flexion occurs is parallel with the fulcral axis of the extracolumella.

The orientation of the bony stapes relative to the extracolumella and tympanic ring is as follows:

The shaft of the stapes and the Processus extracolumellaris lie on a line and are set obliquely to the plane of the tympanic ring. More precisely, the long axis of the stapedial complex forms an angle of *ca.* 68° with the plane of the tympanic ring as measured in a plane normal to that of the tympanic ring and normal to the fulcral axis of the extracolumella. The angle of inclination in a perpendicular plane, i.e. in a plane normal to that of the tympanic ring but parallel with the fulcral axis, is *ca.* 15°. The inclination is such that the footplate of stapes lies anteroventral to the umbo of the eardrum as seen perpendicularly to the base plane of the eardrum. Owing to the oblique orientation of the stapedial complex, the footplate of the

stapes is right under the posteromedial rim of the tympanic ring (figures 35, 36, 38, 43). The attachment of the extracolumella at the umbo of the eardrum cone is located at *ca.* 35% of the length of the tympanic ring diameter (in line with the Ligamentum ascendens) inside the tympanic ring.

*The extracolumella*

The extracolumella is cartilaginous and solid and composed of several processes which are described below.

The extracolumella is firmly fixed to the tympanic ring via the Ligamentum ascendens and the Processi infracolumellaris and supracolumellaris which attach to the tympanic ring, one on either side of the Ligamentum ascendens.

The tip of the Ligamentum ascendens attaches to, and overlaps, the outer tip of the Processus extracolumellaris, and hence marks the position of the long axis of the stapedial complex on the eardrum.

The extracolumella with the Ligamentum ascendens attaches to the tympanic ring almost exactly at the part that is located farthest away from the ear opening of the skull, i.e. at the posteromedial termination of the external auditory meatus (cf. §14.2).

*Processus extracolumellaris.* This process forms a direct and rectilinear continuation of the shaft of stapes. It is *ca.* 1.8 mm long and thus almost 75% the length of the bony stapes. It is the heaviest one of the processes forming the extracolumella. Its anterodorsal surface (facing towards the centre of the middle ear cavity) is convex, the other concave. The process is rather wide and has a crescent-shaped cross section.

At its joint (synarthrosis) with the shaft of the bony stapes the process is strongly flattened in one plane as described under 'The bony stapes'.

The outer end of the process inserts into and attaches firmly to the inner side of the Ligamentum ascendens near its apex. The angle between the Processus extracolumellaris and the ligament is *ca.* 38°. The outer end of the Processus extracolumellaris, thus covered by the distal part of the Ligamentum ascendens, displaces the eardrum outwards and underlies the umbo of the eardrum cone. The attachment of the Processus extracolumellaris to the eardrum via the Ligamentum ascendens occurs eccentrically and is in the posteroventral quadrant of the eardrum, at *ca.* 35% of the length of the tympanic ring diameter (in line with the Ligamentum ascendens) from the eardrum margin.

*Processus infracolumellaris.* From the anteroventral edge of the Processus extracolumellaris at its fusion with the bony stapes, the Processus infracolumellaris juts out at an angle of *ca.* 70° with the stapes. The other end attaches to the tympanic ring *ca.* 1.5 mm anterior to the origin of the Ligamentum ascendens. The process is *ca.* 1.8 mm long and flattened. At its origin from the Processus extracolumellaris the Processus infracolumellaris is flattened along its line of attachment. Towards its attachment to the tympanic ring the process is somewhat widened and twisted through *ca.* 90° such that its edge nearest to the eardrum (the lateral edge) comes to lie nearest the Ligamentum ascendens, its plane of compression being parallel to that of the tympanic ring. From its attachment to the tympanic ring and *ca.* 0.5 mm outwards the process is attached to the eardrum.

*Processus supracolumellaris.* This process originates from the posterodorsal edge of the Processus extracolumellaris at its fusion with the shaft of the bony stapes, i.e. at the same level as the origin of the Processus infracolumellaris. The Processus supracolumellaris is *ca.* 1.2 mm long

and forms an angle of *ca.* 90° with the bony stapes and one of *ca.* 70° with the Processus infracolumellaris. The Processus supracolumellaris is about parallel with the long axis of the footplate of stapes. The process is flattened, the proximal end being compressed along its line of origin. Towards its attachment to the tympanic ring the process is twisted in the same way

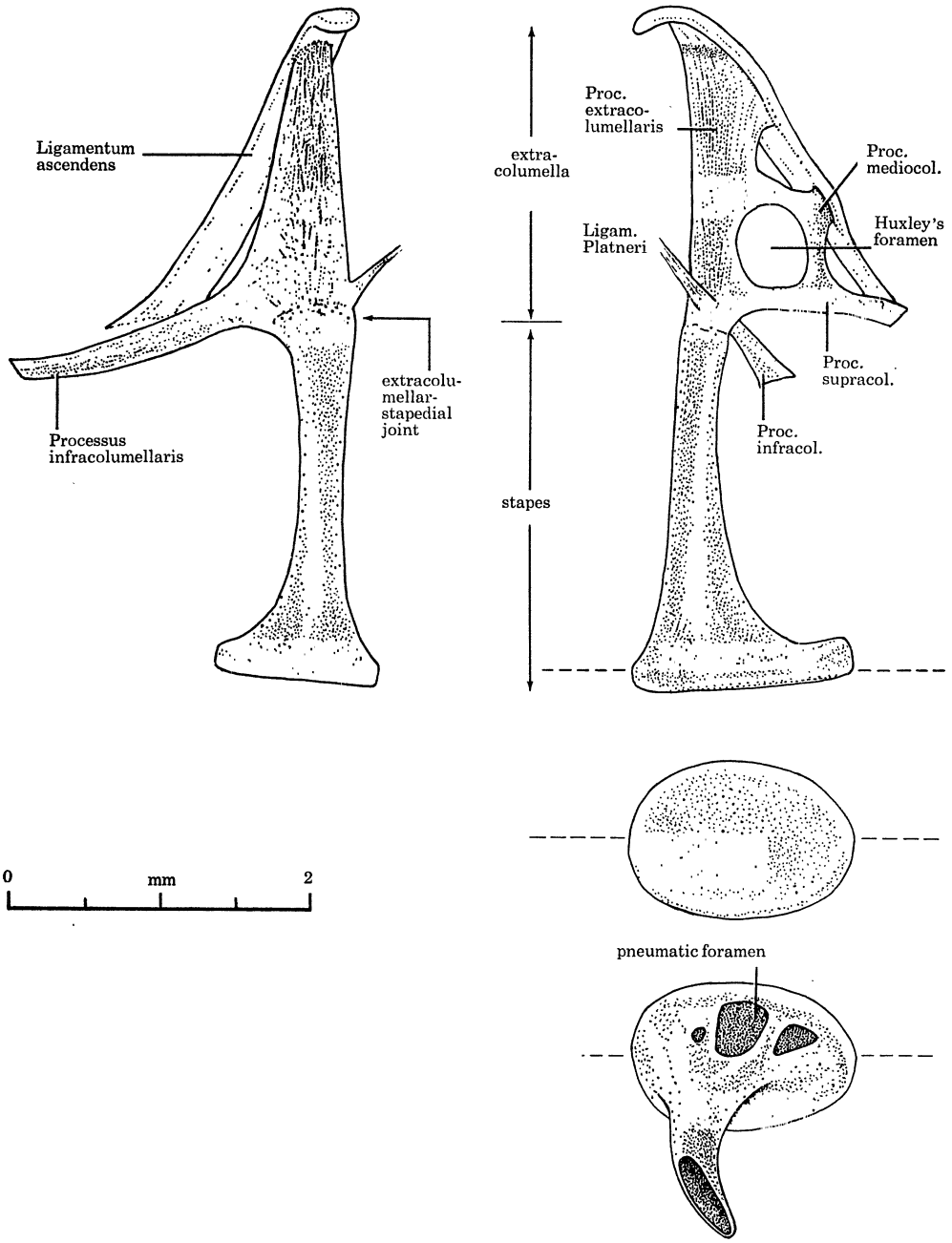


FIGURE 44. The stapedial complex of the right side. *Left*: The long axis of the stapedial complex and the Processus infracolumellaris lie in the plane of the figure. *Upper right*: The long axis of the stapedial complex, the Processus supracolumellaris, and the long axis of the footplate of stapes are parallel with the plane of the figure. *Middle right*: The footplate of the bony stapes. The surface of the footplate lies in the plane of the figure. *Bottom right*: The bony stapes. The long axis of the footplate is oriented as in the two upper figures to the right. Towards the extracolumellar-stapedial joint the shaft of stapes becomes flattened.

as the Processus infracolumellaris, such that the outer edge comes closest to the Ligamentum ascendens and the plane of compression parallel to the plane of the tympanic ring. The attachment to the tympanic ring is *ca.* 0.5 mm posterior to the Ligamentum ascendens. From its attachment to the tympanic ring and outwards until the point where the Processus mediocolumellaris branches off, the process attaches to the eardrum. Also the adjacent, ascending part of the Processus mediocolumellaris, up to its junction with the Ligamentum ascendens, is attached to the eardrum which bulges inwards locally over the Processus supracolumellaris.

*Processus mediocolumellaris.* This process juts out from the middle of the Processus supracolumellaris and is about normal to it. After *ca.* 0.5 mm it attaches to the Ligamentum ascendens, then bends through *ca.* 90° and after another 0.5 mm fuses with the Processus extracolumellaris. The attachment to the Ligamentum ascendens is via a small curved extension penetrating into and reaching the midline of the ligament at about half the distance from base to apex of the ligament. The ascending part, from the Processus supracolumellaris to the Ligamentum ascendens, attaches to the eardrum.

The Processi extracolumellaris, supracolumellaris, and mediocolumellaris enclose a foramen known as *Huxley's foramen* (Bellairs & Jenkin 1960, p. 282).

*Ligamentum Platneri*

This is a slender ligament, *ca.* 0.5 mm long, that connects the extracolumella with the heavy bony ridge that traverses the middle ear cavity. One end attaches to the Processus extracolumellaris close to its junction with the shaft of stapes; the other end attaches to the bony ridge of the middle ear, *ca.* 0.5 mm posteroventral to the articulation of the apex of the internal otic process of quadrate.

From its attachment to the bony ridge the ligament runs obliquely inwards towards the extracolumella, forming an angle of *ca.* 50° with the long axis of the stapedial complex, and an angle of *ca.* 20° with the plane of the tympanic ring.

*Musculus stapedius* (figure 42)

*Origin.* Outside the middle and outer ear, on the external surface of the exoccipital on the skull base, lateral to the occipital condyle.

*Insertion.* Chiefly on the middle part of the Processus infracolumellaris. Fibres also attach to the Processus extracolumellaris, near the base of the Processus infracolumellaris, and to the eardrum.

*Remarks.* From its origin on the exoccipital the muscle passes laterally and it penetrates the base of the paroccipital process of the exoccipital via a foramen (figure 25), thus entering the posteroventral part of the external auditory meatus. The muscle remains under the skin of the meatus. It passes over the edge of the tympanic ring and penetrates the membrana propria of the eardrum at a position between the attachments of the Ligamentum ascendens and the Processus infracolumellaris.

From its origin on the skull base, entirely outside the ear, the muscle thus passes through the inner part of the external auditory meatus, and further through the eardrum into the middle ear, where it inserts in the extracolumella and the inside of the eardrum.

*Function.* The following account of the function of the Musculus stapedius is inferred from the geometrical relations of the stapedial complex, the muscle, and the Ligamentum Platneri.

Because of its insertion on the Processi extracolumellaris and infracolumellaris, contraction

of the M. stapedius tends to result in a displacement of the extracolumellar-stapedial joint towards the tympanic ring. Owing to (1) the oblique orientation of the Ligamentum Platneri relative to the plane of the tympanic ring and (2) the tautness of this ligament, the elastic deformation of the extracolumella, caused by the muscle, results in a force on the bony stapes away from the fenestra ovalis.

It would thus seem that the muscle has a potential function of protecting the inner ear and the attachment of stapes to the fenestra ovalis against high sound pressures.

## 20. The bony cochlea and semicircular canals
(figures 29, 35, 36, 40, 41, 45, 46)

The cochlea and semcircular canals are located ventromedially in the skull, on either side of, and close to, the foramen magnum and occipital condyle. Most of the bony cochlea, the entire anterior vertical semicircular canal, and parts of the other two canals attach to the braincase.

The bony cochlea, the semicircular canals, and the entire braincase exhibit complete bilateral symmetry.

Parts of the bony cochlea and semicircular canals lie free in various air spaces of the middle ear, while other parts are fused with various bony structures. Usually the bone forming the bony cochlea and the tubes of the semicircular canals is much more compact than adjacent bone that is spongy at places. Hence it is rather easy to dissect free the bony cochlea and canals. Only at one place is it somewhat ambiguous where to delimit the bony cochlea, this being at the fenestra rotunda. The ventral boundary of the *recessus scalae tympani* at the base of the cochlea (see below) extends ventrally to the tympanic ring. In figures 45 and 46, showing the isolated bony cochlea and the bony semicircular canals, the bone bounding the recessus scalae tympani ventrally, actually part of the cochlea, is dissected away. The recessus scalae tympani is indicated schematically and in outline only, because of difficulties in delimiting the covering bone.

The spatial relations of the bony cochlea, the semicircular canals, recessus stapediales, and tympanic ring are shown in figures 40 and 41.

Angular relations are described after measurements on several skulls in which the semicircular canals were dissected free (table 5).

### *The bony cochlea*

The bony cochlea lies in the ventromedial part of the middle ear cavity. The fenestra ovalis is located in the bottom of the recessus stapediales while the fenestra rotunda is in its ventromedial wall. The plane of the fenestra ovalis forms an angle of *ca.* 27° with that of the tympanic ring, i.e. the base plane of the eardrum (figure 43). The fenestra rotunda lies in a plane that is about normal to that of the tympanic ring. Hence the fenestrae ovalis and rotunda lie in very different planes, set at *ca.* 120° to each other.

Just inside the *membrana tympanica secundaria*, closing the fenestra rotunda, the bony cochlea is widened to form a chamber known as *recessus scalae tympani* (e.g. Schwartzkopff & Winter 1960, p. 611). This chamber extends *ca.* 2.5 mm medial to the tympanic ring, in direction towards the occipital condyle. The chamber narrows somewhat internally and opens

dorsomedially into the main part of the cochlea via a foramen that is about as large as the fenestra rotunda (figures 40, 41).

The fenestra rotunda as well as the foramen between the recessus scalae tympani and the interior of the cochlea lie just anterior to the ampulla of the posterior vertical semicircular canal at the base of the cochlea.

In the skull, with no membrane as a clue, this well defined intracochlear foramen, readily visible through the tympanic ring and the fenestra rotunda, may easily be mistaken for the fenestra rotunda, which is poorly indicated in the skull and hence difficult to identify. Its boundaries are described in §18 and illustrated in figures 40 and 41.

The basal part of the cochlea, holding the fenestrae ovalis and rotunda, is oriented approximately in the anteroposterior direction of the head. 2 mm distal to the fenestra rotunda the cochlea bends through *ca.* 60° and thereafter runs ventromedially. The tips of the cochleae approach the skull's midline and lie at a distance from each other of *ca.* 1.5 mm. The cochlear tips are indicated externally by two distinct eminences in the skull base, at the line of fusion between the basioccipital posteriorly and the basiparasphenoid anteriorly. The dorsomedial wall of the bony cochlea, along its entire length except for the distal 1.5 mm, is fused with the bottom of the braincase.

The length of the bony cochlea, from the proximal margin of the fenestra ovalis to the apex (externally), measured along the midline at the curvature, is *ca.* 9 mm.

*The horizontal semicircular canal*

The data given on angular relations of the semicircular canals are mean values (cf. table 5). Angles in figures 45 and 46 are for the particular specimen illustrated.

As seen from the side the horizontal canal is parallel with the plane of the jugal bars (to within the error of measurement, i.e. *ca.* 2°), and forms an angle of *ca.* 40° with the plane of the foramen magnum (figure 29). As seen in the anteroposterior direction the plane of the horizontal canal deviates 5° from that of the jugal bars, the medial part of the canal being elevated.

The anterior part of the canal and its ampulla are contained in the posterior part of the heavy bony ridge that crosses the middle ear cavity roughly in the anteroposterior direction.

The horizontal canal encircles the posterior air space that opens into the middle ear anteroventral to the canal.

*The anterior vertical semicircular canal*

The plane of this canal forms an angle of 94° with that of the horizontal canal as measured lateral to the vertical, and dorsal to the horizontal canal, 36° with the median plane of the head (figure 45) and hence 72° with the contralateral anterior vertical canal.

The medial surface of the anterior vertical canal is fused with the braincase wall, which here forms also the medial wall of the superior air space of the middle ear. The bony tube lies on the medial wall of the air space and is easily identified through the tympanic ring (figure 40).

*The posterior vertical semicircular canal*

The posterior vertical canal lies posterior to the tympanic ring and encircles the posterior air space of the middle ear.

The plane of this canal forms an angle of 95° with that of the horizontal canal as measured lateral to the vertical, and dorsal to the horizontal canal, 26° with the median plane of the head (figure 45) and hence 52° with the contralateral posterior vertical canal.

The planes of the anterior vertical and the posterior vertical canals are normal to the

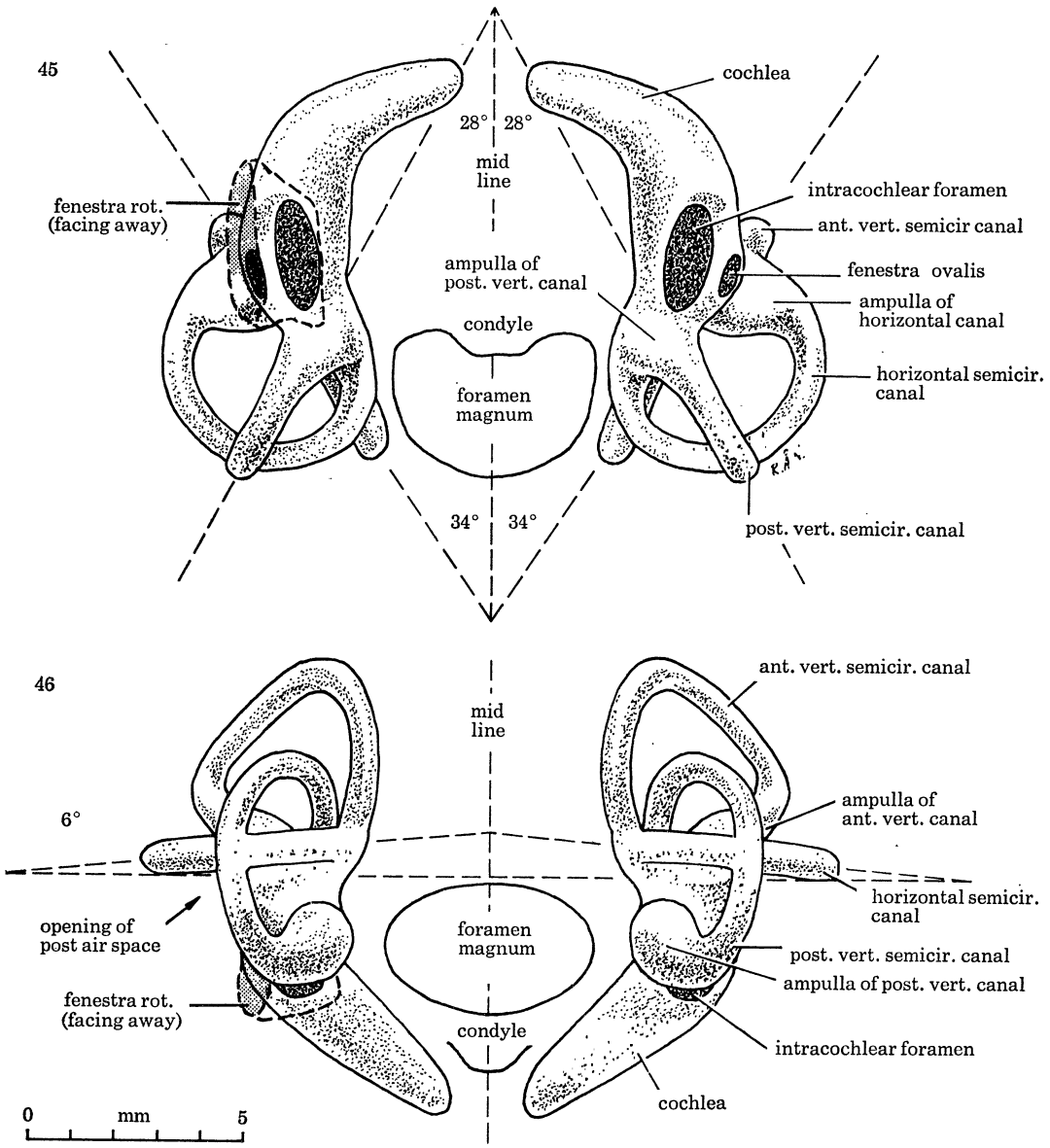


FIGURES 45 AND 46. The bony cochleae and semicircular canals in natural positions in the skull (G 7910). The inner boundary of the recessus scalae tympani and the outline of fenestra rotunda, facing away, are indicated only in the right ear in figure 45, and only in the left ear in figure 46. The bone that forms the ventral wall of the recessus scalae tympani is removed.

For preparation of figures 45 and 46 the bony cochleae and semicircular canals were dissected partly free from adjacent bone. The medial parts were left in connection with the brain case, and so the bony cochlea and semicircular canals remained in natural positions. Figures 45 and 46 drawn with the aid of a camera lucida.

Figure 45 is a ventral view. The horizontal canals lie approximately in the plane of the figure. The plane of the anterior vertical canal is almost parallel with that of the contralateral posterior vertical canal. Figure 46 is a posterior view. The planes of the horizontal canals are normal to the plane of the figure. The scale is for figures 45 and 46.

plane of the jugal bars (to within the error of measurement, *ca.* 2°). The planes of the anterior and the posterior vertical canals of the same side are not set at right angles to each other but form 117° as measured lateral to the canals (figure 45).

The anterior vertical canal lies in a plane that is almost parallel with that of the contralateral posterior vertical canal (*ca.* 9° divergence anterolaterally as calculated from mean values in table 5). This near-coincidence in plane of orientation probably is not accidental. A functional role could be that this geometry brings about perception of angular acceleration via *different* canals for some vertical planes of acceleration. Theoretically this would sharpen the sense.

TABLE 5. ANGULAR RELATIONS OF THE SEMICIRCULAR CANALS

(For spatial relations see figures 45 and 46. The values put in parentheses have been calculated on the assumption that bilateral symmetry prevails (one side measured only in these cases).)

| specimen: | G 7910 | | N.6 | N.7 | | N.8 | | |
|---|---|---|---|---|---|---|---|---|
| | left | right | left | left | right | left | *n* | mean |
| angle between the plane of: | | | | | | | | |
| the horizontal canal and the plane of the foramen magnum, lateral view | 39 | 38 | 40 | | | 41 | 4 | 40 |
| the horizontal canal and the plane of the jugal bars, anteroposterior view | 6 | 6 | 3 | | | 4 | 4 | 5 |
| the anterior vertical canal and the plane of the horizontal canal, measured lateral to the vertical and dorsal to the horizontal canal | 94 | 93 | 94 | 92 | 92 | 96 | 6 | 94 |
| the anterior vertical canal and the median plane of the head | 34 | 34 | 35 | | | 39 | 4 | 36 |
| the posterior vertical canal and the plane of the horizontal canal, measured lateral to the vertical and dorsal to the horizontal canal | 94 | 95 | 95 | 96 | 95 | 93 | 6 | 95 |
| the posterior vertical canal and the median plane of the head | 28 | 28 | 26 | | | 23 | 4 | 26 |
| the anterior vertical canal and the plane of the ipsilateral posterior vertical canal, measured lateral to the canals | 118 | 118 | 119 | 113 | 113 | 118 | 6 | 117 |
| the anterior vertical canal and the plane of the contralateral posterior vertical canal | 6 | 6 | (9) | | | (16) | (4) | (9) |

## 21. SUMMARY OF THE ASYMMETRY

The following is a brief summary of the bilateral ear asymmetry. Details are given in the descriptions of the various structures involved.

The ear openings in the skin are symmetrical with respect to position as well as to form. However, owing to asymmetries of underlying bones, the orientation of the postaural flaps, and hence the ear slits, differs slightly on the two sides.

The feathering of the ear region, namely the facial disk and facial ruff, is symmetrical.

The ear and skull asymmetry reaches its maximum at the ear apertures of the skull. Hence the right ear aperture of the skull lies *ca.* 6.5 mm higher than the left one. This value is the mean of the differences between the two ears in vertical level of the dorsal (6.1 mm) and

ventral (6.8 mm) border of the ear aperture. Viewed from in front, a line connecting the centres of the ear apertures deviates 12° from the horizontal.

The asymmetry then decreases towards the posterior parts of the external auditory meatuses, and the flattened meatus parts extended over the eardrum exhibit complete bilateral symmetry.

As projected on the vertical median plane of the head, an axis through the centre of the eardrum and the centre of the ear aperture of one ear gives an angle of vertical divergence of *ca.* 40° with the corresponding, projected axis of the other ear.

The tympanic ring, the eardrum, the middle ear, the stapedial complex, and the bony cochlea and semicircular canals exhibit complete bilateral symmetry. However, one pair of the three pairs of air spaces communicating with the middle ear, namely the superior air space, is of different shape on the two sides.

The skull bones participating in the asymmetry are: the orbitosphenoid, squamosal, parietal, frontal, and the squamoso-occipital wing.

Of the jaw muscles the M. depressor mandibulae and the aponeurosis 1 portion of M. adductor mandibulae externus exhibit pronounced bilateral asymmetry. Both muscles are related to the highly asymmetrical squamoso-occipital wings.

## 22. A case of outer ear anomaly in *Aegolius* and evolution of ear asymmetry in *Asio*

During field work in 1968 I noticed a slight anomaly of the left external ear in a fledgling of *Aegolius funereus*. In the bottom of the left external auditory meatus, near its orifice, there was a small skin fold forming an erect, small septum. It was low but rather firm. It passed from the posterior surface of the postorbital process on to the quadrate near the quadrate-quadratojugal joint. The septum thus raised mainly from the anterolateral aspect of the body of quadrate. It passed obliquely in a dorsomedial-ventrolateral direction. The ear is illustrated in Norberg (1977, fig. 2).

I have examined the outer ears of well over 100 young and 20 adult *A. funereus* and, except for the above case, have never seen but occasional, very small, loose skin folds that vanished when the skin was manipulated a little. The firm septum described above thus is no commonly occurring type of ear structure in *A. funereus*.

This observation might seem fairly trivial. However, both in its location and orientation the septum resembles very much the one that shuts off the blind cavity below the left ear aperture of the skull in *Asio*. In fact, the ear asymmetry in *Asio* is caused essentially by skin septa, one in each ear.

Presumably the ear asymmetry in *Asio* originated in a similar way through the chance occurrence of skin folds, however, in several steps. The observation in *Aegolius* clearly indicates how accidental may be the origin of novel ear structures that create ear asymmetry and thus open up entirely new evolutionary paths (Norberg 1977).

## 23. Function of the middle ear cavity and associated air spaces

The amplitude of vibration of the ear's sound transmission system depends on (1) the sound pressure (the driving force) and (2) the system's inherent characteristics, namely its friction, mass, and elasticity.

The *mobility* of an oscillating mechanical system such as the middle ear's sound transmission system usually is described in terms of its *mechanical impedance*, which is the inverse of the mobility. It has three constituents, namely (1) the *resistive part* ($R_M$) that expresses the *resistance* or *friction*, and is independent of the frequency, (2) the *mass reactance* ($2\pi fM$) that expresses the *inertia* and increases with the frequency $f$ and mass $M$, and (3) the *stiffness reactance* ($S/2\pi f$) that expresses the elasticity and increases with the stiffness $S$ and decreases with the frequency. They combine into the mechanical impedance $Z$ according to

$$Z = \left(\left(2\pi fM - \frac{S}{2\pi f}\right)^2 + R_M^2\right)^{\frac{1}{2}}. \quad (1)$$

At low oscillating frequencies the stiffness reactance is dominant over the mass reactance and the system is 'stiffness controlled', whereas at high frequencies the reverse is true, the system then being 'mass controlled'. At some intermediate frequency the mass and stiffness reactance cancel, leaving only the resistive part to determine the impedance that then reaches a minimum value. This corresponds to a high mobility of the system, and resonance occurs at this resonant frequency (see for example, Wever & Lawrence 1954, p. 20; Møller 1964).

The air enclosed in the middle ear adds to the stiffness reactance of the middle ear transmission system. Since the stiffness of enclosed air is inversely proportional to its volume, the impedance contribution of the middle ear cavity depends on its volume.

Owing to the large size of the middle ear cavity and to its wide communication with several air cavities, the volume of air inside the eardrum is large in *A. funereus*. Further, the left and right middle ear cavities communicate freely via the left and right anterior air spaces that merge medially in the sphenoid rostrum.

A qualitative evaluation of the function of the large middle ear cavity and associated cavities in *A. funereus* will be made in relation to the function of smaller volumes.

As compared with smaller volumes then, the large volume of air inside the eardrum in *A. funereus* should result in (1) a lowering of the resonant frequency of the middle ear, and (2) a lowering of impedance in the stiffness controlled frequency region below the resonant frequency with a corresponding increase in transmission of these frequencies to the cochlea.

These predictions are based on the theory of sound transmission through the middle ear and on results from experiments on middle ear cavity function in *Dipodomys merriami* and *D. spectabilis* (order Rodentia) (Webster 1962), and in the cat and the rabbit (Møller 1965). In the cat, opening of the bulla, thus eliminating the middle ear cavity's stiffness contribution to impedance, increased sound transmission below 3000 Hz, the gain amounting to 10 dB for low frequencies (Møller 1965, p. 138).

### *Ecological interpretation*

For sound originating from sources that are small relative to the wavelength of sound, the radiation is spherical, resulting in the so-called spreading loss of sensitivity. From this inverse square law, it follows that the pressure level of sound decreases by 6 dB for each doubling of distance.

In natural habitats there are two forms of excess attenuation over the spreading loss, namely (1) atmospheric attenuation that is dependent on the humidity of air, and (2) attenuation due to vegetation. Both kinds of attenuation increase with frequency.

Griffin (1971) compiled data on variation of atmospheric attenuation with frequency and humidity. The following examples read off Griffin's graphs convey some idea of the magnitude

of attenuation. At 75% relative humidity and 10 °C (*ca.* 1% water vapour in the air), atmospheric attenuation per 100 m amounts to about 0.5 dB at 1 kHz, 2 dB at 2 kHz, 7 dB at 4 kHz, 25 dB at 8 kHz, and 70 dB at 16 kHz.

The ability of sound to travel around an obstacle becomes appreciably reduced as the obstacle dimensions approach the wavelength. This is due to sound diffraction and reflexion by the object. With further size increase relative to the wavelength, attenuation increases.

In natural habitats such as forest, both the amount of attenuation by any obstacle and the number of interfering obstacles increase with frequency. Generally then, sound transmission should decrease with frequency due to interference with vegetation.

Morton (1975) measured sound attenuation as a function of frequency at different elevations in various habitats including forest. At ground level and 1.5 m elevation, attenuation in forest, quite unexpectedly, was less at 1500–2500 Hz than at lower and higher frequencies. However, above 2500 Hz, attenuation increased rapidly with frequency (*ca.* 12 dB attenuation per 100 m at 2500 Hz). At 3 m elevation and higher, there was no pronounced 'transmission window' around 2000 Hz, but on the whole an increasing attenuation with frequency.

A consequence of lowered middle ear impedance, and hence a lower threshold of hearing at low frequencies in the owl, is an improvement in far range *detection* of sound containing low frequencies, such as rustling sounds made by prey moving about in vegetation. While high frequencies are potentially more useful for sound localization than are low ones (§28 and Norberg 1968), low frequencies are less attenuated by air and less diffracted and reflected by vegetation, and therefore travel farther and are more useful for detection of sound at some distance.

Acoustic detection by the owl is often the first in a series of events that may lead to prey capture. Once the sound has been detected, a rough azimuth judgement can be made, whereupon the owl can move progressively closer (Norberg 1970, p. 54) and make use of higher frequencies for improved sound localization.

## 24. Transformer action linked to the area ratio between eardrum and footplate of stapes

The ratio between the area enclosed by the tympanic ring, i.e. the base area of the eardrum, and the area of the footplate of stapes, abutting against the perilymph of the inner ear, is 35.3 in *A. funereus*. This is a relatively high value for a bird.

Schwartzkopff (1957) calculated corresponding ratios in 44 bird species. In 40 of these, ratios lay between 15 and 29. Only four species, among them three owls, had ratios of 30 or more. The ratios for the four owl species investigated were: 31 in *Tyto alba* (Scopoli), 20 in *Athene noctua* (Scopoli), 30 in *Strix aluco* Linné, and 40 in *Asio otus* (Linné).

The area ratio between eardrum and footplate of stapes is 36.5 in the cat and 21 in man (Wever & Lawrence 1954, p. 113).

Since most investigations of eardrum displacement pattern and function have been performed on mammals, some definitions pertaining to the mammalian middle ear, and comparisons with the bird ear, are placed here before a functional review.

The outermost ear ossicle, the *malleus*, has a long process, the *manubrium*, that attaches radially to the eardrum much like the Ligamentum ascendens does in birds. The manubrium in mammals and the ligament in birds pass from the margin of the eardrum to its umbo, and

both structures are important in maintaining the conical shape of the eardrum, with the umbo directed inwards in mammals and outwards in birds. The manubrium and the Ligamentum ascendens, with supporting structures of the extracolumella, are functionally analogous, acting as levers picking up vibrations of the eardrum.

The functional interpretation of the area ratio between eardrum and footplate of stapes is critically dependent on the vibration pattern of the eardrum. Two concepts will be reviewed here.

*The stiff-plate concept*

This is the classical concept of von Békésy (1941), shared and supported by Wever & Lawrence (1954). It has been widely accepted until recently.

It states that the eardrum moves as a single stiff plate, or rather cone, that is hinged around the ossicular axis of rotation. Equal displacement lines on the eardrum would run perpendicular to the axis of the manubrium, indicating equal vibration amplitudes for the manubrium and adjacent eardrum points to the sides of it.

Since the eardrum attaches to the tympanic ring, all of it obviously can not move as one rigid cone. Hence the membrane is deformed near its periphery, particularly in a relatively large compliant area at the margin opposite the manubrium. The peripheral compliant area contributes little or nothing to the transformer function. The term *effective area* therefore was introduced, referring to that part of the eardrum that moves as a single plate coupled to the manubrium. The effective area was found to be about two thirds of the whole eardrum (von Békésy 1941; Wever & Lawrence 1954, p. 113).

Hence the effective area ratio would amount to two thirds of the geometrical area ratio of the eardrum and footplate of stapes. The above considerations are restricted to frequencies below 2000 Hz (Khanna & Tonndorf 1972, p. 1916).

*The curved-membrane concept*

This old concept of Helmholtz dates back to 1868. It has since long been regarded as superseded by the stiff-plate concept (see for example, Wever & Lawrence 1954).

However, Khanna & Tonndorf have recently investigated eardrum displacements in the cat and man with the aid of time-averaged holography. They obtained very clear pictures of the eardrum with isoamplitude fringes, revealing a vibration pattern that is consistent with Helmholtz's curved-membrane concept but at variance with the stiff-plate concept (Tonndorf & Khanna 1970, 1972; Khanna & Tonndorf 1972).

In contradistinction to the relatively short Ligamentum ascendens in *A. funereus*, reaching only about 35% of the length of the eardrum diameter along the line of the ligament, the manubrium in man reaches about 60% of the length of the eardrum diameter along the line of the manubrium and that of the cat about 70%. Hence the largest free, unsupported eardrum areas are to either side of the manubrium, especially in the cat.

In man, and more clearly in the cat, equal displacement lines form one set of concentric, elliptical fringes to either side of the manubrium. This reveals that the eardrum does not move as a single stiff cone, but that eardrum displacement amplitudes are larger to either side of the manubrium than on the manubrium itself. This pattern is typical for the frequency range of the first mode of eardrum vibration, which is below about 2000 Hz for the cat (Khanna & Tonndorf 1972, fig. 15; Tonndorf & Khanna 1972, fig. 2).

At higher frequencies the vibration pattern in the cat changed, and beyond 3000 Hz broke up into multiple subpatterns that remained in phase. Along with this there was a gradual decoupling of the membrane vibration from that of the manubrium, suggesting that the sound drives the manubrium directly at high frequencies (Tonndorf & Khanna 1970, pp. 750–751).

These findings for low frequency sound (below about 2000 Hz for the cat) have two important functional implications.

1. The first is that the full eardrum (base) area should be used in estimating the transformer function linked to the area ratio between eardrum and footplate of stapes (Khanna & Tonndorf 1972, p. 1918).

2. The second is that the curved-membrane principle may be in operation and contribute to the final transformer ratio (Khanna & Tonndorf 1972). The principle is that a slightly curved membrane (just as a string or catenary) exerts a greater pull at the points of attachment (in the direction of the tangent plane to the membrane) than the load it is being subjected to.

On the basis of anatomical data only, estimation of the transformer ratio in the owl, due to the curved-membrane principle, would require a detailed working through of membrane curvature and stapedial complex geometry. It is not entered into here.

### 25. Structure and movement of the stapedial complex

The truss system that the Ligamentum ascendens and the various extracolumellar processes form, constitutes a relatively rigid unit resistant to deformation. The geometry of the Ligamentum ascendens and the Processi extracolumellaris, supracolumellaris, and mediocolumellaris seems particularly efficient in rendering stiffness to the extracolumella (figure 44).

The stapedial complex is firmly anchored to the tympanic ring via the Processi infracolumellaris and supracolumellaris with the Ligamentum ascendens in between. The two processi form an angle of *ca.* 70° with each other, and hence prevent any lateral movements of the extracolumella in the plane of the tympanic ring. The Ligamentum Platneri functions as a tension member and adds to lateral rigidity of the extracolumella.

The whole Ligamentum ascendens and the Processi infracolumellaris and supracolumellaris, at their attachments to the tympanic ring, are flattened in the plane of the ring. This weakening against bending of all three structures at the rim of the tympanic ring, and in the same plane, defines the axis of rotation of the extracolumella, and greatly facilitates its rotation.

Another point of great functional importance is that the plane of compression of the region of fusion between the extracolumella and stapes is parallel to the axis of rotation of the extracolumella. Hence the cartilaginous part of this joint (the Processus extracolumellaris) is easily deformed elastically upon rotation of the extracolumella.

The extracolumellar-stapedial joint rotates about the axis of rotation of the extracolumella. The outer end of the shaft of the stapes thus moves along the arc of a circle centred at this axis. The spatial relations are such that a line from the extracolumella's axis of rotation to the extracolumellar-stapedial joint is about normal to the long axis of the Processus extracolumellaris and stapes. At the small vibrational amplitudes set up by sound, vibration of the joint then occurs essentially along the line of the axis of the stapes. This is the geometry that calls for the least possible deformation of the extracolumellar-stapedial joint.

Functionally, the stapedial complex consists of two units that perform two different, but interrelated, movement patterns.

1. The extracolumella and Ligamentum ascendens form one rigid unit that rotates about its axis of rotation at the rim of the tympanic ring. This unit is the functional equivalent to the mammalian ear ossicles malleus and incus. Although basically a diarthrosis, the malleo-incudal joint usually is immobile in most mammals at moderate sound pressure levels (Wever & Lawrence 1954, p. 153). Thus it is immovable in the monotreme echidna, *Tachyglossus* Illiger (Hopson 1966, p. 444), while in the guinea pig there is no such joint, the malleus and incus being solidly fused together (Tonndorf & Khanna 1972, p. 516). In the cat the malleo-incudal joint is immovable except in young animals and at frequencies below about 40 Hz, where there is slippage in the malleoincudal joint (Tonndorf & Khanna 1967, p. 515). Hence, the mammalian malleus and incus usually move as one unit as do the extracolumella and Ligamentum ascendens in *A. funereus*.

2. The bony stapes is driven by the extracolumella but performs a pistonlike motion. It corresponds to the mammalian stapes.

Another kind of motion, inferred from the stapedial complex geometry, is caused by the Musculus stapedius, and was described along with that muscle. This motion of the extra-columellar-stapedial joint is essentially along the arc of a circle with the Ligamentum Platneri as radius and with the centre located at the ligament's origin on the middle ear ridge. Contraction of M. stapedius thus results in a near-axial force on the stapes, away from the fenestra ovalis. The mechanism obviously protects the ear against high sound pressure levels.

Because of the thinness of the extracolumellar processes and the hollow structure of the bony stapes, the stapedial complex has low solidity. The objective of this, obviously, is to keep its mass reactance contribution to the middle ear impedance low. Low mass is particularly important in the bird stapedial complex since the axis of rotation of the extracolumella is located far from the centre of mass of the stapedial complex. The axis of rotation of the ear ossicles in many mammals, including man, passes approximately through the centre of mass of the ossicular system (Wever & Lawrence 1954, ch. 7; Møller 1972, p. 138).

In the owl, the oblique orientation of the stapedial complex helps to bring its centre of mass closer to the axis of rotation, hence slightly reducing moments of inertia.

## 26. Transformer action of the stapedial complex

Three morphological features are essential for the transformer action of the stapedial complex. They are (1) the compressed cross-section area of the extracolumellar-stapedial joint, permitting the two-unit mode of motion of the stapedial complex described in the foregoing section, (2) the oblique orientation of the stapedial complex, and (3) its off-centre attachment to the eardrum.

To begin with, only the membrane force that acts on the outer tip of the stapedial complex, i.e. through the umbo of the eardrum, and normal to the plane of the tympanic ring will be considered. Since the transformer ratio of the stapedial complex will be combined with that due to the area ratio between eardrum and footplate of stapes, the force normal to the plane of the tympanic ring is the pertinent one.

The *force lever arm* is defined as the perpendicular distance between the line of action of the membrane force and the fulcral axis of the extracolumella. The force exerted by the extra-

columella on the bony stapes acts in line with the long axis of stapes. Therefore, the *resistance lever arm* is the perpendicular distance between the long axis of stapes and the fulcral axis of the extracolumella (figure 47).

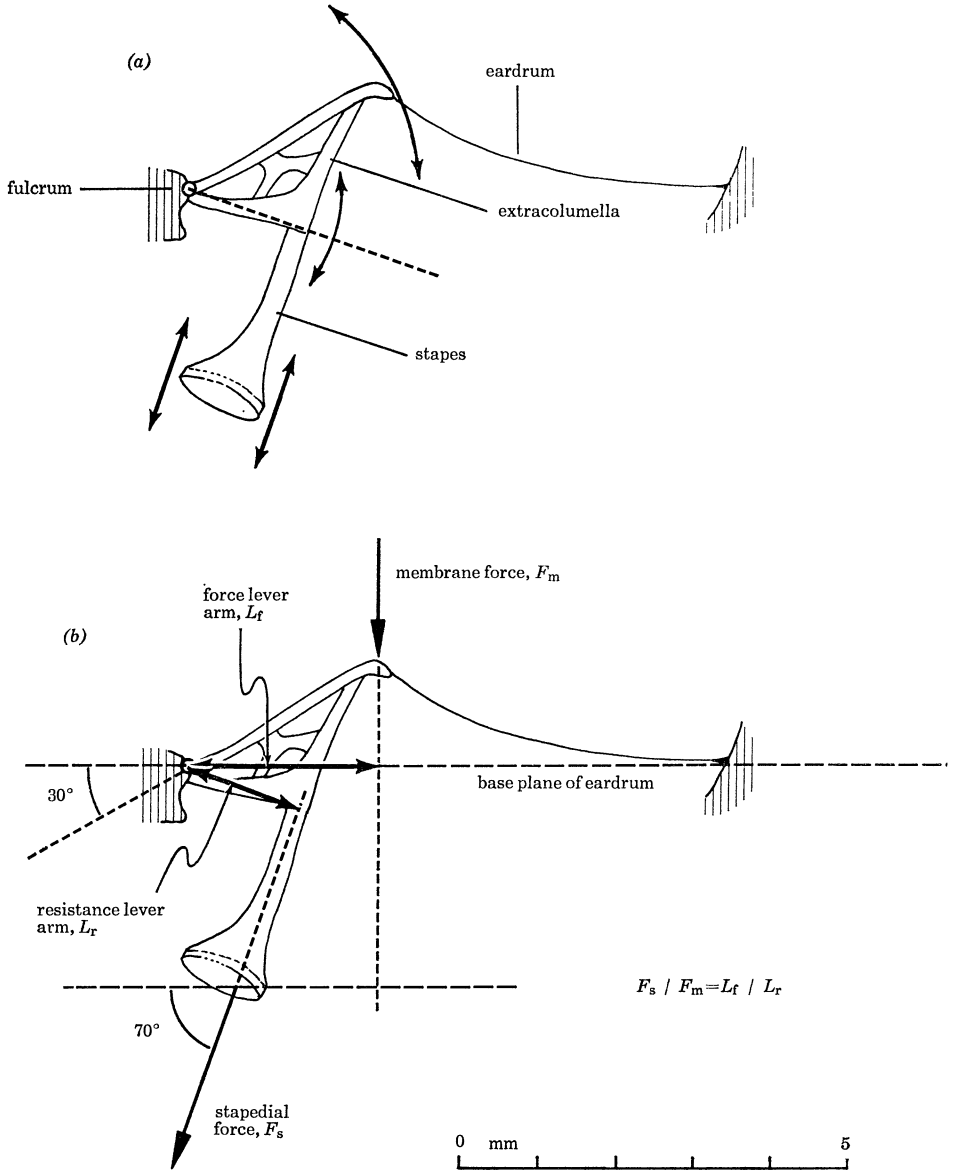


FIGURE 47. Movement pattern (amplitude grossly exaggerated in figure 47*a*) and function (figure 47*b*) of the stapedial complex as inferred from its geometry and structure. Drawings based on figure 43.

(*a*) A radius (broken line) from the fulcral axis and through the extracolumellar-stapedial joint is about perpendicular to the long axis of the bony stapes. Therefore the rotational movement of the cartilaginous extracolumella is transformed to a piston-like motion of the bony stapes (with little or no tilt movement of the stapes). This geometry calls for the least possible deformation of, and thus resistance from, the extracolumellar-stapedial joint. This joint is flattened in a plane parallel to the fulcral axis to facilitate elastic deformation (see §25).

Because of the oblique orientation of the stapedial complex the excursion amplitude is reduced from the umbo of the eardrum to the footplate of stapes, resulting in a corresponding, inversely related, increase in pressure.

(*b*) Geometry and relations used in estimating the force transformation ratio (about 1.6) due to the stapedial complex (cf. §§25 and 26). The membrane force is drawn perpendicularly to the base plane of the eardrum, i.e. the plane of the tympanic ring. The scale is for figures 47*a* and *b*.

Because of the oblique orientation of the stapedial complex relative to the plane of the tympanic ring, the force lever arm becomes longer than the resistance arm. Their respective lengths are 2.4 and 1.5 mm, giving a transformer ratio of 1.6.

This ratio applies only to forces acting on the outer tip of the stapedial complex. Forces distributed along the Ligamentum ascendens have shorter moment arms, thus giving lower transformer ratios. However, because of the off-centre location of the tip of the stapedial complex on the eardrum, most of the membrane forces probably act on the tip of the Ligamentum ascendens. It is probably only forces from the relatively small eardrum parts located lateral to the Ligamentum ascendens that may be distributed along the ligament.

Thus, the transformer ratio of 1.6 is a potential, maximum one. However, the actual ratio is judged to be only slightly smaller because of the off-centre location of the stapedial complex on the eardrum.

## 27. Final transformer ratio

The three transformer ratios, namely those due to (1) the area ratio, (2) the stapedial complex, and (3) the curved-membrane effect, combine multiplicatively into the final transformer ratio.

The area ratio and the lever ratio of the stapedial complex thus combine to give a ratio of $35.3 \times 1.6 = 56$ in *A. funereus* (the possible curved-membrane effect not included).

It should be stressed that the transformer ratio components are estimated solely on the basis of the geometry of the structures involved. Further, it is assumed that the owl's eardrum vibration pattern for low frequencies is basically similar to those in the cat and man, justifying the use of the full area ratio between eardrum and footplate (cf. §24; Khanna & Tonndorf 1972; Tonndorf & Khanna 1972).

The stapedial complex ratio probably is slightly overestimated (cf. the foregoing section). The ratio due to the curved-membrane effect is not estimated here. In the cat, Khanna & Tonndorf (1972, p. 1918) calculated it to be about 2.

From the consideration of the air to sea water impedance ratio, Wever & Lawrence (1954, p. 75) estimated the optimal transformer ratio of the middle ear to be 63. Using data on middle and inner ear impedance, Khanna & Tonndorf (1972, p. 1917) estimated ideal transformer ratios in the cat to be between 57 and 73, varying with frequency, but with 65 as an average value.

The transformation ratio in *A. funereus* thus seems to be close to the optimal one, i.e. that resulting in maximum pressure transfer to the inner ear.

## 28. Function of the ear asymmetry

From circumstantial evidence it seems obvious that bilateral ear asymmetry in owls is linked to directional hearing. Some arguments are given below.

### 28.1. *Inferences from morphology*

The skull and ear asymmetry reaches its maximum at the ear aperture of the skull. Posteriorly in the external auditory meatus as well as in the skull at large, the asymmetry diminishes, and at the eardrums complete symmetry prevails.

The asymmetry thus obviously is designed to bring about differential reception of incoming sound between the two ears.

The eardrum, middle ear (except for the superior air space), and stapedial complex are bilaterally symmetrical, which assures identity of the transmission channels to the inner ears. As far as is known, the inner ears are also symmetrical. Transmission asymmetry in the middle ears should be obviated to assure that any difference in sound reception of the external ears is carried unchanged to the inner ears.

The external ears are bilaterally asymmetrical in the *vertical* plane. This strongly suggests that the asymmetry is linked to *vertical directional hearing.*

The mere fact that there is a *bilateral asymmetry* of the external ears strongly suggests that vertical directional hearing is based on *binaural comparison* of signals from the two ears. Indeed, the entire asymmetry would seem meaningless as to auditory localization, if the information processing at the neural level were not based on binaural comparison.

### 28.2. *Head and ear dimensions and frequency domain of vertical localization*

The external ear asymmetry theoretically makes it possible for the head and external ear to induce a transformation of the incoming sound, such that the heard sounds become some function of the elevation angle of the source and become different in the two ears for most elevation angles in front of the head. Whether the expected information is based on time or on intensity cues, it is dependent on relations between the wavelength of sound and head and ear dimensions. Some general aspects will be considered below.

The sound shadow of the head may be expected to be significant only for sounds with wavelengths about equal to, or shorter than, the linear head dimensions. The head, with plumage, is *ca.* 70 mm wide at the facial ruff in *A. funereus*, and the skull is *ca.* 40 mm wide. This corresponds to the wavelength of frequencies of 5000 and 8500 Hz, respectively, above which head diffraction may be expected to influence significantly the ears' directional sensitivity. Since at least the facial ruff feathers reflect high frequency sound (Konishi 1973, p. 422, on *Tyto alba*), 5000 Hz should be the relevant frequency.

As regards the ear openings in the skin and in the skull, elevation dependent transformation of the sound could be effected in at least two different ways.

1. One is via monaural interference between sound reaching the eardrum directly and via reflexion and delay paths in the external ear as described for the human pinna by Batteau (1967, 1968). Except for the monaural temporal coding of elevation angles, the pinna reflexions in man cause spectral changes. Hence elevation angles could be identified by a traditional spectral analysis of composite signals (Wright, Hebrank & Wilson 1974).

2. Another mechanism is via transverse resonance modes across the external ear which are excited preferentially by sound arriving from certain elevation angles, as inferred from data of the human pinna and models thereof (Shaw & Teranishi 1968, p. 247; Teranishi & Shaw 1968, p. 261; Searle, Braida, Cuddy & Davis 1975, p. 449).

For monaural time delays to influence significantly the ears' vertical directional sensitivity, the pertinent ear dimension, here the height of the ear slit in the skin, would need to be about equal to or larger than a half wavelength ($\frac{1}{2}\lambda$). For the ear slit height of 24 mm in *A. funereus*, a frequency of about 7000 Hz would thus be required. Transverse resonance modes at $\frac{1}{4}\lambda$ might be expected to appear at about this frequency too, as judged by the ear structure and dimensions (notably the distance from the ear aperture of the skull to the lower and upper

terminations of the ear slit which is *ca.* 12 mm; table 1, measurements 5r and 6l). Also, if monaural time delays were decoded directly into elevation angles (as suggested for man by Batteau 1967, 1968), and not via their effect on directional sensitivity, such an analysis would have to rely on high frequencies that give short enough rise and decay times of transients.

The general considerations above indicate that the ear asymmetry in *A. funereus* should be expected to improve vertical directional hearing only at relatively high frequencies.

It could be further hypothesized that the remarkably large height of the symmetrical ear slits in the skin serves the purpose of extending the effect of ear asymmetry to lower frequency domains. The arguments underlying this suggestion are as follows.

The ear openings in the skull must, of necessity, be rather small to have room to be placed on different vertical levels on the two sides. The slits are bilaterally symmetrical and hence may be high. Actually, they occupy the whole height of the skull. Although symmetrical in themselves, the slits combine with the ear apertures of the skull to give bilaterally asymmetrical structures. Hence, as regards relations between ear size and wavelength of sound, it is the size of the ear slit in the skin (*ca.* 24 mm) that is to be considered rather than the size of the ear aperture of the skull (*ca.* 11 mm, table 1, measurements 4 and 7).

### 28.3. *Experimental data on physical cues to vertical localization, provided by the ear asymmetry*

Acoustic measurements have been performed on a carefully made artificial head of *A. funereus* (Norberg 1968). Two acoustic effects of the morphological ear asymmetry were very obvious. One concerns time, the other intensity.

1. *Time.* The directions in front of the head, from which incident sound reached the two eardrums simultaneously, lie in a plane that is inclined 12° to the vertical median plane of the head and intersects this plane in the anterior-posterior direction. This plane, specifying directions of zero interaural time difference, is perpendicular to a line connecting the centres of the ear apertures of the skull. This interaural line deviates 12° from the horizontal plane of the head.

*Interpretation.* The inclination of this reference plane provides no obvious cue to directional hearing, but seems to be a secondary effect.

2. *Intensity.* In the vertical median plane in front of the head there is a great disparity in directional sensitivity between the two ears in the frequency range 10000–16000 Hz. Thus the maximum sensitivity is directed obliquely downwards for the left ear, obliquely upwards for the right one, reflecting the morphological asymmetry. The median-plane sensitivity curves of the two ears intersect near the horizontal plane of the head.

Apart from these measurements on an artificial head, directional characteristics in the vertical median plane have also been recorded on dead but intact specimens of *A. funereus* with entire eardrums (Norberg, unpublished). Sound was picked up close to the eardrum (near its centre) by a probe tube with 2 mm external diameter. It was inserted through a hole in the posteroventral wall of the external auditory meatus. Otherwise the method was essentially as described earlier (Norberg 1968).

The directional characteristics thus obtained at 12500 and 16000 Hz for ears of dead owls were very similar to those of the artificial head, showing essentially the same vertical asymmetry. However, at 8000 and 10000 Hz, and to a lesser extent at 6300 Hz (no intermediate frequencies were used), there was a reversed vertical asymmetry. Thus, the maximum

sensitivity of the left ear was directed obliquely upwards, that of the right ear obliquely downwards. The asymmetry at 8000 Hz was almost as pronounced as the one at 16000 Hz of the artificial head (Norberg 1968, fig. 17). This asymmetry is termed 'reversed' because it is so relative to the morphological asymmetry and also relative to that of the directional characteristics at 12500 and 16000 Hz.

The differences between results from the model head and from dead owls at 6300–10000 Hz are attributed mainly to differences in position of the postaural folds, those of the dead owls being in more natural positions. In particular, the anterior edge of the postaural folds of the dead owls were located further forwards as in living owls when attentive (2–3 mm anterior to the anterolateral edge of the squamoso-occipital wing, not level with it as in the model head). Further, the aural folds did not lie as close against the skull in the real ears as in the artificial head, thus exposing to a higher degree the flat cavities underneath the skin folds, in particular the cavity extending dorsal to the slit. All this tends to enhance the acoustical effect of the ear slit and ear folds. By manipulating the folds, it was found that their position did influence the ears' directionality.

*Interpretation.* In theory, this vertical, binaural disparity in directional sensitivity at high frequencies is an ideal cue for vertical localization. By binaural sound pressure comparison, and with the median plane of the head remaining vertical, a complex sound thus could be localized as to azimuth with the aid of low frequencies and as to elevation with the aid of high frequencies.

### 28.4. *Conclusion*

The results of the acoustic measurements (cf. above) clearly demonstrate that the ear asymmetry in *Aegolius* is capable of producing excellent physical cues to vertical sound localization, based on binaural intensity comparison (essentially as postulated by Pumphrey (1948)).

This leads to the question of whether or not the binaural intensity cues to vertical localization are detectable by the owl?

There are no published data on the frequency range of hearing of *A. funereus*. However, van Dijk (1973) has made an extensive study of hearing sensitivity of 10 other owl species. He presented behavioural audibility curves, or audiograms, for all 10 species, and sensitivity diagrams based on cochlear potentials for two of them. The shape of the curves and the overall sensitivity differed markedly between species.

In the species with the best high-frequency sensitivity, namely *Strix aluco* and *Asio otus*, there was a rapid fall in sensitivity between 8000 and 10000 Hz. Hence no data were obtained for frequencies higher than 10000 Hz, but extrapolation of the curves indicates that the sensitivity is very poor for frequencies beyond 10000 Hz.

Also in *Tyto alba* there is a very rapid fall in sensitivity beyond 10000 Hz (Konishi 1973).

Judging by this, the binaural asymmetry of the vertical directional sensitivity curves of *A. funereus* at 12500 and 16000 Hz probably is not of much use to the owl.

However, it is most likely that a large part of the frequency range 6300–10000 Hz, where the 'reversed asymmetry' occurs, falls within the range of good hearing in *A. funereus*.

To be able to use the intensity cue provided by the binaural vertical asymmetry of the directional characteristics, the owl must also be capable of performing a spectral analysis. No data on this is available for *Aegolius*. However, it is of interest that *Tyto alba* is capable of

an exquisite frequency and spectral discrimination (Quine & Konishi 1974; Konishi & Kenuk 1975).

In conclusion, the following hypothesis on localization of complex sound in *A. funereus* is suggested. It is identical to my earlier version (Norberg 1968) except for the delimitation of frequency domains for azimuth and elevation determinations, respectively, as noted below. Furthermore, it is similar to, but simpler than, the well-known one advanced by Pumphrey in 1948 (further explained in Payne 1971, p. 566). The hypothesis is consistent with modern auditory theory and with owl data, but needs extensive testing.

*Azimuth determination.* 1. By binaural comparison of time of arrival of sound at the two eardrums. Directions in front of the head from which sound reaches the two eardrums simultaneously, lie in a plane that is inclined 12° to the vertical median plane of the head. This is a well defined reference plane for binaural time analysis (Norberg 1968, p. 198).

2. By binaural comparison of intensity at frequencies below 6000 Hz. At these low frequencies the directional characteristics of the two ears are bilaterally symmetrical. When the source is in the vertical median plane, the sound is equally loud in both ears. This plane therefore is a well defined reference plane.

This agrees with Norberg (1968, pp. 200–201) except that the frequency range allocated to azimuth determination is restricted here to be below 6000 Hz (instead of 10000).

*Elevation determination.* By binaural comparison of intensity at frequencies from 6000 Hz and upwards to the upper frequency limit of hearing. The directions in which a source produces no interaural intensity differences are well defined reference directions. For most elevation angles they deviate from the vertical median plane of the head at frequencies beyond 6000 Hz.

In principle, this is in agreement with Norberg (1968, p. 201). The deviation is that 'reversed asymmetry' of the vertical directional characteristics has since been detected for real ears (of dead but intact owls). Therefore, the frequency range allocated here to vertical localization is from 6000 Hz (instead of 10000) and upwards.

With a complex sound, such as prey rustles, at least every major directional sector of incidence in front of the head is likely to be characterized by a unique interaural difference in spectral pattern. With the aid of binaural spectral comparison, this cue could be used for an approximate localization both to azimuth and elevation without head movements.

The interaural difference in spectral pattern should tell the owl in which general direction the source is located relative to the acoustic reference directions (with zero interaural difference in time or intensity). Turning of the head towards the source would permit a more accurate localization close to the acoustic reference directions about the line of sight. This localization should be possible both in the horizontal and vertical plane, and with the median plane of the head remaining vertical. Before striking visible prey the owl turns its face directly towards the prey (Norberg 1970, p. 55), suggesting that the final auditory localization actually occurs near the acoustic reference directions near the line of sight.

In theory, the median plane ambiguity, inherent to symmetrical ears, is removed by the bilateral asymmetry. This is because the asymmetry at some frequencies causes interaural intensity differences at most elevation angles in the median plane.

The use of *interaural differences* in spectral pattern in auditory localization would also remove the problem of distinguishing 'what' from 'where', i.e. the uncertainty as to whether a specific spectral pattern should be attributed to the sound source or to a direction-dependent spectral

transformation imposed by head and ear. The ear asymmetry provides the cue in the vertical plane.

The hypothesis may be summarized in symbols as follows.

Assume an original sound spectrum $P(f)$, which is sound pressure level $P$ against frequency $f$. The transformation $T$ performed by head and ear may be denoted $T(f, \alpha, \epsilon)$, where $\alpha$ is azimuth angle and $\epsilon$ elevation angle. The transformation of azimuth and elevation is performed in different frequency domains. The sounds heard in the left, l, and right, r, ear then are

$$P_l(f) = P(f) \times T_l(f, \alpha, \epsilon) \tag{2}$$

and

$$P_r(f) = P(f) \times T_r(f, \alpha, \epsilon).$$

Binaural comparison may be represented by the ratio between $P_l(f)$ and $P_r(f)$,

$$P_l(f)/P_r(f) = T_l(f, \alpha, \epsilon)/T_r(f, \alpha, \epsilon). \tag{3}$$

Thereby the original spectrum $P(f)$ is eliminated, 'what' is separated from 'where', and the direction of the source is uniquely determined by the difference in transformation between the left and right ear. The contribution of the ear asymmetry would be that of assuring a different transformation in the two ears for most elevation angles $\epsilon$, also in the vertical median plane of the head. This removes the median plane ambiguity associated with localization with symmetrical ears without head movements.

For providing me with dead, intact and fresh owls and/or arranging for me to examine and measure several specimens before preparing them as study skins, I wish to express my sincere thanks to W. Berg, Museum of Natural History, Stockholm, to B. Wennerberg, E. Haack, and Monica Silferstolpe, all at the Museum of Natural History, Göteborg, to T. Hansson, Örebro, and to K. Borg, Department of Veterinary Medicine, Stockholm. Skeletal material was borrowed from several museums, and I thank the following persons for bringing about the loans: J. Lepiksaar, Museum of Natural History, Göteborg; Greta Vestergren, Museum of Natural History, Stockholm; Hj. M.-K. Lund, Museum of Zoology, University of Oslo, Oslo; and H. Olsen, Museum of Zoology, University of Bergen, Bergen.

W. J. Bock, Columbia University, New York, and K. Engström, Museum of Natural History, Stockholm, read the whole manuscript, and A. Møller, The Karolinska Institute, Stockholm, read the functional parts (§§ 23–28). They suggested many improvements, and I am most grateful to them all.

This study was supported by grants from Hierta Retzius' Forskningsfond, Lennanderska Fonden, Längmanska Kulturfonden, and the Faculty of Natural Sciences of the University of Göteborg.

## References

Baird, S. F., Brewer, T. M. & Ridgway, R. 1874 *A history of North American birds.* vol. 3, pp. 4–103, Owls. Boston: Little, Brown, and Company.

Batteau, D. W. 1967 The role of the pinna in human localization. *Proc. R. Soc. Lond.* B **158**, 158–180.

Batteau, D. W. 1968 Listening with the naked ear. In *The neurophysiology of spatially oriented behaviour* (ed. S. J. Freedman), pp. 109–133. Homewood, Illinois: Dorsey Press.

von Békésy, G. 1941 Über die Messung der Schwingungsamplitude der Gehörknöchelchen mittels einer kapazitiven Sonde. *Akust. Z.* **6**, 1–16.

Bellairs, A. D'A. & Jenkin, C. R. 1960 The skeleton of birds. In *Biology and comparative physiology of birds* (ed. A. J. Marshall) vol. 1, pp. 241–300. New York and London: Academic Press.

Bock, W. J. & Shear, Ch. R. 1972 A staining method for gross dissection of vertebrate muscles. *Anat. Anz.* **130**, 222–227.

Collett, R. 1871 On the asymmetry of the skull in *Strix tengmalmi*. *Proc. Zool. Soc. Lond.* (1871), 739–743.

Collett, R. 1872 Om craniets assymetri hos *Nyctala tengmalmi* Gm. *Forh. Vidensk. Selsk. Krist.* (1872), 68–72. (In Norwegian. Content essentially as in Collett 1871.)

Collett, R. 1881 Craniets og øreaabningernes bygning hos de nordeuropaeiske arter af familien Strigidae. *Forh. Vidensk. Selsk. Krist.* (1881), 1–38. (In Norwegian. An unabridged English version was given by Shufeldt 1901, who also added some notes.)

Dijk, T. van. 1973 A comparative study of hearing in owls of the family Strigidae. *Neth. J. Zool.* **23**, 131–167.

Dombrowsky, B. 1925 Das Mittelohr der Vögel. *Rev. Zool. Russ.* **5**, 15–35.

Evans, H. E. 1948 Clearing and staining small vertebrates, in toto, for demonstrating ossification. *Turtox News* **26**, 42–47.

Freye-Zumpfe, H. 1952/53 Befunde im Mittelohr der Vögel. *Wiss. Z. Univ. Halle* **2**, 445–461.

Griffin, D. R. 1971 The importance of atmospheric attenuation for the echolocation of bats (Chiroptera). *Anim. Behav.* **19**, 55–61.

Grossman, M. L. & Hamlet, J. 1964 *Birds of prey of the world.* New York: Clarkson N. Potter Inc.

Helmholtz, H. 1868 Die Mechanik der Gehörknöchelchen und des Trommelfells. *Pflügers Arch.* **1**, 1–60 (transl. as *The mechanism of the ossicles of the ear and the membrana tympani.* New York: W. Wood and Co., 1873). Not seen, cited from Wever & Lawrence (1954) and Tonndorf & Khanna (1972).

Hopson, J. A. 1966 The origin of the mammalian middle ear. *Am. Zool.* **6**, 437–450.

Jollie, M. T. 1957 The head skeleton of the chicken and remarks on the anatomy of this region in other birds. *J. Morph.* **100**, 389–436.

Khanna, S. M. & Tonndorf, J. 1972 Tympanic membrane vibrations in cats studied by time-averaged holography. *J. Acoust. Soc. Am.* **51**, 1904–1920.

Konishi, M. 1973 How the owl tracks its prey. *Am. Sci.* **61**, 414–424.

Konishi, M. & Kenuk, A. S. 1975 Discrimination of noise spectra by memory in the barn owl. *J. comp. Physiol.* **97**, 55–58.

Lucas, A. M. & Stettenheim, P. R. 1972 Avian Anatomy. Integument. Part 1. U.S. Government Printing Office. Washington, D.C.

Marinelli, W. 1936 In *Handbuch der vergleichenden anatomie der wirbeltiere* (ed. Bolk, Göppert, Kallius & Lubosch), vol. 4, pp. 809–838. Urban & Schwarzenberg. Not seen, cited from Jollie (1957).

May, W. (1961). Die Morphologie des Chondrocraniums und Osteocraniums eines Waldkauzembryos (*Strix aluco* L.). *Z. Wiss. Zool.* **166**, 134–202.

Møller, A. R. 1964 The acoustic impedance in experimental studies on the middle ear. *Int. Audiol.* **3**, 1–13.

Møller, A. R. 1965 An experimental study of the acoustic impedance of the middle ear and its transmission properties. *Acta oto-laryngol.* **60**, 129–149.

Møller, A. R. 1972 The middle ear. In *Foundations of modern auditory theory* (ed. J. V. Tobias), vol. 2, pp. 133–194. New York and London: Academic Press.

Morton, E. S. 1975 Ecological sources of selection on avian sounds. *Am. Nat.* **109**, 17–34.

Norberg, R. Å. 1968 Physical factors in directional hearing in *Aegolius funereus* (Linné) (Strigiformes), with special reference to the significance of the asymmetry of the external ears. *Ark. Zool.* **20**, 181–204.

Norberg, R. Å. 1970 Hunting technique of Tengmalm's owl *Aegolius funereus* (L.). *Ornis Scand.* **1**, 51–64.

Norberg, R. Å. 1977 Occurrence and independent evolution of bilateral ear asymmetry in owls and implications on owl taxonomy. *Phil. Trans. R. Soc. Lond.* B **280**, 375–408.

Olson, E. C. 1966 The middle ear – Morphological types in amphibians and reptiles. *Am. Zool.* **6**, 399–419.

Payne, R. S. 1971 Acoustic location of prey by barn owls (*Tyto alba*). *J. exp. Biol.* **54**, 535–573.

Pohlman, A. G. 1921 The position and functional interpretation of the elastic ligaments in the middle-ear region of *Gallus*. *J. Morphol.* **35**, 229–269.

Pumphrey, R. J. 1948 The sense organs of birds. *Ibis* **90**, 171–199. Reprinted with some additions 1948. *Ann. Rep. Smithson. Inst.*, pp. 305–330.

Pycraft, W. P. 1898 A contribution towards our knowledge of the morphology of the owls. Part 1. Pterylography. *Trans. Linn. Soc. Lond.* (2nd ser.) *Zool.* **7**, 223–275.

Pycraft, W. P. 1903 A contribution towards our knowledge of the morphology of the owls. Part 2. Osteology. *Trans. Linn. Soc. Lond.* (2nd ser.) *Zool.* **9**, 1–46.

Quine, D. B. & Konishi, M. 1974 Absolute frequency discrimination in the barn owl. *J. comp. Physiol.* **93**, 347–360.

Romer, A. S. 1962 *The vertebrate body* (3rd edition). Philadelphia and London: W. B. Saunders Company.

Schwartzkopff, J. 1957 Die Grössenverhältnisse von Trommelfell, Columella-Fussplatte und Schnecke bei Vögeln verschiedenen Gewichts. *Z. Morph. Ökol. Tiere* **45**, 365–378.

Schwartzkopff, J. 1962 Zur Frage des Richtungshörens von Eulen (Striges). *Z. vergl. Physiol.* **45**, 570–580.

Schwartzkopff, J. & Winter, P. 1960 Zur Anatomie der Vogelcochlea unter natürlichen Bedingungen. *Biol. Zbl.* **79**, 607–625.

Searle, C. L., Braida, L. D., Cuddy, D. R. & Davis, M. F. 1975 Binaural pinna disparity: another auditory localization cue. *J. Acoust. Soc. Am.* **57**, 448–455.

Shaw, E. A. G. & Teranishi, R. 1968 Sound pressure generated in an external-ear replica and real human ears by a nearby point source. *J. Acoust. Soc. Am.* **44**, 240–249.

Shufeldt, R. W. 1901 Professor Collett on the morphology of the cranium and the auricular openings in the North-European species of the family Strigidae. *J. Morph.* **17**, 119–176. (English version of Collett's 1881 paper.)

Stellbogen, E. 1930 Über das äussere und mittlere Ohr des Waldkauzes (*Syrnium aluco* L.). *Z. Morph. Ökol. Tiere* **19**, 686–731.

Starck, D. & Barnikol, A. 1954 Beiträge zur Morphologie der Trigeminus-muskulatur der Vögel (besonders der Accipitres, Cathartidae, Striges und Anseres). *Gegenbaurs Morphol. Jahrb.* (Jahrb. Morphol. Mikroskopische Anat.) **94**, 1–64.

Stresemann, E. 1934 Sauropsida: Aves. In *Handbuch der Zoologie* (ed. W. Kükenthal & T. Krumbach), vol. 7/2. Berlin and Leipzig: Walter de Gruyter & Co.

Teranishi, R. & Shaw, E. A. G. 1968 External-ear acoustic models with simple geometry. *J. Acoust. Soc. Am.* **44**, 257–263.

Tonndorf, J. & Khanna, S. M. 1967 Some properties of sound transmission in the middle and outer ears of cats. *J. Acoust. Soc. Am.* **41**, 513–521.

Tonndorf, J. & Khanna, S. M. 1970 The role of the tympanic membrane in middle ear transmission. *Ann. Otol. Rhinol. Laryngol.* **79**, 743–753.

Tonndorf, J. & Khanna, S. M. 1972 Tympanic-membrane vibrations in human cadaver ears studied by time-averaged holography. *J. Acoust. Soc. Am.* **52**, 1221–1233.

Webster, D. B. 1962 A function of the enlarged middle-ear cavities of the kangaroo rat, *Dipodomys*. *Physiol. Zool.* **35**, 248–255.

Werner, C. F. 1960 Das Gehörorgan der Wirbeltiere und des Menschen. Beispiel für eine vergleichende Morphologie der Lagebeziehungen. Leipzig: Veb. Georg Thieme.

Wever, E. G. & Lawrence, M. 1954 *Physiological acoustics*. Princeton, New Jersey: Princeton University Press.

Wiener, F. M. & Ross, D. A. 1946 The pressure distribution in the auditory canal in a progressive sound field. *J. Acoust. Soc. Am.* **18**, 401–408.

Wright, D., Hebrank, J. H. & Wilson, B. 1974 Pinna reflections as cues for localization. *J. Acoust. Soc. Am.* **56**, 957–962.

ear opening or slit in the skin
postorbital process
sclerotic ring
preaural fold
external ear cavity
postaural fold
squamoso occipital wing
ear opening in the skull
ext. auditory meatus
facial ruff
facial disk
forehead feathers
facial ruff
lore feathers
jugal bar
chin feathers
throat
locket or
gular region

5

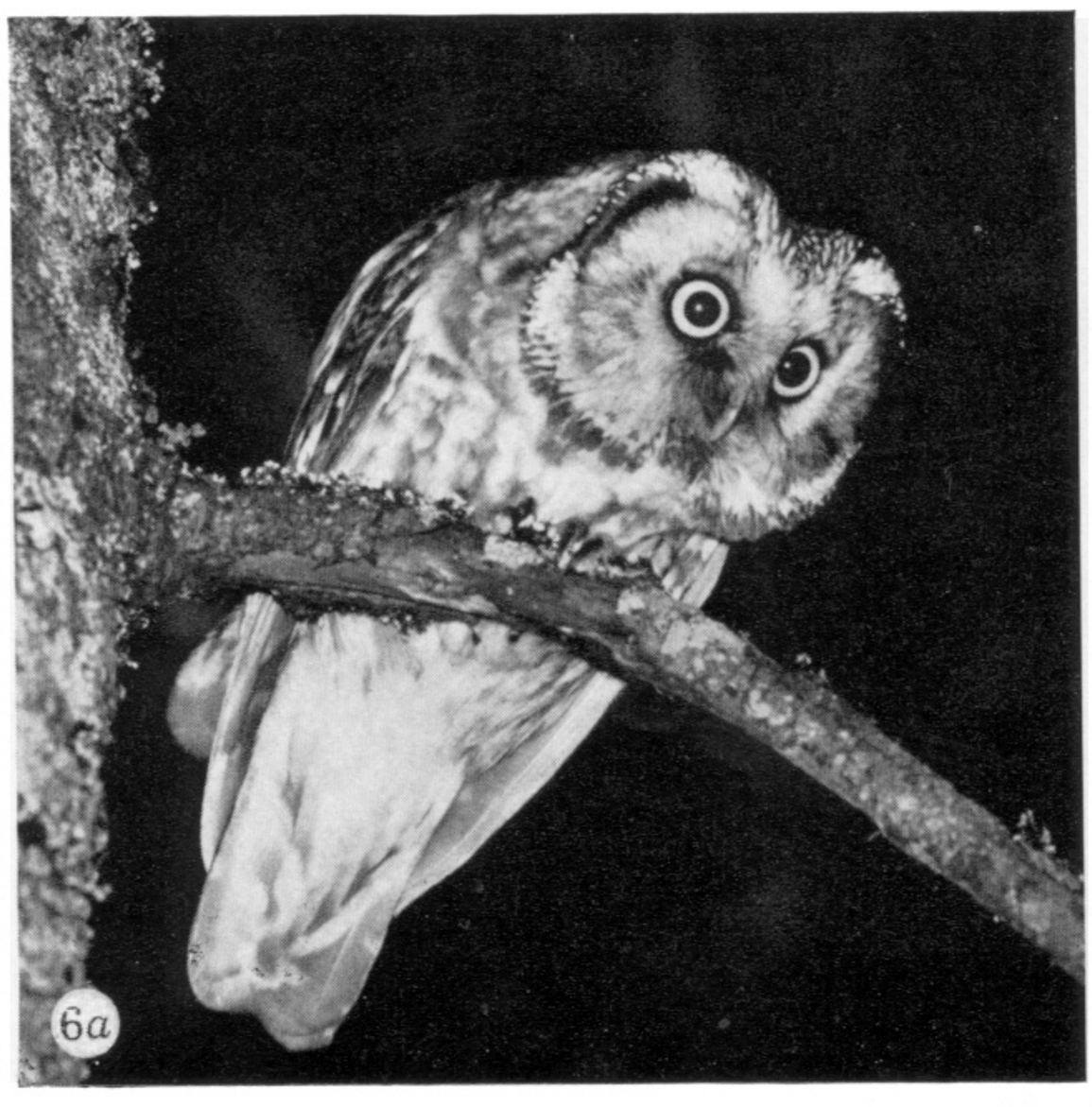

6a

6b

PLATE 1. For description see opposite.

30
mm

8

7

4,5,6

1,2,3

7a

1

2

3

4

5

6

7

8

30 mm

7b

PLATE 2. For description see opposite.